Progress in Particle and Nuclear Physics 116 (2021) 103824

Contents lists available at ScienceDirect

Progress in Particle and Nuclear Physics

journal homepage: www.elsevier.com/locate/ppnp

Review

What comes after the Standard Model?

M. Khlopov *

Institute of Physics, Southern Federal University, Rostov on Don, Russia
National Research Nuclear University MEPhI (Moscow Engineering Physics Institute), Moscow, Russia
Universite de Paris, CNRS, Astroparticule et Cosmologie, F-75013 Paris, France

ARTICLE INFO

Article history:
Available online 10 October 2020

Keywords:
Cosmology
Particle physics
Dark matter
Primordial black holes
Antimatter
Dark atoms

ABSTRACT

The standard model (SM) of elementary particles involves particle symmetry and the mechanism of its breaking. It finds no contradictions in the collider experiments, but appeals to extensions for solutions of its internal problems and in view of its evident incompleteness. The paradigm of the modern cosmology is based on inflationary models with baryosynthesis and dark matter/energy that involves physics beyond the standard model (BSM) of elementary particles. However, studies of the BSM physical basis of the modern cosmology inevitably reveals additional particle model dependent cosmological consequences that go beyond the modern Standard cosmological model. The mutual relationship of the BSM particle physics basis of the modern cosmology and the nontrivial features of the corresponding cosmological scenario are the subject of the present review.

Contents

* Correspondence to: Institute of Physics, Southern Federal University, Rostov on Don, Russia.
E-mail address: khlopov@apc.in2p3.fr.

https://doi.org/10.1016/j.ppnp.2020.103824
0146-6410/

1. Introduction

The answer to the question of the title is that after the old Standard model some new models should come. The contours of such particle physics models may be found in the theoretical solutions for the internal problems of the Standard gauge model of electroweak and strong interactions of elementary particles. They may find esthetical arguments in the trends to unify the fundamental natural forces. These contours acquire the meaning of necessary building blocks for the modern standard model of the Universe. Inflation, baryosynthesis, dark energy and dark matter are the necessary elements of the modern cosmology and their physical nature involves BSM particle models [1–9].

Therefore BSM physics is not only plausible from the particle theoretical viewpoint, but seems to be inevitable in the description of the structure and evolution of the Universe. The problem is the lack of a direct experimental evidence of the BSM particle physics. The principal existence of this physics is favored by the data of precision cosmology, but its experimental signatures are still elusive or controversial in the results of accelerator and non-accelerator searches. Practically only the nonzero mass of neutrino proved by the effect of neutrino oscillations can be considered as the experimentally verified signature of the new physics. However, even in this case the BSM physical nature of the mass of neutrino is still not clear.

In the present review we approach the contours of new physics in a three-fold way. We discuss the basic elements of the SM extension that help to solve the internal SM problems in the relationship with their cosmological signatures. We consider reflection of the structure of the microworld in the cosmological scenario and pay special attention to additional model dependent cosmological features that can provide probes for the basis of the modern cosmology. It inevitably leads to BSM cosmology based on the BSM physics. We finally discuss fundamental relationship of BSM physics and cosmology in the context of cosmoparticle physics that provides methods to study fundamental relationship of micro- and macro-worlds [10–13].

2. BSM physics and its cosmological reflections

2.1. Arguments for extension of the standard model of particle physics

The elementary matter particles content of the Standard model is arranged in three families of fermions (quarks and leptons), displayed in Fig. 1.

The Standard model of fundamental interactions of these elementary particles is based on the principle of a local gauge symmetry and the assumed $SU(2)_L x U(1) x SU(3)_c$ symmetry makes possible to describe electroweak and strong interactions in analogy with quantum electrodynamics (QED) by Lagrangian

$$L_{ij} = g_s \bar{f}_i \gamma_\mu f_j A^\mu_{ij}. \quad (1)$$

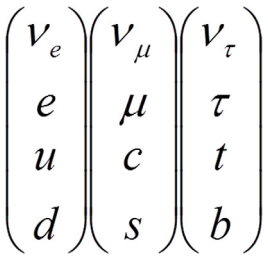

Fig. 1. Three families of quarks and leptons. Each family contains neutrino, charged lepton and up-type and down-type quark.

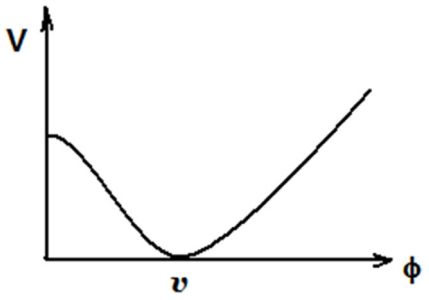

Fig. 2. Higgs potential. Minimum of the Higgs potential determines the nonzero vacuum expectation value of the Higgs field ϕ.

Here g_s are coupling constants for transition from the initial fermion state f_j to a final state f_i that is the source of a gauge field A_{ij}^{μ}. In the extension of QED, charges of electroweak interaction are the source of the electromagnetic field together with W and Z fields of weak interaction. Color charges of Quantum Chromodynamics (QCD) are the source of gluon fields of strong interaction.

The difference in range of electromagnetic and weak interactions is ascribed to the breaking of the $(SU(2)_L xU(1))$ symmetry by Higgs mechanism. The potential of the additional scalar Higgs field ϕ

$$V_H = -\frac{1}{2}m^2\phi^2 + \frac{\lambda}{4}\phi^4, \tag{2}$$

owing to the negative sign of the m^2 term has a minimum at the nonzero vacuum expectation value of the Higgs field $\langle\phi^2\rangle = m^2/\lambda = v^2$. The value of v determines the scale of the electroweak $SU(2)_L xU(1)$ symmetry breaking. The form of the Higgs potential is displayed in Fig. 2.

Interaction of the Higgs field with gauge bosons generates the mass of weak W- and Z- bosons of the order of gv, where g is the gauge coupling, while photon remains massless.

In the Standard model quarks and charged leptons Ψ acquire their mass owing to Yukawa coupling h_f to the Higgs field ϕ.

$$L_f = h_f \phi \bar{\Psi}_R \Psi_L + h.c., \tag{3}$$

where Ψ_L is operator of annihilation of initial left-handed state of fermion f and $\bar{\Psi}_R$ is operator of creation of the right-handed state. The vacuum expectation value of the Higgs field v generates fermion mass $m_f = h_f v$. Only left-handed neutrino take part in weak interactions. There is no right-handed neutrino and neutrino is massless in the Standard model.

The short range of strong nuclear interactions is determined by $(SU(3)_c)$ confinement of colored particles — quarks and gluons. The nature of confinement is related to the self interaction of the gluon field, preventing separation of free colored objects at large distances and giving significant increase of the mass of constituent light u and d quarks. Therefore it is the scale of QCD confinement that dominantly determines the mass of nucleons in the atomic nuclei.

Up to now there is no experimental contradiction to the predictions of the Standard model, but there are serious reasons to consider it as incomplete and to extend its symmetry and particle content:

(1) Discovery of neutrino oscillations reflects nonzero mass of neutrino and presents the first experimentally proven signature of BSM physics (see Section 2.2).
(2) Radiative effects in the mass of Higgs boson are quadratically divergent. This divergence should be either canceled by a contribution of new particles or can be avoided, if Higgs boson is composite. In the both cases BSM physics is needed (see Sections 2.3 and 2.4).
(3) Self-interaction of gluon field leads to CP odd effects that violate CP conservation in QCD. Cancellation of these effects may involve axion solution and BSM physics of axion (see Section 2.5)

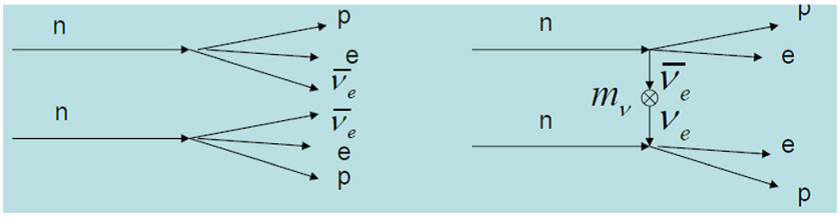

Fig. 3. Two-neutrino and neutrinoless double beta decay.

(4) Symmetry of interactions of quark–lepton families and evident breaking of this symmetry in their mass spectrum appeals to extension of the SM symmetry to broken symmetry of fermion families. Such extension to a local gauge symmetry implies sufficiently nontrivial BSM physics, since the mass of quarks and leptons is within the scale v of the EW symmetry breaking, while the mass M_H of horizontal gauge bosons mediating interaction of Flavor Changing Neutral Currents should be larger, than v by several orders of the magnitude (see Section 2.6).

(5) Parity violation in weak interaction leads to nonequivalence of left- and right-handed coordinate systems. To restore this equivalence a set of mirror partners of ordinary particles should be involved. Their absence in the processes of strong and electroweak interactions implies that they possess the corresponding mirror strong and electroweak interactions. It extends the Standard model by the world of mirror particles and their interactions. (see Section 2.7)

(6) Similarity in the description of strong and electroweak interactions appeals to their unification. Embedding of the group of SM symmetry in the framework of a symmetry group of Grand Unification (GUT) extends the set of particles and involves new interactions. Such interactions violate baryon and lepton number conservation. To provide embedding in the GUT group the three running gauge constants should intersect in one point. It may need addition of new sets of particles with the corresponding gauge charges to support such an intersection. (see Section 2.8)

(7) The esthetical aim to unify all the fundamental forces can involve not only extension of the set of particles and their interactions, but it can also extend the space–time, involving various forms of compactified or infinite extra dimensions. In the latter case our physical world is concentrated in the four-dimensional sheet of a multidimensional space–time. (see Section 2.9)

(8) The data of precision cosmology gives strong evidences for the Standard ΛCDM cosmology, based on inflational models with baryosynthesis and nonbaryonic dark matter/energy. These basic elements of the modern theory of the structure and evolution of the Universe inevitably involve BSM physics. (see Section 4)

These physical, cosmological and esthetical arguments involve extension of the SM model by a rich pattern of the BSM physics.

2.2. BSM physics of the mass of neutrino

The mass term in the Eq. (3) corresponds to transition from right-handed to left handed fermion states. In the lack of right-handed neutrino such mass term is absent for neutrino in the Standard model. Therefore, physics of nonzero mass of neutrino inevitably leads to Physics beyond the Standard model.

There are two principal possibilities for the nature of neutrino mass:

(a) Neutrino is the only electrically neutral elementary particle and can have Majorana mass. In this case, the role of right-handed state plays antineutrino. This solution uses only known particles (left-handed neutrinos and right-handed antineutrinos) but implies lepton number violation, which is preserved in the Standard model. Majorana nature of electron neutrino mass can provide neutrinoless double beta decay. The mechanism of neutrinoless double beta decay due to Majorana mass of electron neutrino is displayed in Fig. 3.

(b) Neutrino has Dirac mass as all the other quarks and leptons. It implies the existence of a sterile right-handed neutrino state, which does not participate in weak interactions. This possibility extends the content of elementary particles by a new state of right handed neutrino.

Both possibilities (a) and (b) are used in the explanation of another puzzle of neutrino mass — it is several order of magnitude smaller, than the mass of the corresponding charged lepton. The see-saw mechanism of neutrino mass generation assumes that neutrino has Dirac mass m_D, which is equal to the mass of the charged lepton, but the right handed neutrino has a very large Majorana mass $M \gg m_D$. It generates a small Majorana mass m_ν of left-handed neutrino, which is equal to

$$m_\nu = \frac{m_D^2}{M} = \frac{m_D}{M} m_D \ll m_D. \tag{4}$$

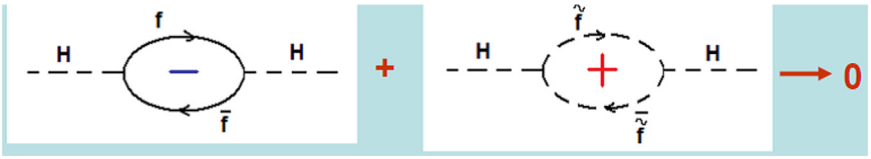

Fig. 4. Cancellation of divergence in the Higgs boson mass.

Direct measurements of neutrino mass give only upper limits on the mass of electron, muon and tau neutrino. The most stringent is the upper limit on the mass of electron neutrino, which is less, than 1 eV.[1] However, neutrino flavor states (electron, muon, tau) do not coincide with the proper mass states. It makes each flavor state, defined by its association with the corresponding lepton, a superposition of states with definite mass and leads to effect of neutrino oscillations — in the course of its propagation neutrino state of definite flavor converts in a superposition of other flavor states owing to the difference of neutrino masses. The oscillation length $l \propto E_\nu/\Delta m^2$ detected in neutrino experiments for neutrinos with the energy E_ν defines the neutrino mass difference, which in combination with upper limits on neutrino mass from experiments with electron neutrino puts a constraint on the mass of all the types of neutrino.

It is the stable prediction of the Big Bang cosmology that together with the observed Cosmic Microwave Background (CMB) radiation relic neutrino background radiation should be inevitably present in the modern Universe. At high temperatures neutrino gas was in thermal equilibrium with cosmological plasma. It determined the relationship between number densities of neutrino–antineutrino pairs $n_{\nu\bar{\nu}}$ and photons n_γ

$$n_{\nu\bar{\nu}} = \frac{3}{4} n_\gamma,$$

where numerical factor 3/4 takes into account the difference in fermion and boson statistics. Adiabatic cosmological expansion after decoupling of neutrino gas preserved separate conservation of entropies of neutrino gas and plasma with radiation. The latter converted into the electromagnetic background radiation after annihilation of the equilibrium electron–positron pairs. The account for the effect of this annihilation leads to an extra factor 4/11 and finally gives the Big Bang prediction for primordial neutrino background with the number density

$$n_{\nu\bar{\nu}} = \frac{3}{4}\frac{4}{11} n_\gamma = n_{\nu\bar{\nu}} = \frac{3}{11} n_\gamma. \tag{5}$$

If we multiply this number density by the mass of neutrino, we get the contribution of relic neutrinos in the modern cosmological density. The current upper limits on neutrino mass make primordial neutrino gas a subdominant component of the modern matter density. In 1980s the results of measurement of electron neutrino mass gave the value around 30 eV. It made massive neutrino dominant in the cosmological density. The analysis of the model of neutrino dominated Universe revealed the necessity in the nonbaryonic dark matter, but the progress in experimental measurements of neutrino mass together with the analysis the cosmological data excludes light massive neutrino as the dominant form of dark matter. Planck collaboration puts the limit of 0.23 eV on the sum of masses of neutrinos [14].

2.3. Supersymmetry

Supersymmetric (SUSY) models put into correspondence to the ordinary particles – fermions and bosons – their partners that have the same gauge charges but differ by spin. They put bosonic partners to quarks and leptons and fermionic partners to gauge and Higgs bosons. For instance, electron with spin 1/2 has a partner selectron with spin 0, or photon with spin 1 has a fermionic partner photon with spin 1/2. Gluon with spin 1 has a SUSY partner gluino, fermion with spin 1/2 and so on.

The advantage of supersymmetric extensions of the Standard Model (SM) made them a mainstream of the high energy physics in the last decades. Indeed, SUSY models provided solutions for several internal SM problems of the Standard model.

- Quadratic divergence of the Higgs boson mass in the radiative effects of the SM particles is canceled by the opposite sign contribution by their supersymmetric partners. Virtual bosons and fermions in such effects contribute with opposite sign due to the difference in the corresponding Bose–Einstein and Fermi–Dirac statistics as displayed in Fig. 4.
- The account for contribution of SUSY particles in the running gauge constants of electroweak (EW) and strong interactions provides intersection of all these three constants at a very high energy scale Λ_{GUT}. It makes possible to embed the symmetry of weak, electromagnetic and strong interactions in the Grand Unified gauge symmetry. The hierarchy of the EW and GUT scales $v \ll \Lambda_{GUT}$ is supported by cancellation by SUSY partners the GUT scale contributions to the EW scale parameters.

[1] (Henceforth, if it is not otherwise specified, we use the units $\hbar = c = k = 1$).

- The Higgs mechanism of the electroweak symmetry breaking finds natural physical origin. At the GUT scale, Higgs potential has positive m^2 term and acquires the form of the Eq. (2) in the course of renormalization to the EW scale.
- Supersymmetry should be broken to explain the absence of SUSY particles by their higher mass than their SM partners. However, to support the hierarchy of EW and GUT scales, SUSY particles should have masses that are not much larger, than the EW scale. It gave the advantage of their search and discovery at the Large Hadron Collider (LHC).

However, the advantage of SUSY models goes far beyond their possibility to solve internal problems of the SM. They naturally offer BSM physics for the basis of the modern cosmology:

- Supersymmetric partners have a property that differs them from the SM particles. In the simplest case it is R-parity, which is positive for SM particles and negative for SUSY partners. R-parity conservation makes stable the Lightest Supersymmetric Particle (LSP). Created in the early Universe, such particles should survive to the present time and be present in the Universe. The LSP candidates are neutral and interact with matter with cross section typical for a weak interaction. It makes LSP natural candidates for Weakly Interacting Massive Particles that explain the cosmological dark matter.
- Scalar partners of quarks and leptons can be in condensate in the early Universe and decay of this condensate can generate the excess of baryons and leptons that can explain the origin the observed baryon asymmetry of the Universe.
- SUSY models can also provide mechanisms of the cosmological inflation (see Section 4).

Local supersymmetric models involve also space–time symmetry. They add to the set of SUSY particles a supersymmetric partner of graviton — gravitino with spin 3/2. Gravitino has semi-gravitational coupling to matter and its direct production at accelerators is strongly suppressed. Gravitino can be metastable and decay to gluon and gluino, or photon and photino with a lifetime

$$\tau \sim \frac{M_{Pl}^2}{m_{3/2}^3}, \tag{6}$$

where $M_{Pl} = 10^{19}$ GeV is the Planck mass and $m_{3/2}$ is the mass of gravitino. Gravitino can be LSP and then play the role of superweakly interacting dark matter particle.

Involvement of space–time symmetry in SUSY models leads to Supergravity that can provide unification of gravity with the other three fundamental interactions.

The expected discovery of SUSY at the LHC still did not happen. There are also no definite positive evidence for WIMPs in the direct dark matter searches in underground detectors. It may mean that the SUSY scale is so high that SUSY particles can be produced neither at the LHC, nor at any future accelerator. The superhigh energy scale supersymmetric models can play important cosmological role and can be studied by their cosmological consequences with the use of methods of astroparticle physics and precision cosmology. However, the solutions for divergence of Higgs boson mass and the origin of the EW symmetry breaking scale may need some other nonsupersymmetric BSM model in this case.

2.4. Composite Higgs boson

The problem of divergence of the mass of an elementary Higgs boson, can be solved, if Higgs boson is composite. Then the electroweak symmetry breaking scale and the mass of Higgs boson are determined by the scale, at which the constituents are confined. The origin of this scale may come from confinement of new nonabelean gauge charges, similar to the QCD case. This idea of a 'technicolor' is now developed in the Walking Technicolor models, in which gauge constants are not running, but walking. This nontrivial dependence of the gauge coupling on distance makes possible to arrange the scale Λ_{WTC} of technicolor confinement above electroweak scale v even if technicolor symmetry is based on $SU(2)$ gauge group. Note that $SU(2)$ confinement with a running constant would take place at macroscopical distances and that would be the case for electroweak $SU(2)$ symmetry without Higgs mechanism.

Together with binding in the composite Higgs boson, technicolor constituents can also form a set of new composite particles. At the energy $E \ll \Lambda_{WTC}$ their composite nature is not feasible and they look like new elementary particles. Since techniquarks have only technicolor and do not possess ordinary QCD color, their bound states look like ordinary leptons.

The minimal walking technicolor model (WTC) [15–21] involves two techniquarks, U and D. They transform under the adjoint representation of a $SU(2)$ technicolor gauge group. Neutral techniquark–antitechniquark state is associated with the Higgs boson. Six bosons UU, UD, DD, and their corresponding antiparticles carry a technibaryon number. If the technibaryon number is conserved, the lightest technibaryon should be stable.

Electric charges of UU, UD and DD are given in general by $q + 1$, q, and $q - 1$, respectively, where q is an arbitrary real number [15,22,23]. To compensate the anomalies the model includes in addition technileptons ν' and ζ that are technicolor singlets. Their electric charges are in terms of q, respectively, $(1 - 3q)/2$ and $(-1 - 3q)/2$.

Fractional value of q would correspond to stable fractionally charged techniparticles. Their creation in the early Universe would lead to their presence in the terrestrial matter that is severely constrained by the experimental data.

Table 1
Integer charged techniparticles. The candidates for even charged constituents of dark atoms are marked bold.

q	$UU(q+1)$	$UD(q)$	$DD(q-1)$	$\nu'(\frac{1-3q}{2})$	$\zeta(\frac{-1-3q}{2})$
1	**2**	1	0	−1	**−2**
3	**4**	3	**2**	**−4**	−5
5	**6**	5	**4**	−7	**−8**
7	**8**	7	**6**	**−10**	−11

On the same reason, stable techniparticles should not have odd charge $2n + 1$. Positively charged $+(2n + 1)$ stable particles are bound with electrons in anomalous isotopes of elements with $Z = 2n + 1$. Negatively charged particles with charge $-(2n + 1)$, created in the early Universe, bind with $n + 1$ nuclei of primordial helium, produced in the Big Bang Nucleosynthesis, and form a +1 charged ion that binds with electrons in atoms of anomalous hydrogen. The experimental data puts severe constraints on such anomalous isotopes.

The case of stable multiple charged particles with even value of negative charge $-2n$ avoids these troubles, since it forms with n nuclei of primordial helium neutral dark atom. Some possible examples of multiple charged techniparticles are shown in Table 1. Their bound states with primordial helium can play the role of dark matter and as we discuss in Section 6.1, can even solve the puzzles of dark matter searches.

New particles are predicted in all the other approaches to solve the problem of the Higgs boson and origin of electroweak symmetry breaking [24–29]. In particular, the approach [30], involving colored twisted partners of top quark, can lead to existence of colored particles with arbitrary charge. In this approach colored particles with charge that differs from $Q = 2/3 + n$ or from $Q = -(n + 1/3)$ cannot decay to SM particles and should be stable or long living [31].

2.5. Axion and pseudo Nambu–Goldstone models

In essence the problem of strong CP violation in QCD comes from the θ term that has the form

$$L_\theta = \theta G_{\mu\nu}\tilde{G}_{\mu\nu}, \tag{7}$$

where $G_{\mu\nu}$ is the tensor of gluon field and $\tilde{G}_{\mu\nu}$ is its dual tensor. It corresponds to a CP odd invariant $\theta\vec{E}_g\vec{H}_g$, where $\vec{E}_g$ and $\vec{H}_g$ are the electric and magnetic strengths of gluon field and θ is constant. This term is generated by instanton transitions originated from nonlinearity of gluon field, since gluon bears color charge, which in turn is the source of gluon field. CP violating phase in the quark mass matrix puts additional contribution in θ.

On the other hand, interference of CP even QCD terms and CP odd θ term generates effects of CP violation in strong interaction. It leads to a nonzero electric dipole moment of neutron d_n. Experimental upper limits on $d_n < 10^{-26}e$ cm, where e is the charge of electron, put severe constraints on the value of $\theta < 10^{-9}$. The different nature of the two contribution to θ each being, in general, not small, cannot a priori provide their cancellation down to the level of $\theta < 10^{-9}$.

The theoretical solution of this problem is related to the mechanism of the natural suppression of θ.

In order to provide such mechanism Peccei and Quinn [32] assumed the additional chiral global $U(1)_{pQ}$ symmetry with nonvanishing color anomaly. If this symmetry is not broken, what corresponds to the existence of at least one massless quark, c.f., u-quark [33,34], all θ vacua are equivalent to the vacuum with $\theta = 0$, since θ-term may be excluded from the Lagrangian by the chiral phase transformation of the u-quark field.

Though a possibility of massless u-quark theoretically is not excluded, the problem of the θ-term finds natural solution in the case of the broken $U(1)_{PQ}$ symmetry. The constant θ acquires in this case the dynamical meaning of the amplitude of the pseudo-Nambu–Goldstone field, related to the broken $U(1)_{PQ}$ symmetry, which, in turn, is manifestly broken by the color anomaly. Hence, in the vacuum the condition $\theta_{vac} = 0$ is automatically satisfied, thus providing the exact mutual compensation of the terms in Eq. (7). Such pseudo-Nambu–Goldstone field is called axion.

The idea of the axion solution for the problem of the strong CP violation can be explained by the following simple argument. If the dynamical solution is found with the use of axion, it means that we should consider the Lagrangian (7) as the Lagrangian of the axion–gluon interaction. The nonvanishing color anomaly means here that the constant of this interaction is nonzero. Zero vacuum expectation value for the axion field provides then the effective cancellation of the 8-term in the QCD vacuum.

The most important parameter, defining the properties of the axion, is the energy scale F_a at which the symmetry $U(1)_{PQ}$ is broken. This scale appears in the Lagrangian of the axion–gluon interaction

$$L_{\alpha gg} = \frac{g^2}{16\pi}\frac{\alpha}{F_a}\tilde{G}^{\mu\nu}G^{\lambda\rho}\epsilon_{\mu\nu\lambda\rho}, \tag{8}$$

where α is the axion field.

Lagrangian of axion interactions with other gauge fields can be expressed in the same form (8) with the suitable change of the gauge coupling constants. So, the axion coupling C with the gauge bosons is generally defined by the scale F_a as $C \propto F_a^{-1}$. Axion–photon interaction can lead to axion–photon conversion in electromagnetic fields, e.g. in magnetic fields

of pulsars and magnetars, or in appearance of light penetrating the wall due to axion conversion to photon in a shielded radi-frequency cavity. At the nonzero mass of axion m_α this interaction should lead to the two-photon decay $\alpha \to \gamma\gamma$ with the lifetime that is given in the complete analogy with the similar decay of neutral pion as

$$\tau(\alpha \to \gamma\gamma) = \frac{64\pi^2}{m_\alpha^3 F_a} \tag{9}$$

Since neutral pion has the similar interaction with gluons, owing to the non-vanishing coupling to the color anomaly, one can express the axion mass in terms of the scale F_a and the respective parameters of pion, $f_\pi \approx m_{pi}$ and m_π, so that the mass of axion m_α is defined by this scale as

$$m_\alpha = A_\alpha \frac{f_\pi}{F_a} m_\pi, \tag{10}$$

where the constant A_α depends on the choice of the specific axion model.

The scale F_a also determines the strength h of the axion interaction with fermions $h \propto F_a^{-1}$.

The simplest variant of the axion model was the model of Weinberg–Wilczek axion [33,34], in which the scale F_a coincided with the scale v of the electroweak symmetry breaking. This model was excluded by the combination of experimental and as trophysical constraints (see review in [35,36]). The analysis of these constraints lead to very high estimation of the lower limit for the axion scale $F_a \gg v$. Thus, the scale F_a should be related to some new high-energy scale in the particle theory. At this scale axion interactions turn out to be elusive, thus making the axion invisible.

In the most general case, the Lagrangian of the invisible axion interaction with fermions (quarks and leptons) and photons has the form

$$L = h_{ij}\alpha\bar{f}_i(\sin\beta_{ij} + i\gamma_5\cos\beta_{ij})f_j + C_{\alpha\gamma\gamma}\alpha F\mu\nu\tilde{F}^{\mu\nu}, \tag{11}$$

where $i, j = 1, 2, 3$ are the indices of fermion families and the constants β_{ij}, $h_{ij} \propto F_a^{-1}$ and $C_{\alpha\gamma\gamma} \propto F_a^{-1}$ depend on the choice of the axion model.

In the model by Dine–Fisher–Srednicki–Zhitnicki (DFSZ) [37,38] non-diagonal axion couplings to fermions are absent and the Yukawa constants of fermion interactions with the DFSZ axion $h \propto m_f$, where m_f is the mass of fermion. Therefore both quarks and leptons have direct couplings to axion in this model. The latter is not the case in the model of hadronic axion of Kim–Shifman–Vainshtein–Zakharov (KSVZ) [39,40]. The KSVZ axion has no direct couplings to quarks and leptons. Thus it does not interact with leptons and its interaction with quarks is induced by the axion mixing with the neutral pion π^0. The model of archion that shares the property of axion with the properties of other Pseudo-Nambu–Glodstone (PNG) bosons — familon and majoron is based on the gauge model of broken family symmetry, which we discuss in the next Section 2.6.

PNG bosons appear in the BSM theory in the result of spontaneous breaking of a global symmetry and axion is an example of a such a boson, originated from spontaneous breaking of the global $U(1)_{PQ}$ symmetry Peccei–Quinn. If the symmetry is anomaly-free, the corresponding Nambu–Goldstone boson in massless. If the anomalies are not canceled the boson acquires a nonzero mass and becomes pseudo-Nambu–Goldstone boson. Typically such $U(1)_{PQ}$-type models involve two energy scales f and $\Lambda \ll f$ and the mass of these axion-like particles is no more determined by the Eq. (10) but is of the order of

$$m_{al} \sim \frac{\Lambda^2}{f}. \tag{12}$$

Lepton number nonconservation due to spontaneous breaking of the symmetry of lepton number results in existence of a PNG boson, called majoron. Spontaneous breaking of the symmetry of quark–lepton families leads to existence of PNG bosons, called familons.

2.6. BSM physics of the quark–lepton families

The problem of fermion families (generations) remains one of the central problems of the particle physics. The standard $SU(3) \times SU(2) \times U(1)$ gauge model is constructed in the framework of one fermion generation and does not contain any deep physical grounds for the existence and properties of the fermion families. Yukawa couplings are arbitrary in the SM and one has to input by hands their values for each fermion to reproduce the experimental data on their masses: one simply takes $h_f = m_f/v$ in the Eq. (3) .

The identity of quark and lepton families (see Fig. 1) relative to strong and electroweak interactions strongly suggests the existence of a "horizontal" symmetry between these families. The family symmetry should be broken in view to the observed hierarchy in the mass pattern of quarks and leptons. For 3 families, one can assume a global $SU(3)_F$ family symmetry and its spontaneous breaking can lead to 8 PNG bosons — familons.

Local gauge family symmetry involves horizontal gauge bosons that interact with Flavor Changing Neutral Currents (FCNC). Such transitions are strictly suppressed. It implies the mass of horizontal gauge bosons m_H to exceed by several orders of magnitude the mass of electroweak Z-boson mediating SM neutral current interaction: $m_H \gg m_Z$. Therefore the

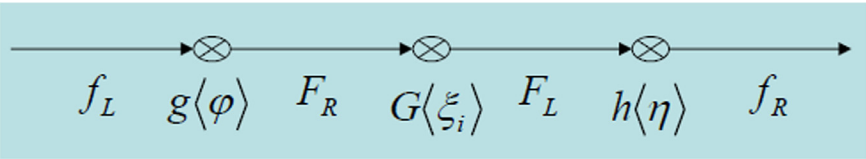

Fig. 5. Dirac see-saw mechanism of quark and lepton mass generation.

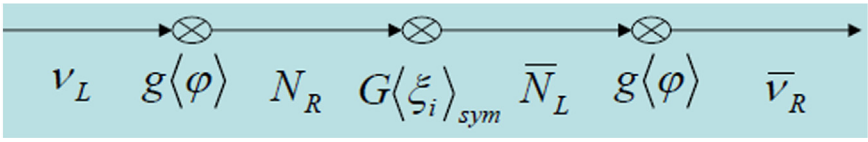

Fig. 6. Majorana see-saw mechanism of neutrino mass generation.

scale V_f of family symmetry breaking by vacuum expectation values of horizontal scalar Higgs bosons should be several orders of magnitude larger, than the electroweak scale v.

On the other hand, all the masses of quarks and leptons are within the electroweak scale v and their mass difference, if ascribed to family symmetry breaking, should be much less than the scale V_f. It involves rather complicated implementation of the broken family symmetry.

A possible solution for this problem was proposed in the framework of the Hypothesis of Horizontal Hierarchy (HHH) [41–43]. The simplest realization of the HHH invokes the introduction of additional superheavy fermions, acquiring their masses via direct coupling with horizontal scalars. The ordinary quark and lepton masses are induced by their "see-saw" mixing [43] with these heavy fermions and their mass matrices m_f have the form

$$m_f = \frac{\mu}{M_F} h_f v, \tag{13}$$

where $f = u, d, e$, M_F is the mass matrix of heavy fermions, $\mu = h_\eta V_\eta$ is determined by Yukawa coupling h_η to a singlet scalar field with vacuum expectation value V_η and h_f is Yukawa coupling of quarks and charged leptons to the electroweak Higgs boson. This mechanism is displayed in Fig. 5. Then the horizontal hierarchy is reflected in the mass hierarchy of quark–lepton families, while the absolute value of their masses is determined by the electroweak scale v. To preserve this hierarchy left-handed and right-handed fermion states should belong to different representations of the family symmetry group. It excludes orthogonal and vector-like gauge groups and in the case of three families leads to unique choice of chiral $SU(3)_F$ family symmetry, first proposed in [44] and considered in [41–43] (see also [45–47]).

To cancel the $SU(3)_F$ anomaly a heavy partner of neutrino N should be added. It makes possible to generate Majorana neutrino mass matrix

$$m_\nu = \frac{(h_\nu v)^2}{M_N}. \tag{14}$$

If $\mu = h_\eta V_\eta$ in Eq. (13) is much larger, than $h_\nu v$, the mass of neutrino is suppressed relative to the mass of the corresponding charged lepton by a factor $h_\nu v/\mu$. The mechanism of Majorana mass generation is displayed in Fig. 6. The natural choice of the horizontal scalar fields potential that contains only terms that can be induced by gauge and Yukawa interactions supports the additional global $U(1)_F$ symmetry making the family symmetry $SU(3)_F x U(1)_F$. The hierarchy of family masses is established by the hierarchy of symmetry breaking

$$SU(3)_F x U(1)_F \to SU(2)_F x U'(1) \to U''(1) \to I, \tag{15}$$

where I is the trivial group of identical transformation and the residual symmetries act on the heavy fermions that remain massless at each intermediate step of Eq. (15). Breaking of the last $U''(1)$ results in the existence of a pseudo-Nambu–Goldstone boson, α, named archion, having both flavor diagonal and flavor non-diagonal couplings with quarks and leptons and thus being familon of the singlet type [48,49]. $U''(1)$ symmetry can be identified with Peccei–Quinn symmetry, making archion a specific type of invisible axion, while its coupling to neutrino adds a property of a singlet majoron.

The inevitable consequences of this model are:

- the flavor-changing neutral transitions, related to archion and horizontal gauge bosons interactions;
- the existence of neutrino Majorana mass and of the neutrino mass hierarchy of different families;

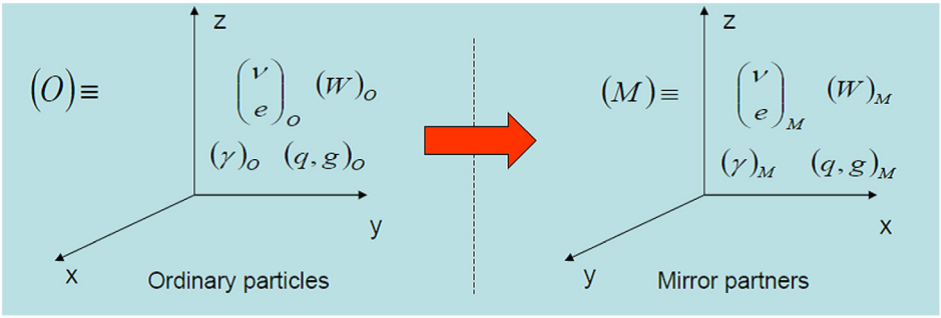

Fig. 7. Mirror partners of ordinary fermions and bosons.

- the instability of heavier neutrino relative to axion decay on lighter neutrino;
- the existence of metastable superheavy fermions.

The model can be tested using a combination of laboratory tests, such as:

- the search for neutrino mass,
- the search for neutrino oscillations,
- the search for double neutrinoless beta decay,
- the study of $K^o - \bar{K}^o$ and $B^o - \bar{B}^o$ transitions,
- the search for axion decays $\mu \to e\alpha$, $K \to \pi\alpha$, etc.

together with the analysis of its predicted cosmological and astrophysical effects.

The latter includes the study of archion emission effects on stellar evolution, investigation of primordial archion field and massive unstable neutrino effects on the dynamics of cosmological large scale structure formation, as well as the analysis of the mechanisms of inflation and baryogenesis, based on the hidden sector of this model.

If the condition that each quark–lepton family has the corresponding heavy fermion partner is relaxed, orthogonal, vector-like or discrete family symmetry is possible. However any explanation of the observed broken family symmetry inevitably involves new set of BSM particles and processes.

2.7. Mirror and shadow worlds

Mirror particles were proposed by T. D. Lee and C. N. Yang [50] to restore the equivalence of left- and right-handed co-ordinate systems in the presence of P- and C-violation in weak interactions. They should be strictly symmetric by their properties to their ordinary twins. After the discovery of CP-violation, it was shown by I. Yu. Kobzarev, et al. in Ref. [51] that mirror partners cannot be associated with antiparticles and should represent a new set of symmetric partners for ordinary quarks and leptons with their own strong, electromagnetic, and weak mirror interactions (see Fig. 7). It means that there should exist mirror quarks, bound in mirror nucleons by mirror QCD forces and mirror atoms, in which mirror nuclei are bound with mirror electrons by mirror electromagnetic interaction [52,53]. If gravity is the only common interaction for ordinary and mirror particles, mirror matter can be present in the universe in the form of elusive mirror objects, having symmetric properties with ordinary astronomical objects (gas, plasma, stars, planets, etc.), but causing only gravitational effects on ordinary matter [54,55].

Even in the absence of any other common interaction except for gravity, the observational data on primordial helium abundance and the upper limits on local dark matter seem to exclude mirror matter evolving in the universe in a fully symmetric way in parallel with the ordinary baryonic matter [56,57]. The symmetry in the cosmological evolution of mirror matter can be broken either by initial conditions [58,59] or by breaking mirror symmetry in the sets of particles and their interactions as it takes place in the shadow world [60,61], arising in the heterotic string model. We refer to Refs. [13,62,63] for a current review of mirror matter and its cosmology.

2.8. Unification of fundamental forces

The similarity in the description of the electromagnetic, weak and strong interactions in the standard model appeals for their unification.

In the grand unified (GUT) models, the gauge symmetry $SU(3)_c \otimes SU(2)_L \otimes U(1)$ of the standard model is embedded into the unifying group G_{GUT} of the grand unified gauge symmetry

$$G_{GUT} \supset SU(3)_c \otimes SU(2)_L \otimes U(1) \tag{16}$$

Quarks and leptons in this construction are placed in the same representation of the unifying group GauT, and the generators of the group related to lepto-quark transitions imply the existence of gauge bosons, mediating baryon and

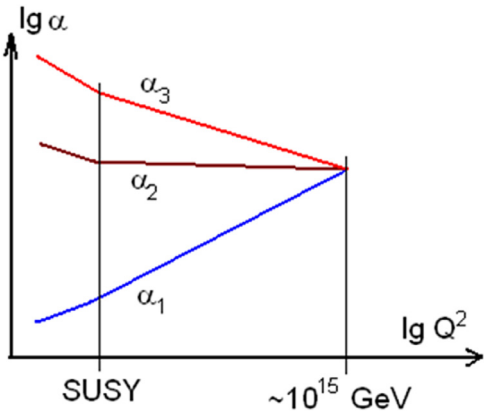

Fig. 8. Contribution of SUSY particles changes the momentum dependence of the running constants and provides intersection of all the three constants in one point.

lepton number non conserving processes. These processes can play a very important role in the mechanisms of generation of baryon excess in the initially baryon symmetric Universe. The simplest unifying group, which can completely embed the symmetry of the standard model is the $SU(5)$ group. The number of its generators is 24, so even in the simplest realization of grand unification one should assume the existence of 12 new gauge bosons in addition to 12 bosons mediating strong (8 gluons), weak (3 - W^+, W^- and Z bosons) and electromagnetic (photon) interactions.

In the $SU(5)$ gauge model these twelve new bosons mediate the processes violating baryon and lepton number conservation, such as proton decay. In particular, the proton decay to the channel $p \to \pi^0 + e^+$ was predicted in the $SU(5)$ gauge model with the lifetime $\tau_p \leq 10^{30} \div 10^{31}$ years that is excluded by the results of the experimental searches for proton decay. It implies the use of a larger embedding group of GUT symmetry. Moreover, all three curves, describing the energy dependencies of the SM gauge constants, do not intersect in one point, if the SM particle content does not change up to the GUT scale. To reach the intersection of all three curves in one point, one should involve an additional set of particles in the theory, such as the supersymmetric particles. The intersection of the three running constants due to the contribution of SUSY particles is displayed in Fig. 8.

In all the GUT models, unifying electromagnetism with other interactions within a compact group of symmetry, magnetic monopole solutions appear. These solutions follow from the topology of the GUT symmetry breaking. The GUT magnetic monopoles are stable topological defects, having the Dirac magnetic charge

$$g = \frac{\hbar c}{2e} \tag{17}$$

and the mass of the order of

$$m = \frac{\Lambda}{e}, \tag{18}$$

where Λ is the scale, at which electromagnetic $U(1)$ symmetry separates from the other interactions.

Taking $\Lambda \sim 10^{15}$ GeV of the order of the GUT scale, one obtains that the mass of the GUT magnetic monopole should be of the order of $m \sim 10^{16}$ GeV. It makes the production of such monopoles impossible at accelerators and in collisions of cosmic rays with ultra high energy. However, magnetic monopoles should have been produced, if the phase transition with GUT symmetry breaking took place at high temperature in the very early Universe. Their calculated primordial abundance turned out to be very high [64–66] and that lead to the serious problem of magnetic monopole overproduction. The solution of this problem implied the development of both cosmology and particle physics.

The problems of the minimal $SU(5)$-based unification lead to nonminimal GUT models that extend the embedding Eq. (16) of the gauge SM symmetry by additional symmetries. If rang $r > 4$ of such models (the number of conserved quantum numbers) is larger than the rang of SM, equal to 4, new conservation laws makes stable the lightest particles that possess these new quantum numbers.

In addition to new stable particles the pattern and nontrivial topology of GUT symmetry breaking can lead to a variety of topological defects other than magnetic monopoles.

In the case of spontaneously broken discrete symmetry, the two-dimensional topological defects – domain walls – should exist at the boundary of the degenerated vacua, labeled by the underlying discrete symmetry. The energy density per unit surface of the domain wall is determined by the scale Λ of the discrete symmetry breaking, being proportional to $\rho_w \propto \Lambda^3$.

If the continuous $U(1)$ symmetry is spontaneously broken, the one-dimensional defect (cosmic string) should exist as a result of symmetry breaking. The corresponding energy density per unit length is proportional to $\rho_s \propto \Lambda^2$, where Λ is the scale of the symmetry breaking.

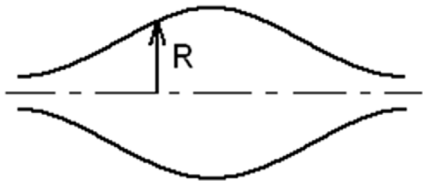

Fig. 9. Geometrical description of interactions can be illustrated by the analogy with a fluid moving along the tube of variable radius.

The combination of continuous and discrete symmetry breaking leads to more sophisticated types of topological defects, such as wall surrounded by strings predicted in the cosmology of invisible axion, which we discuss in 3.6.

In the models of unification, more extensive than the minimal SU(5) model, one can hope to find natural place for the physics of neutrino mass, for axion solution of strong CP violation in QCD, for supersymmetry and for mirror matter. Such unification can be related with unification of all the fundamental forces including gravity.

2.9. Unification of all the four fundamental forces, including gravity

Local supersymmetry involves local space–time transformations. It makes possible to unify weak, electromagnetic and strong interactions with gravity on the base of supergravity.

The models of supergravity are specified by the number of sets of supersymmetric partners and of different types of gravitino N. The $N = 1$ supergravity realizes the simplest case of a single gravitino. The maximal number of gravitino is present in the $N = 8$ supergravity. Supergravity has many attractive features [67]:

- it has SUSY unifying bosons and fermions,
- it automatically includes General Relativity (GR),
- it is the conservative extension of GR and field theory (without violating their basic principles), which restricts a number of independent coupling constants,
- SUSY Grand Unified Theories (GUTs) gives rise to the perfect unification of electro-weak and strong interactions,
- the spectrum of matter-coupled supergravities with spontaneously broken SUSY has the natural candidate for dark matter particle, given by the Lightest SUSY Particle (LSP),
- SUSY can be used to stabilize the fundamental scales, towards solving the hierarchy problem,
- SUSY results in cancellation of quadratic UV-divergences in quantum loops,
- some supergravity theories can be considered as the low-energy effective actions of superstring theories, i.e., in quantum gravity.

Supergravity involves the symmetry of space–time in the course of extension of the particle gauge symmetry. The opposite approach that determines particle gauge symmetry in terms of geometry of multi-dimensional space–time by extension of space–time symmetry comes back to the early ideas of 1920s by T.Kaluza [68] and O.Klein [69]. In the essence this approach assumes that metric tensor g_{MN} of $4+d$ dimensional space–time contain together with usual 4-dimensional components $g_{\mu\nu}$ the components that involve N extra dimensional coordinates, denoted by Latin indices m and n. The nondiagonal components $g_{\mu n}$ and $g_{m\nu}$ transform in 4 dimensions as 4-vectors, which can describe vector potentials of particle interactions, e.g. electromagnetic field. Such 'geometrical' description of interactions can be illustrated by the analogy with a fluid moving along the tube of variable radius displayed in Fig. 9. Acceleration and slowing down of the water flux moving in such a tube is interpreted by an observer in the longitudinal dimension as result of a force, acting on the water.

Practically all the main trends to the unification: gauge symmetry, multidimensional space–time, supergravity and mirror symmetry are combined on the basis of the string theory in superstring models. Strings are here the most fundamental elementary objects reduced to the effective quantum field theory in the four-dimensional space–time.

The following features made this approach widespread and popular [70]:

- Anomaly cancellation mechanism [71], which showed that supersymmetric gauge theories can be consistent in ten dimensions provided they are coupled to supergravity and the gauge group is either $SO(32)$ or $E_8 \otimes E_8'$. Any other group necessarily would give uncanceled gauge anomalies and hence inconsistency at the quantum level.
- The discovery of two superstring theories – called heterotic string theories – with precisely these gauge groups [72]
- The realization that the $E_8 \otimes E_8'$ heterotic string theory admits solutions in which six of the space dimensions form a Calabi–Yau space, and that this results in an effective theory in 4-dimensional space–time at low energies that can naturally embed supersymmetry and symmetry of the Standard model [73]

There are five distinct superstring theories with consistent weak coupling perturbation expansions, each in ten dimensions. Three of them, the*type I* theory and the two heterotic theories, have $N = 1$ supersymmetry in the ten-dimensional sense. Since the minimal 10d spinor is simultaneously Majorana and Weyl, this corresponds to 16 conserved

Fig. 10. Winding over the tube corresponds to the string configuration (19) which is stable relative to string intersections and has the mass, proportional to the radius of compactification R.

supercharges. The other two theories, called *type IIA* and *type IIB*, have N = 2 supersymmetry (32 supercharges) [74]. In the IIA case the two spinors have opposite handedness so that the spectrum is left–right symmetric (nonchiral). In the IIB case the two spinors have the same handedness and the spectrum is chiral. In studies of these five superstring theories it was largely proved, that there are consistent perturbation expansions of on-shell scattering amplitudes [70].

In such an approach, the fundamental constants of the quantum field theory are shown to be finite for one-loop quantum corrections. It may provide the quantitatively definite grounds for all the fundamental physics, but the problem is that such models have enormous variety of possible realizations of compactification and contain a very extensive hidden sector elusive for direct experimental probes. So, in the widely discussed heterotic string model, the initial $E_8 \otimes E'_8$ gauge symmetry, postulated in the 10 space–time-dimensional string model, assumes exact symmetry between the ordinary (E_8) and mirror (E'_8) worlds. The initial mirror symmetry is broken due to the combined action of compactification and gauge symmetry breaking, so that the shadow matter appears. The initially mirror partners lose the discrete symmetry with the corresponding ordinary particles.

In the 4-dimensional effective field model, to which the heterotic string model is reduced after compactification, the gauge symmetry of the ordinary matter comes from the E_8 symmetry, which is broken down to E_6 symmetry in order to compensate the effect of the compactification. Euler characteristics of compactified manifold defines the number of fermion multiplets that remain massless at the unification scale and thus define the number of quark–lepton families. This number of families can be 3, as needed to reproduce the structure of the Standard model. But this number may be also 4, involving a new quark–lepton family. The existence of fermions of the 4th family may avoid severe constraints on their contribution into the precisely measured SM parameters [75] or the Higgs boson width [76].

E_6 symmetry, embedding the SM symmetry has rang 6. It means that there can exist new conserved quantum numbers and new types of stable particles that possess them, such as quarks and leptons of the 4th family [77–79]. The extra E_6 gauge bosons mediate new types of particle interactions.

The ordinary matter is accompanied not only by new particles by the enormously large world of shadow particles and their interactions, corresponding to the (broken?) E'_8 gauge group.

Thus, even in the simplest realization of the superstring models, one faces the problem of test for E'_8 symmetry model of the shadow world. To understand the complexity of the problem, remind that there are 248 fundamental fermions and 248 gauge bosons in the E_8 group. Cosmological effects can provide some probes for their existence [60,61,80].

The mechanism of the gauge symmetry breaking in compactification onto Calaby–Yao manifolds or orbifolds, used in superstring models, implies homotopically stable solutions with the mass [81]

$$m \sim \frac{R}{\alpha'}, \tag{19}$$

where R is the radius of compactification and α' is the string tension. These objects are sterile relative to gauge interactions and may act on the ordinary matter by gravitation only. The dependence of these configuration on the radius of the compact dimension is displayed in Fig. 10.

BSM models involve new types of particles and interactions. Most of them correspond to superhigh energy scale which cannot be probed by direct methods of the experimental high energy physics and implies indirect tests. The theory of Big Bang Universe states that the super high energy physics phenomena should have naturally taken place at the very early stages of cosmological evolution. It makes cosmological consequences an important and in some cases unique probe for BSM physics.

3. Cosmological tracers of BSM physics

3.1. Big Bang cosmology

Cosmology studies the Universe as a whole. Stars and interstellar medium, galaxies and intergalactic space, clusters of galaxies and galaxy superclusters, surrounding giant voids, in which galaxies are not observed, exhibit strongly inhomogeneous distribution of luminous matter in the Universe. However at scales, exceeding the largest scale of cosmological structure one finds the distribution of matter to be almost homogeneous and isotropic.

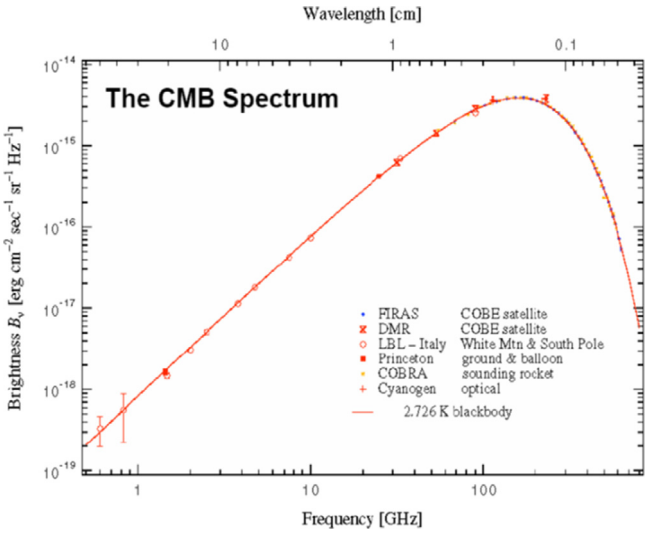

Fig. 11. Black body spectrum of CMB.

The simplest and reasonable conjecture is to consider homogeneous and isotropic cosmological model. Such model accounts for the presence of the matter in the modern Universe via the unique parameter — cosmological density ρ, which is the density of matter averaged over scales, exceeding the scale of the observed structure.

The discovery of other galaxies and the analysis of their luminosity lead to the discovery of systematic red shift in their spectra. Observed red shifts in spectra of distant galaxies, interpreted as the Doppler effect, correspond to recession of galaxies.

The recession velocity of a galaxy v is proportional to its distance r according to the Hubble law

$$v = Hr, \tag{20}$$

where the coefficient H with the dimension of the inverse time is the Hubble constant. The Hubble constant is constant in space, not in time. Having the dimension of the inverse time, it defines the time scale of cosmological expansion. The quantity, proportional to the inverse Hubble constant $1/H$, determines the time from the beginning of expansion t_U, called the age of the Universe. The Hubble constant determines the critical density

$$\rho_c = \frac{3H^2}{8\pi G} \tag{21}$$

that separates closed ($\rho > \rho_c$), flat ($\rho = \rho_c$) and open ($\rho < \rho_c$) cosmological models.

In the nonstationary Universe, all distances change proportionally to the scale factor $a(t)$.

Tracing back the history of the expanding Universe, one inevitably comes to the conclusion, that the physical conditions in the Universe should have changed with time. The modern picture of the Universe, full of galaxies and stars, should have appeared as a result of the evolution of expanding dense nearly homogeneous and isotropic plasma. Such plasma might have been in the state of cold degenerated matter, as it is now in white dwarfs and neutron stars.

The alternative idea of G.Gamov, that the primeval plasma was hot, found for more than three decades no observational confirmation, because it predicted the existence of relic thermal electromagnetic background radiation, which should be conserved in this model from the early hot stage of cosmological evolution.

The discovery in 1965 by Penzias and Wilson of the thermal electromagnetic radiation background favored the model of hot expanding Universe.

The existence of the black body radiation background with the Planck intensity distribution $F_{em}(\nu)$, given by

$$F_{em}(\nu) = \frac{2h\nu^3}{c^2}\frac{1}{\exp\left(\frac{h\nu}{kT}\right) - 1} \tag{22}$$

with the temperature $T = 2.7$ K proves the existence of early hot stages of cosmological evolution. The black body spectrum of the Cosmic Microwave Background radiation (CMB) is displayed in Fig. 11.

In the early Universe the role of thermal background radiation turns out to be dominant in the dynamics of expansion. The reason lies both in the high photon to baryon ratio and in the different dependence of the matter and radiation density on the scale factor. The density of matter ρ_m is inversely proportional to the cube of the scale factor, whereas in the case of radiation density one should also take into account the red shift in the average energy of photons.

The frequency of a photon, emitted in the early Universe, experiences the red shift z, defined as

$$z = \frac{\nu_{em}}{\nu_{abs}} - 1, \tag{23}$$

where ν_{em} and ν_{abs} are the frequencies of emitted and absorbed photon, respectively.

Similarly the black body spectrum is red shifted in the course of expansion, so that the radiation temperature $T(t)$ at some earlier time t is related to the modern temperature T_o as

$$T(t) = (1 + z(t))T_o = \frac{a(t = t_U)}{a(t)}T_o, \tag{24}$$

where the red shift z(t) is determined by the ratio of the scale factors, taken now at $t = t_U$ and at the moment t. With the account for the temperature decrease in the course of expansion, one obtains

$$\rho_\gamma \propto \epsilon_\gamma(t) \propto T(t)^4 \propto a(t)^{-4}. \tag{25}$$

Going back in time (to large red shifts and respectively small scale factors) we come inevitably to the period of radiation dominance, when the energy density of radiation dominated in the total cosmological density and in the dynamics of cosmological expansion.

At radiation-dominant stage the equation of state of the Universe is $p = 1/3\epsilon$ and the Einstein equations have the form

$$\left(\frac{\dot{a}}{a}\right)^2 = \frac{8\pi G}{3}\epsilon \tag{26}$$

$$\frac{\ddot{a}}{a} - \frac{4\pi G}{3}(\epsilon + 3p). \tag{27}$$

With the account for the relationship between pressure and density, given by the equation of state, one finds from these equations the time dependence of the scale factor at the radiation-dominant stage as

$$a(t) \propto t^{1/2} \tag{28}$$

On the basis of the known laws of atomic and nuclear physics, one may easily prove, that the baryon matter in the early Universe was in the state of plasma in equilibrium with radiation. One could follow the thermodynamic equilibrium conditions up to the earliest stages of the expansion, when the formal cosmological solution of the general relativity leads to singularity. The Planck time

$$t_{pl} = \left(\frac{G\hbar}{c^5}\right)^{1/2} = 510^{-44}\,\mathrm{s} \tag{29}$$

and the Planck length

$$l_{pl} = \left(\frac{G\hbar}{c^3}\right)^{1/2} = 1.510^{-33}\,\mathrm{cm} \tag{30}$$

are the natural border for the interpolation of the classical picture of the expansion, given by the general relativity. They define the time and length scales, at which the quantum effects should be involved into the space–time description.

The period $t_{pl} < t < 1\,\mathrm{s}$ is referred to as the very early Universe. Physical processes in this period are determined by the high-energy physics. In the lack of the information on the particle properties at superhigh energies, the old Big Bang scenario simply postulated the relativistic particle dominance in the very early Universe and the general trend of the cosmological evolution given by

$$\rho = \frac{3}{32\pi G t^2} = \frac{3}{32\pi}\frac{m_{pl}^2}{t^2}, \tag{31}$$

where m_{pl} is the Planck mass

$$m_{pl} = \left(\frac{\hbar c}{G}\right)^{1/2} = 210^{-5}\,\mathrm{g}. \tag{32}$$

Thermodynamics of the relativistic gas leads to the following relationship between the temperature T and cosmological time t

$$T = \frac{1}{\kappa^{1/4}}\left(\frac{45}{32\pi^3}\right)^{1/4}\left(\frac{m_{pl}}{t}\right)^{1/2}, \tag{33}$$

where κ is the effective number of species of relativistic particles with account for their statistical properties.

The thermodynamic equilibrium is established in any system, if the rate of processes, maintaining the equilibrium, exceeds the rate of the variation of the parameters of the system, such as its density, temperature etc.

In the expanding Universe the latter rate coincides with the rate of expansion.

If the time scale of the physical process exceeds the cosmological time scale, the system goes out of the equilibrium relative to the considered process. If the system contains several types of different particles, and there exist transitions between the particles of different type, the equilibrium distribution is established under the constant conditions. This distribution further does not change with time. If the parameters of the system change more rapidly, than the most rapid process, leading to the creation of particles of given type or to their annihilation, the particles of this type go out of the equilibrium with other particles.

In the old Big Bang scenario, the physical motivation for the simple thermodynamically equilibrium picture of the very early Universe was based on the fact that among the known particles only nucleons, electrons, photons and neutrino are of the cosmological significance. The cosmological effect of all other known particles is reduced to their contribution to the factor κ, when the considered species (quarks and charged leptons) are in equilibrium.

To the end of the first second of expansion the net result of the very early Universe in the old Big Bang scenario was practically reduced to the conditions of the equilibrium for the gas of photons, electron–positron and neutrino–antineutrinos pairs and to the small but fundamentally important admixture of nucleons with the concentration of the order of $n_b \sim 10^{-9} n_\gamma$. In that period the rate of expansion exceeds the rate of processes of weak interactions. It leads to decoupling of neutrino from plasma and radiation and to the freeze out of the neutron to proton ratio. In the first three minutes Big Bang Nucleosynthesis (BBN) took place, when the primordial chemical composition was formed. Its main components are hydrogen and helium-4, with weight fractions about 75% and 25%, respectively. There is small ($\sim 10^{-5}$) fraction of deuterium and helium-3 and much more smaller amount of lithium-7.

In the course of expansion radiation dominated stage was changed at t_{RD} by the matter domination. The gravitational instability of neutral gas evolves on this stage. Small matter density fluctuations grow, forming the observed structure of inhomogeneities, to which belong galaxies, their clusters and superclusters, stellar clusters, stars, etc.

The growth of density fluctuations lasts considerable time. Long after the moment t_{RD} matter expands almost homogeneously, and the growth of inhomogeneities is reduced to the growth of density contrasts between different regions.

Baryonic matter can participate in this process only after recombination of hydrogen — the dominant element of the Universe. Before recombination growth of density contrasts in plasma is hindered by radiation pressure, converting baryonic density fluctuations into the sound waves. The last photon scattering in plasma in the period of recombination is reflected in the modern anisotropy of the Cosmic Microwave Background radiation. This measured anisotropy corresponds to the amplitude of baryon density fluctuations, which is too small to provide sufficient growth of density fluctuations of the neutral gas to form the observed large scale structure of the Universe. It was one of the crucial quantitative inconsistencies of the Old Big Bang model.

Still, based on the physical laws, well proven in laboratories, the old Big Bang scenario was physically self consistent. Moreover, its main predictions for decades seemed to find qualitative confirmation in observations. The discovery of black body background radiation, measurements of the light element abundance seemed to confirm this picture [82,83].

However, the development of particle theory and the attempts to apply its prediction to cosmology initiated the critical analysis of the old Big Bang model and starting from late-1970s–early 1980s the theoretical analysis of the cosmological consequences of particle theory has uncovered the internal inconsistency of the old Big Bang model. The set of troubles, unrecoverable in the framework of the old Standard Big Bang model, was clarified in this analysis. It opened the way to the new Standard model of the Universe based on the inflationary models with baryosynthesis and non-baryonic dark matter. The physical grounds of these models lose the possibility of the direct experimental tests, and need special methods for their probe. It makes cosmological test of BSM physics more complicated, since it should use the cosmological framework that is based itself on the BSM physics.

3.2. Big Bang probes for new physics

The self-consistent treatment of cosmological consequences of BSM model would imply their analysis in the framework of cosmological scenario that is based on the considered model itself. However, the existing models are either not complete to provide the basis for all the necessary elements of cosmological scenario, or contain such a huge variety of various scenarios that makes impossible their complete analysis.

In the former case the model involves some minimal extension of the SM symmetry $SM \otimes G$, in which BSM physics is related to the additional symmetry G. In the latter case, like in the GUT models, heterotic string models or approach unifying spins and charges [84,85], the basic unifying symmetry U embeds the SM symmetry and contains in the result of in general multi-step U symmetry breaking $U \to SM \otimes G$ residual group of symmetry G in addition to the SM symmetry.

Cosmological consequences are related to the properties of additional or residual symmetry and to the pattern of the basic symmetry breaking. If the additional symmetry is strict, the lightest particles that possess it should be stable. The approximate symmetry results in metastable but sufficiently long-living particles. The pattern of symmetry breaking determines the energy scale Λ of new interactions and the masses $m \sim \Lambda$ of new particles.

In the early Universe transition to the phase of broken symmetry is reflected in cosmological phase transitions that can lead to creation of topological defects and primordial nonlinear structures.

The cosmological impact of these effects can influence the picture of the evolution of the Universe and result in the observable signatures of such influence.

3.3. Stable particles

New particles are characterized by their mass, m, cross section σ_m of their interaction with SM particles, cross section of their annihilation σ_a and lifetime, τ. At the temperature $T > m$ they were in the thermal equilibrium, provided that the rate of their interaction with plasma and radiation $n\sigma_m v$ and the rate of their pair annihilation $n_m\sigma_a v$ exceeds the rate of cosmological expansion $H \sim T^2/m_{Pl}$. Here $n \sim T^3$ and $n_m \sim T^3$ are, correspondingly, number densities of SM species and the considered particles and m_{Pl} is the Planck mass.

For a particle with the mass m, the particle physics time scale is $t \sim 1/m$, so in the particle world we refer to particles with lifetime $\tau \gg 1/m$ as metastable. To be of cosmological significance in the Big Bang Universe, a metastable particle should survive after $t \sim (m_{Pl}/m^2)$, when the temperature of the universe T fell below $T \sim m$, and particles go out of thermal equilibrium. It means that the particle lifetime should exceed

$$\tau \gg (m_{Pl}/m) \cdot (1/m), \tag{34}$$

and such a long lifetime should be explained by the existence of an (approximate) symmetry. From this viewpoint, cosmology is sensitive to the conservation laws reflecting strict or nearly strict symmetries of particle theory.

If the symmetry is strict, the particles are stable and, created in the early Universe, should be present in the modern time.

In the charge symmetric case, concentration of particles, n_m and antiparticles $\bar{n}_m = n_m$ in equilibrium is determined by the process of their pair creation and annihilation. At $T < m$, the rate of this process $n_m\sigma_a v$ becomes smaller than the rate of expansion $H = T^2/m_{Pl}$. Particles and antiparticles go out of equilibrium and their frozen out concentration n_m changes in the course of expansion $\propto a(t)^{-3}$, where $a(t)$ is the scale factor. At the present time the product of their mass m on primordial concentration n_m $\rho_m = mn_m$ determines their contribution into the modern cosmological density.

More weakly interacting and/or more light species decouple from plasma and radiation, being relativistic at $T \gg m$, when

$$n \cdot \sigma v \cdot t \sim 1$$

i.e., at

$$T_{dec} \sim (\sigma m_{Pl})^{-1} \gg m$$

After decoupling, these species retain their equilibrium distribution until they become non-relativistic at $T < m$. Conservation of partial entropy in the cosmological expansion links the modern abundance of these species to the number density of relic photons with the account for the increase of the photon number density due to the contribution of heavier ordinary particles, which were in equilibrium in the period of decoupling, as it is the case for primordial thermal neutrino background discussed in Section 2.2.

Right-handed neutrinos and left-handed antineutrinos, involved in the seesaw mechanism of neutrino mass generation, are sterile relative to ordinary weak interaction. If these species were in thermal equilibrium in the early universe, they should decouple much earlier than ordinary neutrinos in the period when there were much more particle species (leptons, quarks, gluons, etc.) in the equilibrium, what leads to the primordial abundance of sterile neutrinos much smaller than the ordinary ones. Therefore, cosmological constraints permit sterile neutrinos with mass in the keV range. We refer to the Ref. [86] for a recent review of models of sterile neutrinos and their possible effects.

The maximal temperature which is reached in inflationary universe is the reheating temperature, T_r, after inflation. So, the very weakly interacting particles with the annihilation cross section

$$\sigma < 1/(T_r m_{Pl})$$

as well as very heavy particles with mass

$$m \gg T_r$$

cannot be in thermal equilibrium, and the detailed mechanism of their production should be considered to calculate their primordial abundance.

In particular, gravitino with its semi-gravitational interaction could not be in the thermal equilibrium with plasma and radiation. Its production in rare processes of thermal particle collisions gives the example of freeze-in. This thermal freeze-in gravitino abundance is proportional to the reheating temperature T_r, which puts an upper limit on this temperature from constraints on primordial gravitino abundance [87–93].

BSM physics can provide the existence of new interactions, which only new particles possess. Historically, one of the first examples of such self-interacting dark matter was presented by the model of mirror and shadow matter, which we discussed in Section 2.7.

If new particles possess new y-charge, interacting with massless bosons or intermediate bosons with sufficiently small mass (y-interaction), for slow y-charged particles a Coulomb-like factor of "Sommerfeld–Gamov–Sakharov enhancement" [94–98] should be added in the annihilation cross section

$$C_y = \frac{2\pi\alpha_y/v}{1 - \exp(-2\pi\alpha_y/v)},$$

where v is relative velocity and α_y is the running gauge constant of the y-interaction. This factor may not be essential in the period of particle freezing out in the early universe (when v was only a few times smaller than c), but can cause strong enhancement in the effect of annihilation of nonrelativistic dark matter particles in the galaxy.

For weakly interacting massive particles (WIMPs) with mass $m \sim 100 \div 10^3$ GeV their contribution to the total density can explain the observed matter density of the Universe. Such particles start to dominate in the Universe at $T \geq 1$ eV and trigger development of gravitational instability and cosmological structure formation. WIMP gas is collisionless in the Galaxy, but rare processes of WIMP annihilation can produce fluxes of cosmic SM particles and put significant contribution to the galactic cosmic rays and gamma background as it was first found in [99]. It provides indirect searches for dark matter in cosmic ray experiments [100]. This effect is sensitive even to a tiny subdominant component of annihilating WIMPs [101].

The process of WIMP annihilation to ordinary particles, considered in t-channel, determines their scattering cross section on ordinary particles, and thus relates the primordial abundance of WIMPs to their scattering rate in ordinary matter. Forming a non luminous massive halo of our galaxy, WIMPs can penetrate terrestrial matter and scatter on nuclei in underground detectors. The strategy of direct WIMP searches implies the detection of recoil nuclei from this scattering.

The process inverse to the annihilation of WIMPs corresponds to their production in the collisions of ordinary particles. It should lead to effects of missing mass and energy–momentum, being the challenge of the experimental search for the production of dark matter candidates at accelerators—e.g., at the LHC.

If charge-symmetric stable particles (and their antiparticles) represent the only subdominant fraction of cosmological dark matter, a more detailed analysis of their distribution in space, of their condensation in galaxies, of their capture by stars, Sun, and Earth, as well as the effects of their interaction with matter and of their annihilation provides more sensitive probes for their existence.

In particular, fourth-generation hypothetical stable neutrinos with mass about 50 GeV should be the subdominant form of modern dark matter, contributing less than 0.1% to the total density [99,101]. However, direct experimental search for cosmic fluxes of weakly interacting massive particles (WIMPs) may be sensitive to existence of such components (see [102–110] and references therein). It was shown in Refs. [111–114] that annihilation of fourth generation neutrinos and their antineutrinos in the galaxy is severely constrained by the measurements of gamma-background, cosmic positrons, and antiprotons. Fourth generation neutrino annihilation inside the Earth should lead to the flux of underground monochromatic neutrinos of known types, which can be traced in the analysis of the already existing and future data of underground neutrino detectors [113,115–117].

New stable particles with electric charge and/or strong interaction can form anomalous atoms and be contained in ordinary matter as anomalous isotopes. For example, if the lightest fourth generation quark is stable, it can form stable charged hadrons, serving as nuclei of anomalous atoms of, for example, anomalous helium [118–123]. Therefore, stringent upper limits on anomalous isotopes, especially on anomalous hydrogen, put severe constraints on the existence of new stable charged particles. However, as we discuss in Section 6.1, stable even charged particles cannot only exist, but even dominate in cosmological dark matter, being effectively hidden in neutral "dark atoms" [124].

3.4. Metastable particles

Decaying particles with lifetime τ, exceeding the age of the universe (t_U, $\tau > t_U$) can be treated as stable. By definition, primordial stable particles survive to the present time and should be present in the modern universe. The net effect of their existence is given by their contribution to the total cosmological density. However, even the small effect of their decay can lead to a significant contribution to cosmic rays and gamma background [125]. Leptonic decays of dark matter are considered as a possible explanation of the cosmic positron excess, measured in the range above 10 GeV by PAMELA [126], FERMI/LAT [127], and AMS02 [128] (see Ref. [129] for a review of the AMS02 experiment).

The fact that particles are not absolutely stable means that the corresponding charge is not strictly conserved and the generation of particle charge asymmetry is possible, as is assumed for ordinary baryonic matter. At sufficiently strong particle annihilation cross section, excessive particles (antiparticles) can dominate in the relic density, leaving an exponentially small admixture of their antiparticles (particles) in the same way that primordial excessive baryons dominate over antibaryons in the baryon asymmetric universe. In this case, *asymmetric dark matter* does not lead to a significant effect of particle annihilation in the modern universe and can be searched for either directly in underground detectors or indirectly by effects of decay or condensation and structural transformations of, e.g., neutron stars (see Ref. [130] for recent review and references). If particle annihilation is not strong enough, primordial pairs of particles and antiparticles dominate over excessive particles (or antiparticles), and this case has no principle difference from the charge symmetric case. In particular, for very heavy charged leptons (with mass above 1 TeV), like "tera electrons" [131], discussed in Section 6.1, their annihilation due to electromagnetic interaction is too weak to provide effective suppression of primordial tera electron–positron pairs relative to primordial asymmetric excess [118].

Primordial unstable particles with a lifetime less than the age of the universe ($\tau < t_U$) cannot survive to the present time. However, if their lifetime is sufficiently large to satisfy the condition $\tau \gg (m_{Pl}/m) \cdot (1/m)$, their existence in the early universe can lead to direct or indirect traces [132].

Weakly interacting particles decaying to invisible modes can influence Large Scale Structure formation. Such decays prevent the formation of structure if they take place before the structure is formed. Invisible products of decays after

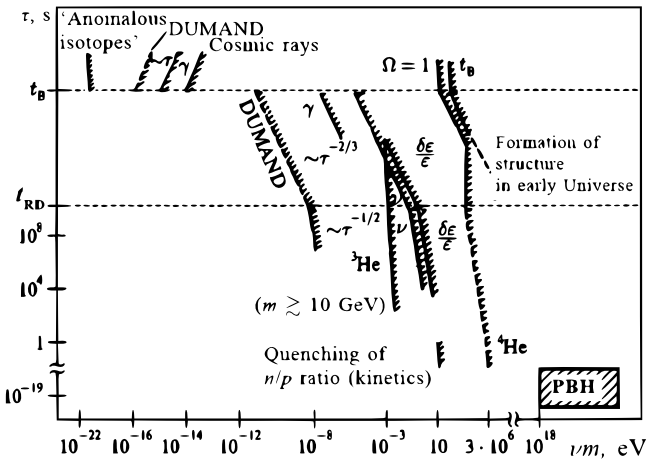

Fig. 12. Constraints on particles with mass m, lifetime τ and relative concentration r.

the structure is formed should contribute to the cosmological dark energy. The unstable dark matter [133–141] implied weakly interacting particles that form structure in the matter-dominated stage and then decay to invisible modes after the structure is formed.

The cosmological flux of decay products contributing to the cosmic and gamma ray backgrounds represents the direct trace of unstable particles [132,142]. If the decay products do not survive to the present time, their interaction with matter and radiation can cause indirect trace in the light element abundance [89–91,143] or in the fluctuations of thermal radiation [144]. Electromagnetic energy release in such decays causes distortions of the thermal spectrum of CMB

If the particle lifetime is much less than 1 s, the multi-step indirect traces are possible, provided that particles dominate in the universe before their decay. In the dust-like stage of their dominance, black hole formation takes place, and the spectrum of such primordial black holes traces the particle properties (mass, frozen concentration, lifetime) [145–147]. The particle decay in the end of the dust-like stage influences the baryon asymmetry of the universe. Cosmophenomenological chains link the predicted properties of even unstable new particles to the effects accessible in astronomical observations. Such effects may be important in the analysis of the observational data.

The set of constraints on particles with mass m, abundance $r = n_m/n_r$ and lifetime τ is given in Fig. 12.

3.5. Cosmological phase transitions

Parameters of new stable and metastable particles are also determined by a pattern of particle symmetry breaking. This pattern is reflected in a succession of phase transitions in the early Universe.

According to the Standard model there should have been two phase transitions:

- QCD phase transition at the confinement temperatureT_{QCD}, when hadronization took place and quark–gluon plasma transformed in the plasma of hadrons and
- The electroweak phase transition at T_{EW}, when the $SU(2)_L$x$U(1)$ symmetry was broken.

At high temperature T the potential (2) of the Higgs field ϕ acquired a high-temperature correction and had the form

$$V_H = \left(CT^2 - \frac{1}{2}m^2\right)\phi^2 + \frac{\lambda}{4}\phi^4. \tag{35}$$

Therefore at $T > T_{EW} \sim m/\sqrt{C}$ the $SU(2)_L$x$U(1)$ symmetry of the Standard model was restored and quarks, leptons and gauge bosons were massless.

Extension of symmetry in the BSM models and the mechanisms of its breaking can give rise to various forms of cosmological phase transitions and their observable consequences [148].

First order phase transitions proceed through bubble nucleation, which can result in black hole formation (see Refs. [149,150] for review and references). Phase transitions of the second order can lead to the formation of topological defects, such as walls, string, or monopoles. The observational data puts severe constraints on magnetic monopole [64, 66,151] and cosmic wall production [152], as well as on the parameters of cosmic strings [153,154]. The structure of cosmological defects can be changed in a succession of phase transitions. More complicated forms, like walls-surrounded-by-strings, can appear. Such structures can be unstable, but their existence can leave a trace in the nonhomogeneous distribution of dark matter and give rise to large scale structures of nonhomogeneous dark matter like *archioles* [155–157]. This effect should be taken into account in the analysis of the cosmological effects of weakly interacting slim particles (WISPs) (see Ref. [158] for current review) that can play the role of cold dark matter in spite of their small mass.

3.6. Structures of cosmological defects

A wide class of particle models possesses a symmetry breaking pattern, which can be effectively described by pseudo-Nambu–Goldstone (PNG) field and which corresponds to the formation of unstable topological defect structure in the early universe (see Ref. [150] for review and references). The Nambu–Goldstone nature in such an effective description reflects the spontaneous breaking of global U(1) symmetry, resulting in continuous degeneracy of vacua. The explicit symmetry breaking at smaller energy scale changes this continuous degeneracy by discrete vacuum degeneracy.

At high temperatures, such a symmetry breaking pattern implies the succession of second order phase transitions. In the first transition, continuous degeneracy of vacua leads – at scales exceeding the correlation length – to the formation of topological defects in the form of a string network; in the second phase transition, continuous transitions in space between degenerated vacua form surfaces: domain walls surrounded by strings. This last structure is unstable, but, as was shown in the example of the invisible axion [155–157], it is reflected in the large scale inhomogeneity of the distribution of the energy density of coherent PNG (axion) field oscillations. This energy density is proportional to the initial phase value, which acquires a dynamical meaning of the amplitude of the axion field, when axion mass is switched on as a result of the second phase transition.

The value of phase changes by 2π around string. This strong nonhomogeneity of phase leads to corresponding nonhomogeneity of the energy density of coherent PNG (axion) field oscillations. The usual argument (see Ref. [35] and references therein) is essential only at scales corresponding to the mean distance between strings. This distance is small, being on the order of the scale of the cosmological horizon in the period when PNG field oscillations start. However, since the nonhomogeneity of phase follows the pattern of the axion string network, this argument misses large scale correlations in the distribution of oscillations' energy density.

Indeed, numerical analysis of the string network (see the review in [159]) indicates that large string loops are strongly suppressed, and the fraction of about 80% of string length (corresponding to long loops) remains virtually the same in all large scales. This property is the other side of the well known scale invariant character of the string network. Therefore, the correlations of energy density should persist on large scales, as was revealed in Refs. [155–157].

The large scale correlations in topological defects and their imprints in primordial inhomogeneities is the indirect effect of inflation, if phase transitions take place after the reheating of the universe. Inflation provides, in this case, the equal conditions of phase transition, taking place in causally disconnected regions.

3.7. Primordial black holes

Any object of mass M can become a black hole, being put within its gravitational radius $r_g = 2GM/c^2$. At present time, black holes can be created only by a gravitational collapse of compact objects with mass more than about three solar mass [160,161]. It can be a natural end of massive stars or can result from the evolution of dense stellar clusters. However, in the early universe, there were no limits on the mass of BH.

Ya. B. Zeldovich and I. D. Novikov (see Ref. [162]) noticed that if cosmological expansion stops in some region, a black hole can be formed in this region within the cosmological horizon. This corresponds to strong deviation from general expansion and reflects strong inhomogeneity in the early universe. There are several mechanisms for such strong inhomogeneity and formation of Primordial Black Holes (PBHs) [163,164].

Here we outline the role of PBHs as a link in cosmoarcheological chain, connecting cosmological reflections of particle symmetry with observational data. We discuss the way in which the spectrum of PBHs reflects the properties of superheavy metastable particles and of phase transitions on inflationary and post-inflationary stages. We illustrate in Section 3.8 some mechanisms of PBH formation on the stage of dominance of superheavy particles and fields (Section 3.8.3) and from second order phase transition on the inflationary stage. An effective mechanism of BH formation during bubble nucleation provides a sensitive tool to probe the existence of cosmological first order phase transitions by PBHs (Section 3.9.2). The existence of stable remnants of PBH evaporation can strongly increase the sensitivity of such a probe, and we demonstrate this possibility in Section 3.10 on an example of gravitino production in PBH evaporation. Being formed within the cosmological horizon, PBHs seem to have masses much less than the mass of stars, constrained by the small size of the horizon in the very early universe.

However, if phase transition takes place in the inflationary stage, closed walls of practically any size can be formed, and their successive collapse can give rise to clouds of massive black holes, which can play the role of seeds for galaxies as discussed below in subsection Section 5.1.

3.8. PBHs from early dust-like stages

The possibility of forming a black hole is highly improbable in a homogeneous expanding universe, since it implies metric fluctuations of order 1. For metric fluctuations distributed according to Gaussian law with dispersion

$$\langle \delta^2 \rangle \ll 1 \tag{36}$$

a probability for fluctuation of order 1 is determined by an exponentially small tail of the high amplitude part of this distribution. This probability can be further suppressed in the case of non-Gaussian fluctuations [165].

In the universe with equation of state

$$p = \gamma\epsilon \tag{37}$$

with numerical factor γ being in the range

$$0 \leq \gamma \leq 1 \tag{38}$$

the probability of forming a black hole from fluctuations within the cosmological horizon is given by [166]

$$W_{PBH} \propto \exp\left(-\frac{\gamma^2}{2\langle\delta^2\rangle}\right) \tag{39}$$

This provides the exponential sensitivity of the PBH spectrum to the softening of the equation of state in the early universe ($\gamma \rightarrow 0$) or to the increase of ultraviolet part of the spectrum of density fluctuations ($\langle\delta^2\rangle \rightarrow 1$). These phenomena can appear as a cosmological consequence of particle theory.

3.8.1. Dominance of superheavy particles in the early universe

Superheavy particles cannot be directly studied at accelerators. If they are stable, their existence can be probed by cosmological tests, but there is no direct link between astrophysical data and the existence of superheavy metastable particles with lifetime $\tau \ll 1s$. It was first noticed in Ref. [146] that the dominance of such particles in the universe before their decay at $t \leq \tau$ can result in the formation of PBHs, remaining in the universe after the particles decay and keeping some information on particle properties in their spectrum. This provided (though indirect) a possibility to probe the existence of such particles in astrophysical observations. Even the absence of observational evidence for PBHs is important. It puts restrictions on the allowed properties of superheavy metastable particles, which might form such PBHs on a stage of particle dominance, and thus constrains the parameters of models predicting these particles.

After reheating, at

$$T < T_0 = rm \tag{40}$$

particles with mass m and relative abundance $r = n/n_r$ (where n is the frozen out concentration of particles and n_r is the concentration of relativistic species) must dominate in the universe before their decay. Dominance of these nonrelativistic particles at $t > t_0$, where

$$t_0 = \frac{m_{pl}}{T_0^2} \tag{41}$$

corresponds to a dust-like stage with equation of state $p = 0$, at which particle density fluctuations grow as

$$\delta(t) = \frac{\delta\rho}{\rho} \propto t^{2/3} \tag{42}$$

and the development of gravitational instability results in the formation of gravitationally-bound systems which decouple at

$$t \sim t_f \approx t_i\delta(t_i)^{-3/2} \tag{43}$$

from general cosmological expansion, when $\delta(t_f) \sim 1$ for fluctuations entering the horizon at $t = t_i > t_0$ with amplitude $\delta(t_i)$.

The formation of these systems can result in black hole formation, either immediately after the system decouples from expansion or as a result of the evolution of the initially formed nonrelativistic gravitationally-bound system.

3.8.2. Direct PBH formation

If density fluctuation is especially homogeneous and isotropic, it directly collapses to BH as soon as the amplitude of fluctuation grows to 1 and the system decouples from expansion. A probability for direct BH formation in the collapse of such homogeneous and isotropic configurations gives minimal estimation of BH formation in the dust-like stage.

This probability was calculated in Ref. [146] with the use of the following arguments. In the period $t \sim t_f$, when fluctuation decouples from expansion, its configuration is defined by averaged density ρ_1, size r_1, deviation from sphericity s, and by inhomogeneity u of internal density distribution within the fluctuation. Having decoupled from expansion, the configuration contracts and the minimal size to which it can contract is

$$r_{min} \sim sr_1 \tag{44}$$

being determined by a deviation from sphericity

$$s = \max\{|\gamma_1 - \gamma_2|, |\gamma_1 - \gamma_2|, |\gamma_1 - \gamma_2|\} \tag{45}$$

where γ_1, γ_2, and γ_3 define a deformation of configuration along its three main orthogonal axes. It was first noticed in Ref. [146] that in order to form a black hole as a result of such a contraction it is sufficient that the configuration returns to the size

$$r_{min} \sim r_g \sim t_i \sim \delta(t_i) r_1 \tag{46}$$

which had the initial fluctuation $\delta(t_i)$ when it entered the horizon at cosmological time t_i. If

$$s \leq \delta(t_i) \tag{47}$$

the configuration is sufficiently isotropic to concentrate its mass in the course of collapse within its gravitational radius, but such a concentration also implies sufficient homogeneity of configuration. Density gradients can result in gradients of pressure, which can prevent collapse to BH. This effect does not take place for the contracting collisionless gas of weakly interacting massive particles, but due to the inhomogeneity of collapse, the particles which have already passed the caustics can free stream beyond the gravitational radius before the whole mass is concentrated within it. Collapse of nearly spherically symmetric dust configuration is described by the Tolman solution. Its analysis [145,147,167,168] has provided a constraint on the inhomogeneity $u = \delta\rho_1/\rho_1$ within the configuration. It was shown that for both collisionless and interacting particles, the condition

$$u < \delta(t_i)^{3/2} \tag{48}$$

is sufficient for the configuration to contract within its gravitational radius.

The probability of direct BH formation is then determined by a product of probability for sufficient initial sphericity W_s and homogeneity W_u of configuration, which is determined by the phase space for such configurations. In a calculation of W_s, one should take into account that the condition (47) implies five conditions for independent components of the tensor of deformation before its diagonalization (two conditions for three diagonal components to be close to each other, and three conditions for nondiagonal components to be small). Therefore, the probability of sufficient sphericity is given by [145–147,167,168]

$$W_s \sim \delta(t_i)^5 \tag{49}$$

and together with the probability for sufficient homogeneity

$$W_u \sim \delta(t_i)^{3/2} \tag{50}$$

results in the strong power-law suppression of probability for direct BH formation

$$W_{PBH} = W_s \cdot W_u \sim \delta(t_i)^{13/2} \tag{51}$$

Though this calculation was originally done in Refs. [145–147,167,168] for Gaussian distribution of fluctuations, it does not imply a specific form of the high amplitude tail of this distribution, and thus should not change strongly in a case of non-Gaussian fluctuations [165].

The mechanism [12,13,145–147,167,168] is effective for the formation of PBHs with mass in an interval

$$M_0 \leq M \leq M_{bhmax} \tag{52}$$

The minimal mass corresponds to the mass within the cosmological horizon in the period $t \sim t_0$, when particles start to dominate in the universe and it is equal to [12,13,145–147,167,168]

$$M_0 = \frac{4\pi}{3}\rho t_0^3 \approx m_{pl}(\frac{m_{pl}}{rm})^2 \tag{53}$$

The maximal mass is indirectly determined by the condition

$$\tau = t(M_{bhmax})\delta(M_{bhmax})^{-3/2} \tag{54}$$

that fluctuation in the considered scale M_{bhmax}, entering the horizon at $t(M_{bhmax})$ with an amplitude $\delta(M_{bhmax})$, can manage to grow up to nonlinear stage, decouple, and collapse before particles decay at $t = \tau$. For scale-invariant spectrum $\delta(M) = \delta_0$, the maximal mass is given by [150]

$$M_{bhmax} = m_{pl}\frac{\tau}{t_{Pl}}\delta_0^{-3/2} = m_{pl}^2\tau\delta_0^{-3/2} \tag{55}$$

The probability, given by Eq. (51), is also appropriate for the formation of PBHs in the dust-like preheating stage after inflation [12,13,169]. The simplest example of such a stage can be given by the use of a model of a homogeneous massive scalar field [12,13]. Slow rolling of the field in the period $t \ll 1/m$ (where m is the mass of the field) provides a chaotic inflation scenario, while at $t > 1/m$, the field oscillates with period $1/m$. Coherent oscillations of the field correspond to an average over a period of oscillations in a dust-like equation of state $p = 0$, at which gravitational instability can develop. The minimal mass in this case corresponds to the Jeans mass of scalar field, while the maximal mass is also determined by the condition that fluctuation grows and collapses before the scalar field decays and reheats the universe.

The probability $W_{PBH}(M)$ determines the fraction of total density

$$\beta(M) = \frac{\rho_{PBH}(M)}{\rho_{tot}} \approx W_{PBH}(M) \tag{56}$$

corresponding to PBHs with mass M. For $\delta(M) \ll 1$, this fraction (given by Eq. (51)) is small. This means that the bulk of particles do not collapse directly into black holes, but form gravitationally-bound systems. The evolution of these systems can give a much larger amount of PBHs, but it strongly depends on particle properties.

3.8.3. Evolutional formation of PBHs

Superweakly interacting particles form gravitationally bound systems of collisionless gas, which resemble modern galaxies with collisionless gas of stars. Such a system can finally collapse to a black hole, but energy dissipation within it – and consequently, its evolution – is a relatively slow process [12,13,170]. The evolution of these systems is dominantly determined by the evaporation of particles, which gain velocities exceeding the parabolic velocity of the system. In the case of binary collisions, the evolution timescale can be roughly estimated [12,13,170] as

$$t_{ev} = \frac{N}{\ln N} t_{ff} \tag{57}$$

for a gravitationally-bound system of N particles, where the free fall time t_{ff} for a system with density ρ is $t_{ff} \approx (4\pi G\rho)^{-1/2}$. This time scale can be shorter due to collective effects in collisionless gas [171] and at large N can be on the order of

$$t_{ev} \sim N^{2/3} t_{ff} \tag{58}$$

However, since the free fall time scale for gravitationally-bound systems of collisionless gas is on the order of cosmological time t_f for the period when these systems are formed, even in the latter case the particles should be very long-living ($\tau \ll t_f$) to form black holes in such a slow evolutional process.

The evolutional time scale is much smaller for gravitationally-bound systems of superheavy particles interacting with light relativistic particles and radiation. Such systems have analogy with stars, in which evolution time scale is defined by energy loss by radiation. An example of such particles is superheavy color octet fermions of asymptotically free SU(5) model [172] or magnetic monopoles of GUT models. Having decoupled from expansion, frozen out particles and antiparticles can annihilate in gravitationally-bound systems, but detailed numerical simulation [173] has shown that annihilation cannot prevent the collapse of the majority of mass, and the timescale of collapse does not exceed the cosmological time of the period when the systems are formed.

3.9. PBH formation from cosmological phase transitions

3.9.1. PBHs from phase transitions in the inflationary stage

Scale non-invariant spectrum of fluctuations – in which the amplitude of small scale fluctuations is enhanced – can be another factor, increasing the probability of PBH formation. The simplest functional form of such a spectrum is represented by a blue spectrum with a power law dispersion

$$\left\langle \delta^2(M) \right\rangle \propto M^{-k} \tag{59}$$

with the amplitude of fluctuations growing at $k > 0$ to small M. The realistic account for the existence of other scalar fields together with inflaton in the period of inflation can give rise to spectra with distinguished scales, determined by the parameters of the considered fields and their interaction.

In the chaotic inflation scenario, interaction of a Higgs field ϕ with an inflaton η can give rise to phase transitions in the inflationary stage if this interaction induces positive mass term $+\frac{\nu^2}{2}\eta^2\phi^2$. When in the course of slow rolling, the amplitude of an inflaton decreases below a certain critical value $\eta_c = m/\nu$, the mass term in Higgs potential

$$V(\phi, \eta) = -\frac{m_\phi^2}{2}\phi^2 + \frac{\lambda_\phi}{4}\phi^4 + \frac{\nu^2}{2}\eta^2\phi^2 \tag{60}$$

changes sign, and phase transition takes place. Such phase transitions in the inflationary stage lead to the appearance of a characteristic spike in the spectrum of initial density perturbations. These spike-like perturbations, on scales that cross the horizon ($60 \geq N \geq 1$), e-fold before the end of inflation and reenter the horizon during the radiation or dust-like era and could in principle collapse to form primordial black holes. The possibility of such spikes in the chaotic inflation scenario was first pointed out in Ref. [174] and realized in Ref. [175] as a mechanism of PBH formation for the model of horizontal unification [133,176–178].

For the vacuum expectation value of a Higgs field

$$\langle\phi\rangle = \frac{m}{\lambda} = v \tag{61}$$

and $\lambda \sim 10^{-3}$, the amplitude δ of a spike in the spectrum of density fluctuations, generated in phase transition in the inflationary stage is given by [175]

$$\delta \approx \frac{4}{9s} \tag{62}$$

with

$$s = \sqrt{\frac{4}{9} + \kappa 10^5 \left(\frac{v}{m_{pl}}\right)^2} - \frac{3}{2} \tag{63}$$

where $\kappa \sim 1$.

If phase transition takes place at e-folding N before the end of inflation, the spike re-enters the horizon at the radiation dominance (RD) stage and forms a Black hole of mass

$$M \approx \frac{m_{Pl}^2}{H_0} \exp\{2N\} \tag{64}$$

where H_0 is the Hubble constant in the period of inflation.

If the spike re-enters the horizon in the matter dominance (MD) stage, it should form black holes of mass

$$M \approx \frac{m_{Pl}^2}{H_0} \exp\{3N\}. \tag{65}$$

3.9.2. First order phase transitions as a source of black holes in the early universe

First order phase transitions go through bubble nucleation, recalling the common example of boiling water. The simplest way to describe first order phase transitions with bubble creation in the early universe is based on a scalar field theory with two non-degenerated vacuum states. Being stable at a classical level, the false vacuum state decays due to quantum effects, leading to the nucleation of bubbles of true vacuum and their subsequent expansion [179]. The potential energy of the false vacuum is converted into the kinetic energy of bubble walls, thus making them highly relativistic in a short time. The bubble expands until it collides with another one. As it was shown in Refs. [180,181], a black hole may be created in a collision of several bubbles. The probability of the collision of two bubbles is much higher. The opinion of the absence of BHs in such processes was based on strict conservation of the original O(2,1) symmetry. As shown in Refs. [149,182,183], there are ways to break it. Firstly, radiation of scalar waves indicates increasing entropy, and hence the permanent breaking of the symmetry during bubble collision. Secondly, the vacuum decay due to thermal fluctuation does not possess this symmetry from the beginning. The investigations [149,182,183] have shown that BH can also be created with a probability of order unity in collisions of only two bubbles. This initiates an enormous production of BH that leads to essential cosmological consequences discussed below.

Inflation models ended by a first order phase transition hold a dignified position in the modern cosmology of the early universe (see for example [184–190]). The interest in these models is due to the fact that such models are able to generate the observed large-scale voids as remnants of the primordial bubbles for which the characteristic wavelengths are several tens of Mpc [189,190]. A detailed analysis of a first order phase transition in the context of extended inflation can be found in Ref. [191]. Hereafter, we will be interested only in a final stage of inflation when the phase transition is completed. Remember that a first order phase transition is considered completed immediately after establishing the true vacuum percolation regime. Such a regime is established approximately when at least one bubble per unit Hubble volume is nucleated. Accurate computation [191] shows that first order phase transition is successful if the following condition is valid:

$$Q \equiv \frac{4\pi}{9} \left(\frac{\Gamma}{H^4}\right)_{t_{end}} = 1 \tag{66}$$

Here Γ is the bubble nucleation rate. In the framework of first order inflation models, the filling of all space by true vacuum takes place due to bubble collisions, nucleated at the final moment of exponential expansion. The collisions between such bubbles occur when they have comoving spatial dimension less than or equal to the effective Hubble horizon H_{end}^{-1} at the transition epoch. If we take $H_0 = 100$ h km/s/Mpc in $\Omega = 1$ universe, the comoving size of these bubbles is approximately $10^{-21} h^{-1}$ Mpc. In the standard approach it is believed that such bubbles are rapidly thermalized without leaving a trace in the distribution of matter and radiation. However, in the previous section it was shown that for any realistic parameters of the theory, the collision between only two bubbles leads to BH creation with a probability close to 100% . The mass of this BH is given by [149,182,183]

$$M_{BH} = \gamma_1 M_{bub} \tag{67}$$

where $\gamma_1 \simeq 10^{-2}$ and M_{bub} is the mass that could be contained in the bubble volume at the epoch of collision in the condition of the full thermalization of bubbles. The discovered mechanism leads to a new direct possibility of PBH creation at the epoch of reheating in first order inflation models. In the standard picture, PBHs are formed in the early universe if density perturbations are sufficiently large, and the probability of PBH formation from small post-inflation

initial perturbations is suppressed (see Section 3.8). A completely different situation takes place at the final epoch of the first order inflation stage; namely, collision between bubbles of Hubble size in the percolation regime leads to copious PBH formation with masses

$$M_0 = \gamma_1 M_{end}^{hor} = \frac{\gamma_1}{2}\frac{m_{pl}^2}{H_{end}} \tag{68}$$

where M_{end}^{hor} is the mass of the Hubble horizon at the end of inflation. According to (67), the initial mass fraction of this PBH is given by $\beta_0 \approx \gamma_1/e \approx 6 \times 10^{-3}$. For example, for a typical value of $H_{end} \approx 4 \times 10^{-6}\, m_{pl}$, the initial mass fraction β is contained in PBHs with mass $M_0 \approx 1\,\mathrm{g}$.

In general, the Hawking evaporation of mini BHs [192] could give rise to a variety of possible end states. It is generally assumed that evaporation proceeds until the PBH vanishes completely [193], but there are various arguments against this proposal (see Refs. [194–197]). If one supposes that BH evaporation leaves a stable relic, then it is natural to assume that it has a mass of order $m_{rel} = km_{pl}$, where $1 \leq k \leq 10^2$. We can investigate the consequences of PBH formation at the percolation epoch after first order inflation, supposing that the stable relic is a result of its evaporation. As it follows from the above consideration, the PBHs are preferentially formed with a typical mass M_0 at a single time t_1. Hence, the total density ρ at this time is

$$\rho(t_1) = \rho_\gamma(t_1) + \rho_{PBH}(t_1) = \frac{3(1-\beta_0)}{32\pi t_1^2} m_{pl}^2 + \frac{3\beta_0}{32\pi t_1^2} m_{pl}^2 \tag{69}$$

where β_0 denotes the fraction of the total density corresponding to PBHs in the period of their formation t_1. The evaporation time scale can be written in the following form

$$\tau_{BH} = \frac{M_0^3}{g_* m_{pl}^4} \tag{70}$$

where g_* is the number of effective massless degrees of freedom.

Let us derive the density of PBH relics. There are two distinct possibilities to consider.

The universe is still radiation dominated (RD) at τ_{BH}. This situation will hold if the following condition is valid: $\rho_{BH}(\tau_{BH}) < \rho_\gamma(\tau_{BH})$. It is possible to rewrite this condition in terms of Hubble constant at the end of inflation

$$\frac{H_{end}}{m_{pl}} > \beta_0^{5/2} g_*^{-1/2} \simeq 10^{-6} \tag{71}$$

Taking the present radiation density fraction of the universe to be $\Omega_{\gamma_0} = 2.5 \times 10^{-5} h^{-2}$ (h being the Hubble constant in the units of $100\,\mathrm{km\,s^{-1}\,Mpc^{-1}}$), and using the standard values for the present time and time when the density of matter and radiation become equal, we find the contemporary densities fraction of relics

$$\Omega_{rel} \approx 10^{26} h^{-2} k \left(\frac{H_{end}}{m_{pl}}\right)^{3/2} \tag{72}$$

It is easily to see that relics overclose the universe ($\Omega_{rel} \gg 1$) for any reasonable k and $H_{end} > 10^{-6}\, m_{pl}$.

The second case takes place if the universe becomes PBHs dominated at period $t_1 < t_2 < \tau_{BH}$. This situation is realized under the condition $\rho_{BH}(t_2) < \rho_\gamma(t_2)$, which can be rewritten in the form

$$\frac{H_{end}}{m_{pl}} < 10^{-6} \tag{73}$$

The present day relics density fraction takes the form

$$\Omega_{rel} \approx 10^{28} h^{-2} k \left(\frac{H_{end}}{m_{pl}}\right)^{3/2} \tag{74}$$

Thus, the universe is not overclosed by relics, only if the following condition is valid

$$\frac{H_{end}}{m_{pl}} \leq 2 \times 10^{-19} h^{4/3} k^{-2/3} \tag{75}$$

This condition implies that the masses of PBHs created at the end of inflation have to be larger then

$$M_0 \geq 10^{11}\,\mathrm{g} \cdot h^{-4/3} \cdot k^{2/3} \tag{76}$$

On the other hand, there are a number of well-known cosmological and astrophysical limits [198–204] which prohibit the creation of PBHs in the mass range (76) with initial fraction of mass density close to $\beta_0 \approx 10^{-2}$.

So, one has to conclude that the effect of the false vacuum bag mechanism of PBH formation makes the coexistence of stable remnants of PBH evaporation with the first order phase transitions at the end of inflation impossible.

3.10. PBH evaporation as universal particle accelerator

Presently, there is no observational evidence proving the existence of PBHs. However, even the absence of PBHs provides a very sensitive theoretical tool to study the physics of the early universe. PBHs represent a nonrelativistic form of matter, and their density decreases with scale factor a as $\propto a^{-3} \propto T^3$, while the total density is $\propto a^{-4} \propto T^4$ in the period of radiation dominance (RD). Being formed within the horizon, a PBH of mass M can be formed not earlier than at

$$t(M) = \frac{M}{m_{pl}} t_{pl} = \frac{M}{m_{pl}^2} \tag{77}$$

If they are formed in the RD stage, the smaller the masses of PBHs, the larger becomes their relative contribution to the total density in the modern MD stage. Therefore, even the modest constraint for PBHs of mass M on their density

$$\Omega_{PBH}(M) = \frac{\rho_{PBH}(M)}{\rho_c} \tag{78}$$

in units of critical density $\rho_c = 3H^2/(8\pi G)$ from the condition that their contribution $\alpha(M)$ into the total density

$$\alpha(M) \equiv \frac{\rho_{PBH}(M)}{\rho_{tot}} = \Omega_{PBH}(M) \tag{79}$$

for $\rho_{tot} = \rho_c$ does not exceed the density of dark matter

$$\alpha(M) = \Omega_{PBH}(M) \leq \Omega_{DM} = 0.23 \tag{80}$$

converts into a severe constraint on this contribution

$$\beta \equiv \frac{\rho_{PBH}(M, t_f)}{\rho_{tot}(t_f)} \tag{81}$$

in the period t_f of their formation. If formed in the RD stage at $t_f = t(M)$ (given by (77)), which corresponds to the temperature $T_f = m_{pl}\sqrt{m_{pl}/M}$, PBHs contribute to the total density in the end of the RD stage at t_{eq}, corresponding to $T_{eq} \approx 1$ eV, by a factor of $a(t_{eq})/a(t_f) = T_f/T_{eq} = m_{pl}/T_{eq}\sqrt{m_{pl}/M}$ larger than in the period of their formation. The constraint on $\beta(M)$, following from Eq. (80) is then given by

$$\beta(M) = \alpha(M)\frac{T_{eq}}{m_{pl}}\sqrt{\frac{M}{m_{pl}}} \leq 0.23\frac{T_{eq}}{m_{pl}}\sqrt{\frac{M}{m_{pl}}} \tag{82}$$

The possibility of PBH evaporation, revealed by S. Hawking [192], strongly influences the effects of PBHs. In the strong gravitational field near the gravitational radius r_g of PBH, a quantum effect of the creation of particles with momentum $p \sim 1/r_g$ is possible. Due to this effect, PBHs turn out to be a black body source of particles with temperature (in the units $\hbar = c = k = 1$)

$$T = \frac{1}{8\pi GM} \approx 10^{13}\ \text{GeV}\frac{1\ \text{g}}{M} \tag{83}$$

The BH evaporation timescale is $\tau_{BH} \sim M^3/m_{pl}^4$ (see Eq. (70) and discussion in previous section), and at $M \leq 10^{14}$ g is less than the age of the universe. Such PBHs cannot survive to the present time, and their magnitude Eq. (80) should be re-defined and has the meaning of contribution to the total density in the moment of PBH evaporation. For PBHs formed in the RD stage and evaporated in the RD stage at $t < t_{eq}$, the relationship Eq. (82) between $\beta(M)$ and $\alpha(M)$ is given by [145,205]:

$$\beta(M) = \alpha(M)\frac{m_{pl}}{M} \tag{84}$$

The relationship between $\beta(M)$ and $\alpha(M)$ has a more complicated form if PBHs are formed in early dust-like stages [12,145,167,206], or if such stages take place after PBH formation [12,206]. The relative contribution of PBHs to total density does not grow in the dust-like stage, and the relationship between $\beta(M)$ and $\alpha(M)$ depends on the details of a considered model. Minimal model independent factor $\alpha(M)/\beta(M)$ follows from the account for enhancement, taking place only during the RD stage between the first second of expansion and the end of the RD stage at t_{eq}, since radiation dominance in this period is supported by observations of light element abundance and the spectrum of CMB [12,145,167,206].

Effects of PBH evaporation make astrophysical data much more sensitive to the existence of PBHs. Constraining the abundance of primordial black holes can lead to invaluable information on cosmological processes, particularly as they are probably the only viable probe for the power spectrum on very small scales which remain far from the Cosmological Microwave Background (CMB) and Large Scale Structures (LSS) sensitivity ranges. To date, only PBHs with initial masses between $\sim 10^9$ g and $\sim 10^{16}$ g have led to stringent limits (see Refs. [145,195,207,208]) from consideration of the entropy

per baryon, the deuterium destruction, the ^{4}He destruction, and the cosmic-rays currently emitted by the Hawking process [192]. The existence of light PBHs should lead to important observable constraints, either through the direct effects of the evaporated particles (for initial masses between 10^{14} g and 10^{16} g) or through the indirect effects of their interaction with matter and radiation in the early universe (for PBH masses between 10^9 g and 10^{14} g). In these constraints, the effects taken into account are those related to known particles. However, since the evaporation products are created by the gravitational field, any quantum with a mass lower than the black hole temperature should be emitted, independently of the strength of its interaction. This could provide a copious production of superweakly interacting particles that cannot be in equilibrium with the hot plasma of the very early universe. This makes evaporating PBHs a unique source of all the species which can exist in the universe.

Following Refs. [12,13,132,206] and [209,210] (but in a different framework and using more stringent constraints), limits on the mass fraction of black holes at the time of their formation ($\beta \equiv \rho_{PBH}/\rho_{tot}$) were derived in Ref. [211] using the production of gravitinos during the evaporation process. Depending on whether gravitinos are expected to be stable or metastable, the limits are obtained using the requirement that they do not overclose the universe and that the formation of light nuclei by the interactions of ^{4}He nuclei with nonequilibrium flux of D,T, ^{3}He and ^{4}He does not contradict the observations. This approach is more constraining than the usual study of photo-dissociation induced by photons–photinos pairs emitted by decaying gravitinos. This opened a new window for the upper limits on β below 10^9 g, and correspondingly on various mechanisms of PBH formation [211].

4. BSM physics of the modern cosmology

It followed from the old Big Bang Scenario that the early cosmological evolution should have taken place at superhigh temperatures. This conjecture made the conditions in the very early Universe dependent on the laws of superhigh-energy physics. Our modern knowledge of these laws is based on the predictions of particle theory. Thus, the development of particle theory implies natural influence on the picture of the very early Universe. In principle, all cosmologically significant phenomena, predicted by particle theory, can find their place in the history of the Universe.

Since the true theory of superhigh-energy physics is not developed yet, we can only make some reasonable guess on the phenomena that should exist in cosmology. The development of particle theory and its application to the Big Bang model found at least three phenomena, which are widely accepted as being necessary in the Big Bang scenario both on esthetical and practical reasons. It led to the change of the cosmological paradigm. The modern Big Bang model is now generally referred to as the inflational scenario with baryosynthesis and dark matter.

The development of this scenario offers the exciting possibility to explain the main cosmological parameters by physical mechanisms. So, the choice of open, closed or flat cosmological model is related to the mechanism of inflation. In the simplest cases, this mechanism leads to the prediction of a flat Universe with

$$\Omega = 1. \tag{85}$$

The observed baryon-to-photon ratio is considered as a result of baryosynthesis, defining the modern baryon density.

The difference between the modern total and baryon density is ascribed to the nonbaryonic dark matter. In the simplest case, the dark matter density is determined by the mass and the concentration of frozen out weakly interacting particles. The attractive idea to determine cosmological parameters through the parameters of particles and fields is not the only advantage of the new paradigm. Inflation, baryosynthesis and dark matter recover internal inconsistencies of Big Bang cosmology.

However,- the price is the unknown physical grounds and the wide variety of possible realizations on the base of different approaches. Our hope to remove this ambiguities is related to cosmoparticle physics. Assuming that the inflationary baryon-asymmetrical cosmology with the nonbaryonic dark matter is more realistic, than Gamow's original Big Bang scenario, one faces the problem of observational evidences, specifying the choice of the inflationary model, the mechanism of baryosynthesis and with the proper form of nonbaryonic dark matter.

4.1. Inflation

Inflation is the necessary element of cosmological picture. Inflationary models explain, why the Universe expands. They provide solution for horizon, flatness, magnetic monopole, etc., problems [212,213]. The solution is based on superluminous expansion, which takes place in the case of the cosmological equation of state

$$p < -\frac{1}{3}\epsilon. \tag{86}$$

Under the condition (86), the acceleration in the cosmological equation

$$\frac{\ddot{a}}{a} = -\frac{4\pi G}{3c^2}(\epsilon + 3p) \tag{87}$$

is positive and the formal solution for the law of expansion is given by

$$a(t) \propto \exp\left(\int H dt\right) \tag{88}$$

where H is defined from the Eq. (26) as

$$\frac{\dot{a}}{a} = H = \sqrt{\frac{8\pi G\epsilon}{3c^2}}. \tag{89}$$

Neither the matter, nor the radiation dominance can lead to the equation of state with the negative pressure. One needs some hypothetical phenomena to occur in the very early Universe, inducing unstable negative pressure stage of cosmological evolution. The simplest possibility, mentioned in [214,215], was first considered in [216,217]. It assumed the initial state of the cosmological expansion to be maximally symmetric in space–time. It corresponds to the De Sitter vacuum equation of state given by

$$p = -\epsilon = -\Lambda. \tag{90}$$

The time dependence of the scale factor is then given by the exponential law $a(t) \propto \exp(Ht)$ with

$$H = \sqrt{\frac{8\pi G\epsilon}{3c^2}}. \tag{91}$$

Bugrii and Trushevsky [218] found the possibility for the exponential stage of expansion in the hadron stage but the conditions they assumed were not supported by the hadron physics based on QCD.

A. Starobinsky has noticed that quantum corrections to the gravitational field can induce R^2 term in gravitational lagrangian, which naturally leads to exponential expansion [219–221]

D. Kazanas has drawn attention to a possibility of exponential expansion in the cosmological phase transition, associated with spontaneous symmetry breaking [222].

However, the general clear understanding that inflation is necessary both for cosmology and particle theory, came only after the work by A. Guth [212]. Inspired by the solution of the cosmological GUT magnetic monopole overproduction problem, this work has stipulated in the transparent form the list of internal inconsistencies of the old Big Bang model to be removed by inflation. They are:

- The horizon problem, which is related to the remarkable homogeneity of the Universe within the modern cosmological horizon originated from different initially causally disconnected regions.
- In the case of a non-flat Universe the horizon problem is strengthen by the flatness problem that corresponds to very fine tuning in the initial deviation from the flat Universe.

The exponential growth of the scale factor naturally removes both problems. Provided that the e-folding, defined as the power in the exponent in Eq. (88) exceeds 72, the size of the region, causally connected at the Planck time, grows so that it embeds the size of the modern cosmological horizon. It explains the similarity of the initial conditions for the observed part of the modern Universe. For the non-flat Universe, such e-folding provides the exponential growth of the scale factor making the contribution of the curvature effect in deviations from the flat Universe exponentially suppressed. The cosmological expansion itself is explained by inflation. The acceleration at the inflational stage (its positive sign in the Eq. (89)) gives the initial momentum to the expansion. Fluctuations on inflational stage induce the spectrum of initial density fluctuations, giving rise to galaxy and large scale structure formation in respective scales.

The appealing idea of inflation should find proper basis in the BSM physics.

In the "old inflationary model", the strong first-order phase transition, driving inflation, results in the "boiling" of the Universe. The dominance of the false vacuum finishes, when the bubbles of the true vacuum nucleate, expand and collide. The energy release in bubble collisions leads to the reheating of the Universe. But the thermalization of this energy needs the small size of bubbles, that corresponds to rapid bubble nucleation.

On the other side, the e-folding, being necessary for the explanation of the global properties of the modern Universe, assumes sufficiently slow bubble nucleation. The large size of bubbles in this case means that all energy released in the phase transition transforms into the kinetic energy of bubble walls. It leads to the large empty space inside the true vacuum bubble which can be hardly reheated after the bubble wall collisions. The Universe turns to be strongly inhomogeneous.

In the "new inflationary scenario" [223,224] (for review, see [1,213]), the transition from the inflational stage proceeds due to slow rolling of the effective potential down to the true vacuum state. This scenario removes the problem of inhomogeneities induced by the bubble nucleation. But the fluctuations of the scalar field induce density fluctuations. To provide sufficiently low amplitude of these density fluctuations, the effective potential should be very flat at the origin. It implies very slow rolling of the field from the symmetric phase down to the true vacuum of the asymmetric phase.

The same condition of slow rolling appears in the chaotic inflation scenario [225]. The equation of state (90) appears at the initial stage of cosmological evolution of any scalar field, provided that its derivative terms are negligible as compared with the potential. On the basis of the chaotic inflation scenario, a wide variety of possibilities seem to appear for the inflaton, i.e., the field driving the inflation. displayed in Fig. 13.

To make the proper choice between these possibilities, or, at least, to make some reduction of their number, observational signatures of the inflationary mechanism and its theoretical framework should be considered. It makes very interesting supergravity basis for inflationary models (see [226] for review and references). This approach can offer simultaneous solution for inflation and supeheavy gravitino as dark matter in Starobinsky Supergravity [67,227,228].

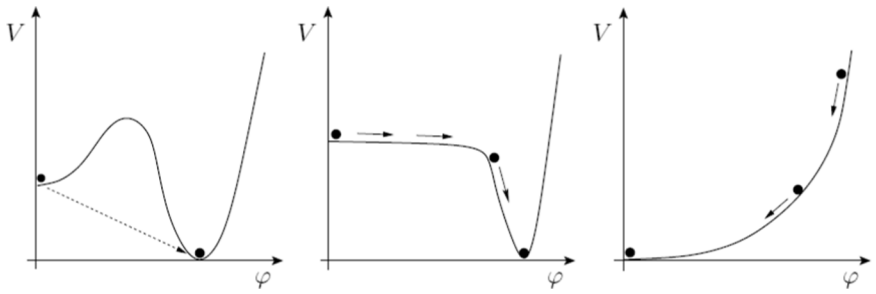

Fig. 13. Old, new and chaotic inflation scenario.

Fluctuations on inflational stage induce the spectrum of initial density fluctuations, giving rise to galaxy and large scale structure formation in respective scales. The amplitude of these fluctuations is constrained by the observed isotropy of the thermal electromagnetic background radiation.

It rules out all inflationary models with high amplitude of predicted fluctuations, the most of GUT-induced phase transition scenarios, in particular.

In the simplest models with the equation of state on the inflationary stage close to Eq. (90), the form of the spectrum is predicted rather close to the flat Harrison–Zeldovich. The slow roll inflationary models predict this spectrum a bit tilted with power index $n_s < 1$, corresponding to slight suppression of the amplitude of fluctuations at small scales. Then the estimated amplitude of initial fluctuations at the modern scale of the cosmological large scale structure provides some information on the possible properties of inflaton, e.g. on the form and parameters of the scalar field potential. Together with scalar density perturbations inflationary models also predict spectrum of tensor perturbations — primordial gravitational waves that cause a B-mode polarization of the CMB.

In the framework of standard single-field inflationary models with Einstein gravity, the results of Planck experiment [229] imply that:

(a) the predictions of slow-roll models with a concave potential, $V''(\phi) < 0$, are increasingly favored by the data; and
(b) based on two different methods for reconstructing the inflaton potential, no evidence for dynamics beyond slow roll is found

Planck measurements of the potential tilt give $n_s = 0.9649 \pm 0.0042$ (68% CL), and for the tensor-to-scalar ratio: $r = T/S < 0.064$ (95% CL).

For more complicated inflationary models, e.g., multicomponent inflation, the form of the predicted spectrum of fluctuations can differ from the simple flat one.

Phase transitions on the inflationary stage lead to specific peaks or plateaux in the spectrum with the position and amplitude defined by the parameters of the model. One should also account for the phase transitions after the global inflationary stage, in which the initial spectrum can be modified.

Both in R^2 and scalar-field-driven (e.g., chaotic) inflationary scenarios long dust-like post-inflational stage can appear, induced by coherent inflaton field oscillations.

The scale, corresponding to the maximal e-folding given by inflation, puts the physical constraint on the homogeneity of the Universe.

The other side of the inflationary mechanism of the homogeneity of the observed part of the Universe is the inhomogeneity of the Universe far beyond the modern cosmological horizon. In studies of the Universe as a whole the physical mechanism offered as the basis for the homogeneous and isotropic cosmological model inevitably leads to much more complicated cosmological picture.

4.2. Baryosynthesis

The idea on the baryon-asymmetric Universe follows from the observed absence of antimatter at macroscopic scales up to the scales of clusters of galaxies. In the baryon-asymmetric Universe, the observed baryonic matter originated from the initial baryon excess, surviving after the local nucleon–antinucleon annihilation, that was taking place at the first millisecond of cosmological evolution.

The baryon excess is assumed to be generated in the process of baryogenesis [230,231], resulting in the baryon asymmetry of the initially baryon symmetrical Universe.

In the original Sakharov's scenario [230] of baryosynthesis, the baryon excess originated from the CP violating effects in out-of-equilibrium baryon-nonconserving processes.

To illustrate the idea of the Sakharov's mechanism consider the baryon-symmetric Universe in which the out of equilibrium decays of some particles X and of equal amount of their antiparticles $\bar{X}$ take place. The baryon non-conservation in these decays means that the products of decay along different channels have different baryon number.

Assume, for definiteness, that there are two different decay modes of the particle X, namely, the channel

$$X \to qq \tag{92}$$

and the channel

$$X \to \bar{q}l, \tag{93}$$

where q denotes quark $\bar{q}$ denotes antiquark and l denotes a lepton. The corresponding channels for the antiparticle are

$$\bar{X} \to \bar{q}\bar{q} \tag{94}$$

and

$$\bar{X} \to q\bar{l}. \tag{95}$$

Owing to CPT invariance, the total widths of particle and antiparticle are strictly equal. However, due to CP-violation the relative probabilities (branching ratios) for particular decay mode of particle and antiparticle do not coincide.

Let the total decay probability be equal to 1, the relative probability of the decay (92) be r and of the decay (93) be $(1-r)$, respectively. For the antiparticle, the corresponding probabilities are $\bar{r}$ and $(1-\bar{r})$.

With the account for baryon charges of quarks $B_q = 1/3$ and antiquarks $B_{\bar{q}} = -1/3$ one finds that as a result of the out-of-equilibrium decays (92)–(95) in the baryon symmetric Universe with the equal initial concentrations of particles and antiparticles $n_X = n_{\bar{X}}$ the baryon excess is generated, equal to

$$n_q = (r - \bar{r})n_X \tag{96}$$

The magnitude of the baryon excess (96) is determined by the concentration of the decaying particles as well as by the difference of branching ratios of respective modes for particles and antiparticles. This difference is determined by the magnitude and the sign of the CP-violation.

Supersymmetric (SUSY) models offer another possible origin of the baryon asymmetry of the Universe. The supersymmetric scalar partners of quarks can form the Bose condensate. Affleck, Dine [232] and Linde [233] found that the superpotential is flat relative to the baryon charge, and the existence of scalar quark condensate is not forbidden. Such a condensate, being formed with the positive baryon charge ($B > 0$), induces the baryon asymmetry, after the decay of scalar quarks on quarks and gluinos. However, the mechanism does not fix the value and the sign of the baryon charge of condensate, opening the possibilities for inhomogeneous baryon charge distribution as well as for antibaryon domains (see 5.2).

At the high temperature the standard model of electroweak (EW) interactions predicts baryon and lepton charge nonconservation owing to sphaleron transitions [234]. This effect puts severe constraints on the mechanisms of baryosynthesis. Electroweak non-conserving processes follow the selection rule

$$B + L = O \tag{97}$$

and wash out any initial baryon asymmetry, which follows the selection rule

$$B - L = O \tag{98}$$

In particular, the electroweak baryon nonconservation (EW BNC) makes impossible to generate the observed baryon asymmetry by the processes, predicted in the $SU(5)$ GUT model, since they obey the selection rule (98).

On the other hand, the EW BNC opens the new approach to baryosynthesis, because one can use it for the generation of the observed baryon asymmetry.

It was found [235] that one cannot generate the baryon excess sufficient to explain this asymmetry in the framework of the minimal standard model. The extensions of the standard model are necessary to provide the mechanism for baryosynthesis based on EW BNC. It proves the general statement that the physical grounds for baryosynthesis are related to the hidden sector of particle theory. Among the possible extensions of the standard model needed for the baryosynthesis based on EW BNC, an interesting possibility exists related with the physics of the mass of neutrino. The Majorana mass of neutrino is induced by the violation of lepton number with the selection rule

$$\Delta L = 2. \tag{99}$$

CP violation in the out-of-equilibrium lepton number-non-conserving processes implied by neutrino mass physics can lead to lepton excess, which is transformed into baryon excess owing to EW BNC.

4.3. Dark universe

The main arguments favoring nonbaryonic nature of dark matter in the Universe are Big Bang nucleosynthesis (BBN) in the inflational cosmology and the formation of large scale structure of the Universe in conditions of the observed isotropy of relic radiation. Evolution of density fluctuations of dark matter and baryons is displayed in Fig. 14. The amplitude of

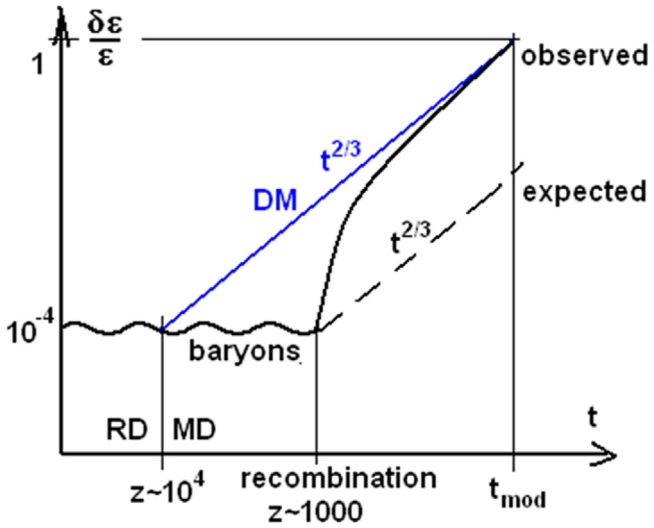

Fig. 14. Evolution of dark matter and baryonic matter density fluctuations. Before recombination, fluctuations of the ionized baryonic matter are converting into the sound waves, while density fluctuations of dark matter grow. After recombination of hydrogen, constituting the main component of baryonic dark matter, amplitude of fluctuations of the neutral atomic gas reaches the amplitude of dark matter fluctuations and joins their common growth.

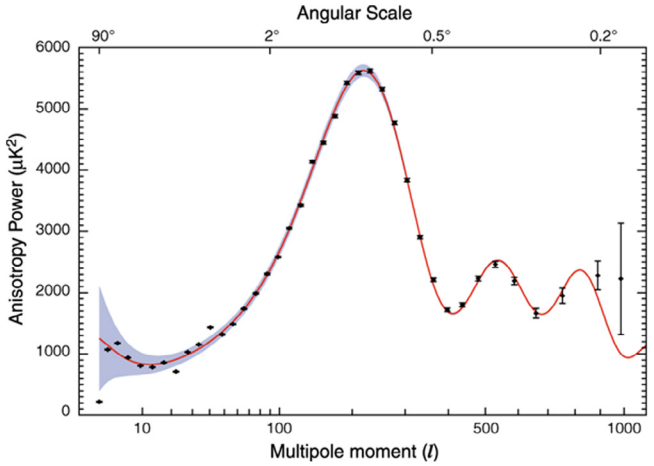

Fig. 15. Positions of peaks in the CMB angular fluctuations determine the total, total matter and baryon densities.

baryonic density fluctuations in the period of recombination is reflected in anisotropy of the CMB and is constrained by the CMB data.

The positions of peaks in CMB angular fluctuations displayed in Fig. 15 determine the total density of the Universe, the total matter density and the baryon density.

The difference between the total matter density ($\Omega_m \approx 30\%$) and the baryon density ($\Omega_b \leq 5\%$) corresponds to the nonbaryonic dark matter and it turns out that the dark matter density dominates in the matter content of the Universe. The difference between the total density ($\Omega = 1$) and the total matter density corresponds to the dark energy with negative pressure equation of state close to the Eq. (90). Dark energy dominates in the modern Universe and drives acceleration of the cosmological expansion. The relative contribution to the total density by dark energy, dark matter and baryons is displayed in Fig. 16.

The second type of arguments is that the formation of the large scale structure is compatible with the observed isotropy of thermal electromagnetic background only if some weakly interacting form of matter triggers the structure formation with the minor effect in the angular distribution of relic radiation.

There are several scenarios of structure formation by hot (HDM), cold (CDM), unstable (UDM), mixed hot+cold (H+CDM), hierarchical decaying (HDS), etc. dark matter. These scenarios physically differ by the ways and succession in which the elements of structure are formed, as well as by the number of model parameters. But having in mind the

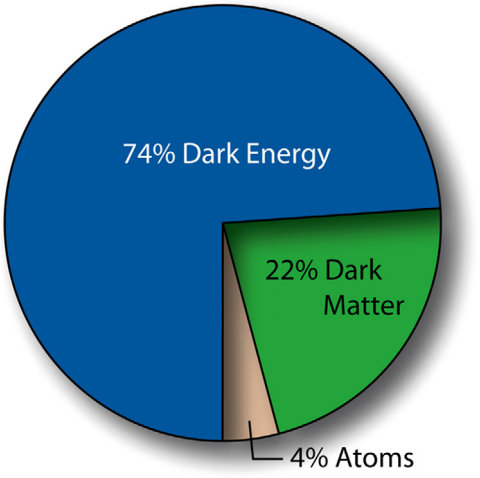

Fig. 16. Relative contribution of dark energy, dark matter and baryonic matter (Atoms).

general independence of motivations for each type of dark matter candidates, one finds from the particle physics viewpoint that the hot, cold, unstable, etc. dark matter are not alternatives and rather supplementary options to be taken together, accounting for the whole set of reasonable physical arguments .

5. BSM cosmology from BSM physics

5.1. Primordial nonlinear structures in inflationary universe

If the phase transitions take place at the inflational stage, new forms of primordial large scale correlations appear. The example of global U(1) symmetry—broken spontaneously in the period of inflation and successively broken explicitly after reheating was considered in Ref. [236]. In this model, spontaneous U(1) symmetry breaking at the inflational stage is induced by the vacuum expectation value $\langle\psi\rangle = f$ of a complex scalar field $\Psi = \psi \exp(i\theta)$, also having an explicit symmetry breaking term in its potential $V_{eb} = \Lambda^4(1 - \cos\theta)$. The latter is negligible in the period of inflation if $f \gg \Lambda$, so there appears a valley relative to values of phase in the field potential in this period. Fluctuations of the phase θ along this valley—being of the order of $\Delta\theta \sim H/(2\pi f)$ (here H is the Hubble parameter at the inflational stage)—change in the course of inflation, its initial value within the regions of smaller size. Owing to such fluctuations, for the fixed value of θ_{60} in the period of inflation with *e-folding* $N = 60$ corresponding to the part of the universe within the modern cosmological horizon, strong deviations from this value appear at smaller scales, corresponding to later periods of inflation with $N < 60$. If $\theta_{60} < \pi$, the fluctuations can move the value of θ_N to $\theta_N > \pi$ in some regions of the universe. After reheating, when the universe cools down to temperature $T = \Lambda$, the phase transition to the true vacuum states, corresponding to the minima of V_{eb}, takes place. For $\theta_N < \pi$, the minimum of V_{eb} is reached at $\theta_{vac} = 0$; whereas in the regions with $\theta_N > \pi$, the true vacuum state corresponds to $\theta_{vac} = 2\pi$. For $\theta_{60} < \pi$ in the bulk of the volume within the modern cosmological horizon $\theta_{vac} = 0$. However, within this volume there appear regions with $\theta_{vac} = 2\pi$. These regions are surrounded by massive domain walls, formed at the border between the two vacua. Since regions with $\theta_{vac} = 2\pi$ are confined, the domain walls are closed. After their size equals the horizon, closed walls can collapse into black holes (BHs). This qualitative feature of formation of closed walls is displayed in Fig. 17.

The mass range of formed BHs is constrained by fundamental parameters of the model, f and Λ. The maximal BH mass is determined by the condition that the wall does not dominate locally before it enters the cosmological horizon. Otherwise, local wall dominance leads to a superluminal $a \propto t^2$ expansion for the corresponding region, separating it from the other part of the universe. This condition corresponds to the mass [150]

$$M_{max} = \frac{m_{pl}}{f} m_{pl} \left(\frac{m_{pl}}{\Lambda}\right)^2 \tag{100}$$

The minimal mass follows from the condition that the gravitational radius of BH exceeds the width of wall, and it is equal to [150,237]

$$M_{min} = f \left(\frac{m_{pl}}{\Lambda}\right)^2 \tag{101}$$

Closed wall collapse leads to primordial gravitational wave (GW) spectrum, peaked at and it is equal to [150,237]

$$\nu_0 = 3 \times 10^{11} (\Lambda/f)\,\mathrm{Hz} \tag{102}$$

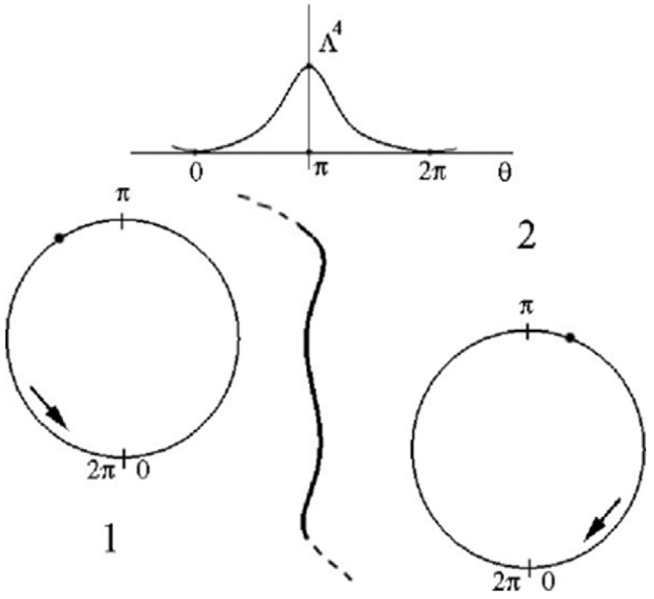

Fig. 17. Formation of closed domain walls in the succession of phase transitions of global $U(1)$ symmetry breaking. Fluctuations of phase in inflational stage can lead to its value $\theta > \pi$ at some step of inflation. After the second phase transition the regions with $\theta > \pi$ correspond to vacuum with $\theta_{vac} = 2\pi$, while the surrounding space is in the state $\theta_{vac} = 0$. Such regions are thus surrounded by a closed domain wall.

with energy density up to

$$\Omega_{GW} \approx 10^{-4}(f/m_{pl}) \tag{103}$$

At $f \sim 10^{14}$ GeV this primordial gravitational wave background can reach $\Omega_{GW} \approx 10^{-9}$. For the physically reasonable values of

$$1 < \Lambda < 10^8\,\text{GeV} \tag{104}$$

the maximum of the spectrum corresponds to

$$3 \times 10^{-3} < \nu_0 < 3 \times 10^5\,\text{Hz} \tag{105}$$

In the range from tens to thousands of Hz, such background may be a challenge for LIGO experiment. Another profound signature of the considered scenario are gravitational wave signals from merging of BHs in the primordial black hole (PBH) cluster. These effects can provide a test of the considered approach in eLISA experiment.

This mechanism can lead to the formation of primordial black holes of a whatever large mass (up to the mass of active galactic nuclei (AGNs) [238,239], see for latest review Ref. [240]). Such black holes appear in the form of primordial black hole clusters, exhibiting fractal distribution in space [150,237,241]. This can shed new light on the problem of galaxy formation [150,239].

Another profound signature of the considered scenario are gravitational wave signals from merging of BHs in PBH cluster. Being in cluster, PBHs with the masses of tens $M_\odot$ form binaries much easier, than in the case of their random distribution. In this aspect detection of signals from binary BH (BBH) coalescence in the gravitational wave experiments [242–246] may be considered as a positive evidence for this scenario. Repeatedly detected signals localized in the same place would provide successive support in its favor.

Critical analysis by [247] of constraints [248–252] on relative contribution of PBHs into dark matter density shows that PBH formation in clusters can influence the constraints [251] excluding PBH dominance in dark matter.

Even subdominant component of massive PBH clusters can lead to important consequences for interpretation of gravitational wave signals from coalescence of massive black holes. The latest GWTC catalog [253] contains now 11 events of coalescence of compact binaries, with only one event of neutron star–neutron star binary coalescence. All the other 10 events correspond to coalescence of binary systems of black holes with mass, exceeding 10–20 Solar masses each. Formation of such systems in the evolution of massive stars is rather problematic, while it is rather natural for clusters of massive PBHs, in which formation of binaries is much more probable as compared with the case of random PBH distribution. Recent detection by LIGO and VIRGO collaborations of gravitational wave signal from a BBH merging with total mass $150M_{odot}$ [254], corresponding to the gap in the predicted BH masses from first massive stars, can evidence for primordial origin of massive BHs [255].

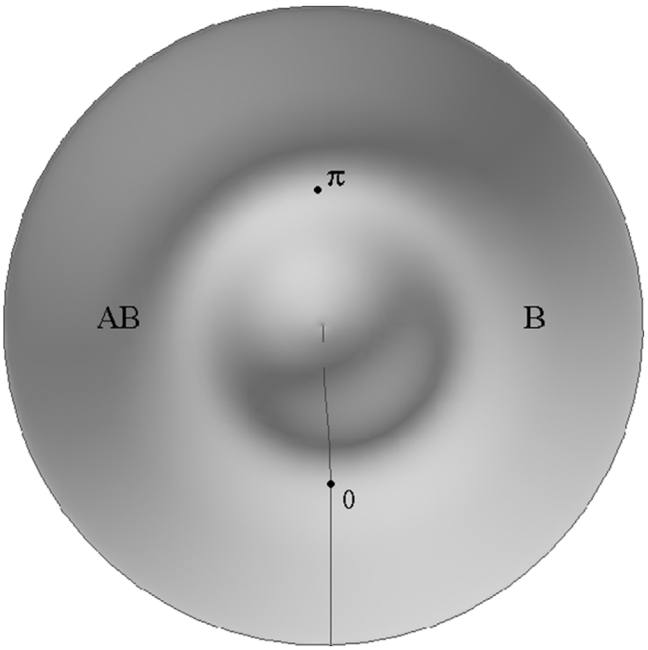

Fig. 18. Formation of baryon and antibaryon excess in spontaneous baryosynthesis.

Repeating merging of black holes in clusters may be another signature for massive PBH clusters [247,256]. The existing statistics is evidently not sufficient to make any definite conclusion on this possibility. However, repeating detection of four GW signals in the August of 2017 may be an interesting hint to such a possibility.

5.2. Antimatter in baryon asymmetric universe

The appearance of antibaryon domains in the baryon asymmetrical universe (reflecting the inhomogeneity of baryosynthesis) is the profound signature of such strong inhomogeneity [257,258]. The matter-antimatter symmetry of the Universe with survival of antimatter in large domains is excluded within the all the now observed part of the Universe [259–262]. In an example of a model of spontaneous baryosynthesis (see Ref. [263] for review), the possibility of the existence of antimatter domains surviving to the present time in the inflationary baryon asymmetrical universe with inhomogeneous baryosynthesis was revealed in [264].

The mechanism of spontaneous baryogenesis [263,265,266] implies the existence of a complex scalar field $\chi = (f/\sqrt{2})\exp(\theta)$ carrying the baryonic charge. The $U(1)$ symmetry – which corresponds to the baryon charge – is broken spontaneously and explicitly. The explicit breakdown of $U(1)$ symmetry is caused by the phase-dependent term

$$V(\theta) = \Lambda^4(1 - \cos\theta) \tag{106}$$

The possible baryon and lepton number violating interaction of the field χ with matter fields can have the following structure [263]:

$$\mathcal{L} = g\chi\bar{Q}L + \text{h.c.} \tag{107}$$

where fields Q and L represent a heavy quark and lepton, coupled to the ordinary matter fields.

In the early universe, at a time when the friction term induced by the Hubble constant becomes comparable with the angular mass $m_\theta = \frac{\Lambda^2}{f}$, the phase θ starts to oscillate around the minima of the PNG potential and decays into matter fields, according to (107). The coupling (107) gives rise to the following [263]: as the phase starts to roll down in the clockwise direction (Fig. 19), it preferentially creates an excess of baryons over antibaryons, while the opposite is true as it starts to roll down in the opposite direction. This qualitative feature of spontaneous baryosynthesis is displayed in Fig. 18.

The fate of such antimatter regions depends on their size. If the physical size of some of them is larger than the critical surviving size $L_c = 8h^2$ kpc [264,267], they survive annihilation with surrounding matter. The evolution of sufficiently dense antimatter domains can lead to the formation of antimatter globular clusters [268]. The existence of such clusters in the halo of our galaxy should lead to the pollution of the galactic halo by antiprotons. Their annihilation can reproduce [269] the observed galactic gamma background in the range of tens–hundreds MeV. The prediction of an

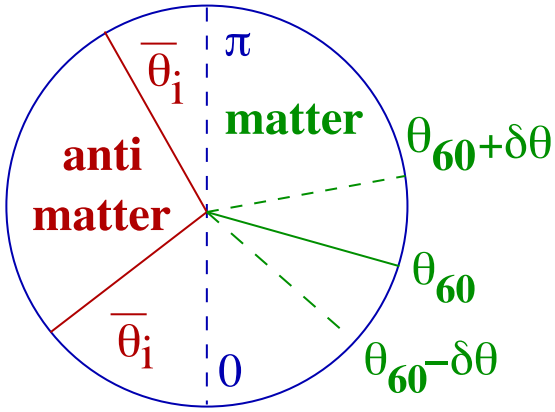

Fig. 19. Generation of antibaryon excess on inflational stage in the mechanism of spontaneous baryosynthesis.

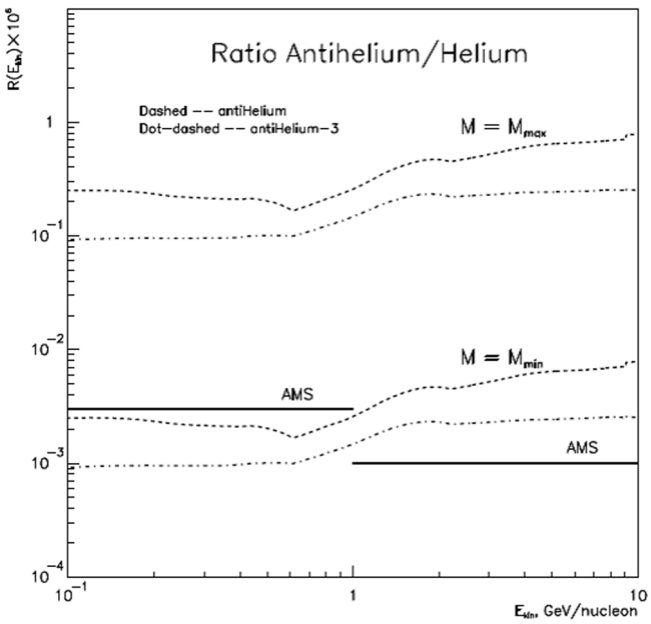

Fig. 20. Expected sensitivity of AMS02 experiment to antihelium flux from antimatter globular cluster in our Galaxy.

antihelium component of cosmic rays [270] – accessible to future searches for cosmic ray antinuclei in PAMELA and AMS II experiments – as well as of antimatter meteorites [271] provides the direct experimental test for this hypothesis.

Generation of antibaryon excess on inflationary stage in the mechanism of spontaneous baryosynthesis schematically presented in Fig. 19.

Predictions for cosmic antihelium flux from antimatter globular cluster in our Galaxy are displayed in Fig. 20. This prediction is not only accessible to searches for cosmic ray antinuclei in the AMS02 experiment, but also provide decisive experimental test for antimatter globular cluster hypothesis.

AMS collaboration continuously presents results of these searches (see review in [272]). There are about ten clear candidates for antihelium-3. Two events may be interpreted as antihelium-4. It is expected that more statistics will be available to 2024 and the result with the significance level of 5 standard deviation can be obtained. The expected progress will shed light on the reasons of dominance of events with anti-helium-3 over anti-helium-4, as well as of the absence of candidates for anti-deuterium in the presented results. In any case antihelium-3 events cannot be explained as the secondary effect from cosmic ray interactions [272]. Therefore their confirmation would be a strong argument, favoring antimatter globular cluster hypothesis.

Formation of dense antistars and their possible search were considered in [273] within an extension of the supersymmetric Affleck–Dine mechanism of baryosynthesis.

6. Dark matter puzzles

The existence of nonbaryonic dark matter is strongly supported by the data of precision cosmology, but the experimental direct search for dark matter particles in underground detectors gives controversial results. The continuous increase of confidence level of positive results of DAMA/NaI and DAMA/LIBRA dark matter searches [102–105,274] seems to be in apparently growing tension with the negative results of other groups like CDMS [106–108] , XENON100 [109] and LUX [275]. A possible explanation for this apparent contradiction may be related with the difference in strategy, methods and chemical content of detectors in these experiments. With the account for such difference even interpretation of DAMA result in terms of Weakly Interacting Massive Particles (WIMPs) may not be completely ruled out [274]. However, such interpretation seems highly unprobable and the coexistence of positive result of DAMA and negative results of other groups can appeal to non-WIMP dark matter effect, detected by DAMA.

WIMPs are the simplest miraculous solution for cosmological dark matter. This solution found strong theoretical motivation in supersymmetric models, predicting a few hundred GeV Lightest Supersymmetric Particle as a natural WIMP dark matter candidate. However, the lack of supersymmetric particles at the LHC as well as negative results of WIMP searches by most of experimental groups may be a hint to a non-WIMP nature of dark matter, which is detected by DAMA but missed in the strategy of other searches, aimed specifically to detection of WIMPs.

Here we draw attention to a possibility to explain these puzzles of direct dark matter searches in the model of dark atoms [22,121,122,276,277]. The model assumes that, similar to ordinary matter, dark matter consists of neutral atoms called *O*-helium (*O*He), in which hypothetical stable -2 charged massive particles are bound by ordinary Coulomb force with primordial helium nucleus. This model is a simplest extension of the Standard model, since it involves only one parameter of new physics (the mass of double charged particle O^{--}) and reduces effects of dark atoms to the nuclear interaction of their helium shells that can be based on known laws of nuclear and atomic physics. The complication of the problem of *O*He nuclear interaction still leaves open its complete quantum mechanical solution, but the qualitative features of *O*He dark matter scenario and the possibility of its explanation for the puzzles of direct dark matter searches and some astrophysical anomalies appeal to development of this interesting approach.

6.1. Dark atoms

Here we concentrate on the properties of OHe atoms, their interaction with matter, and the qualitative picture of OHe cosmological evolution [22,121,122,278–281] and observable effects. We show from the following Refs. [124,282] that the interaction of OHe with nuclei in underground detectors can explain the positive results of dark matter searches in DAMA/NaI (see for review Ref. [103]) and DAMA/LIBRA [104] experiments by annual modulations of the radiative capture of O-helium, resolving the controversy between these results and the results of other experimental groups.

After it is formed in the Standard Big Bang Nucleosynthesis (SBBN), ^4He screens the excessive O^{--} charged particles in composite ($^4He^{++}O^{--}$) *O-helium* (*OHe*) "atoms" [122].

In all the considered forms of O-helium, O^{--} behaves either as lepton or as a specific "heavy quark cluster" with strongly-suppressed hadronic interaction. Therefore, O-helium interaction with matter is determined by nuclear interaction of He. These neutral primordial nuclear interacting species can play the role of a nontrivial form of strongly interacting dark matter [283–291], giving rise to a Warmer than Cold dark matter scenario [278,292,293].

6.2. OHe atoms and their interaction with nuclei

The structure of an OHe atom follows from the general analysis of the bound states of O^{--} with nuclei.

Consider a simple model [294–296] in which the nucleus is regarded as a sphere with uniform charge density and in which the mass of the O^{--} is assumed to be much larger than that of the nucleus. Spin dependence is also not taken into account, so both the particle and nucleus are considered as scalars. Then, the Hamiltonian is given by

$$H = \frac{p^2}{2Am_p} - \frac{ZZ_o\alpha}{2R} + \frac{ZZ_o\alpha}{2R}\cdot(\frac{r}{R})^2 \tag{108}$$

for short distances $r < R$ and

$$H = \frac{p^2}{2Am_p} - \frac{ZZ_o\alpha}{R} \tag{109}$$

for long distances $r > R$, where α is the fine structure constant, $R = d_nA^{1/3} \sim 1.2A^{1/3}/(200\,\mathrm{MeV})$ is the nuclear radius, Z is the electric charge of the nucleus, and $Z_o = 2$ is the electric charge of the negatively charged particle O^{--}. Since $Am_p \ll M_o$, the reduced mass is $1/m = 1/(Am_p) + 1/M_o \approx 1/(Am_p)$.

For small nuclei, the Coulomb binding energy is like in hydrogen atom and is given by

$$E_b = \frac{1}{2} Z^2 Z_o^2 \alpha^2 A m_p \tag{110}$$

For large nuclei, O^{--} is inside the nuclear radius and the harmonic oscillator approximation is valid for the estimation of the binding energy

$$E_b = \frac{3}{2}\left(\frac{ZZ_o\alpha}{R} - \frac{1}{R}\left(\frac{ZZ_o\alpha}{Am_pR}\right)^{1/2}\right) \tag{111}$$

For the intermediate regions between these two cases with the use of trial function of the form $\psi \sim e^{-\gamma r/R}$, variational treatment of the problem [294–296] gives

$$E_b = \frac{1}{Am_pR^2} F(ZZ_o\alpha Am_pR) \tag{112}$$

where the function $F(a)$ has limits

$$F(a \to 0) \to \frac{1}{2}a^2 - \frac{2}{5}a^4 \tag{113}$$

and

$$F(a \to \infty) \to \frac{3}{2}a - (3a)^{1/2} \tag{114}$$

where $a = ZZ_o\alpha Am_pR$. For $0 < a < 1$ the Coulomb model gives a good approximation, while at $2 < a < \infty$ the harmonic oscillator approximation is appropriate.

In the case of OHe $a = ZZ_o\alpha Am_pR \leq 1$, which proves its Bohr-atom-like structure, assumed in Refs. [22,122,279,297,298]. The radius of Bohr orbit in these "atoms" [122,278] is $r_o \sim 1/(Z_oZ_{He}\alpha m_{He}) \approx 2 \times 10^{-13}$ cm. However, the size of the He nucleus rotating around O^{--} in this Bohr atom turns out to be on the order of and even a bit larger than the radius r_o of its Bohr orbit, and the corresponding correction to the binding energy due to non-point-like charge distribution in He is significant.

The Bohr atom-like structure of OHe seems to provide a possibility to use the results of atomic physics for the description of OHe interaction with matter. However, the situation is much more complicated. The OHe atom is similar to hydrogen, in which the electron is hundreds of times heavier than the proton, so that it is a proton shell that surrounds an "electron nucleus". Nuclei that interact with such "hydrogen" would interact first with the strongly interacting "protonic" shell, and such interaction can hardly be treated in the framework of perturbation theory. Moreover, in the description of OHe interaction, accounting for the finite size of He – which is even larger than the radius of the Bohr orbit – is important. One should consider, therefore, the analysis presented below as only a first step approaching the true nuclear physics of OHe.

The approach of Refs. [278,292] assumes the following picture of OHe interaction with nuclei: OHe is a neutral atom in the ground state, perturbed by the Coulomb and nuclear forces of the approaching nucleus. The sign of OHe polarization changes with the distance: at larger distances, Stark-like effect takes place—nuclear Coulomb force polarizes OHe so that the nucleus is attracted by the induced dipole moment of OHe, while as soon as the perturbation by nuclear force starts to dominate, the nucleus polarizes OHe in the opposite way so that He is situated more closely to the nucleus, resulting in the repulsive effect of the helium shell of OHe. When helium is completely merged with the nucleus, the interaction is reduced to the oscillatory potential of O^{--} with a homogeneously charged merged nucleus with the charge $Z + 2$.

Though OHe scenario seems to involve dominantly known atomic and nuclear physics, there is no small parameter in OHe–nucleus interaction. It makes the problem very complicated as compared with ordinary atoms that have electroweakly interacting electronic shells and strongly interacting nuclei of much smaller size. These two features proved small parameters in the ordinary atomic physics, which are not the case for OHe. Indeed, the size of the He shell is equal to the size of He nucleus and creation of barrier in OHe–nucleus interaction should be the result of a simultaneous action of nuclear attraction and Coulomb repulsion between He and approaching nucleus. Qualitatively, a possibility for such a solution can be illustrated by the following picture. At large distances Coulomb field of nucleus polarizes OHe so that Stark-effect attraction takes place. At some distance nuclear attraction changes the sign of polarization, but Coulomb repulsion moves it back, and then nuclear attraction moves He again towards nucleus and so on. Such oscillatory behavior can provide creation of potential barrier and this approach is now under quantitative investigation.

Therefore OHe–nucleus potential can have a qualitative feature, presented in Fig. 21: the potential well at large distances (regions III–IV) is changed by a potential wall in region II. The existence of this potential barrier is crucial for all the qualitative features of the OHe scenario: it causes suppression of reactions with the transition of the OHe–nucleus system to levels in the potential well of the region I, provides the dominance of elastic scattering while transitions to levels in the shallow well (regions III–IV) should dominate in reactions of OHe–nucleus capture. The proof of this picture implies accurate and detailed quantum-mechanical treatment, which was started in Ref. [299]. With the use of perturbation theory, it was shown that OHe polarization changes sign as the nucleus approaches OHe (as is given in Fig. 22), but the perturbation approach was not valid for the description at smaller distances, while the estimates indicated that this

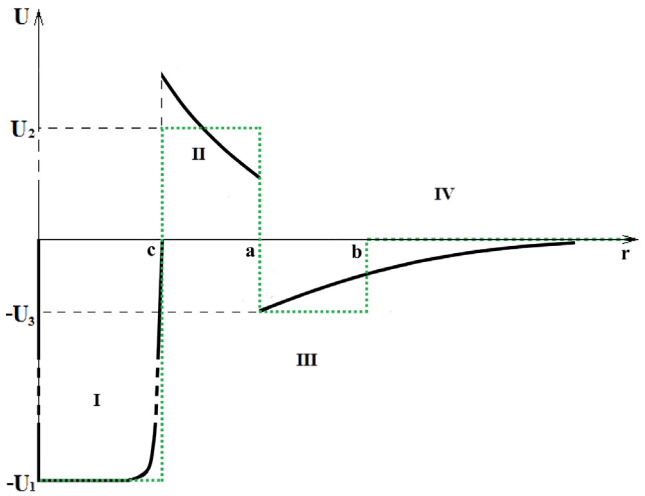

Fig. 21. The potential of the O-Helium (OHe)-nucleus system and its rectangular well approximation.

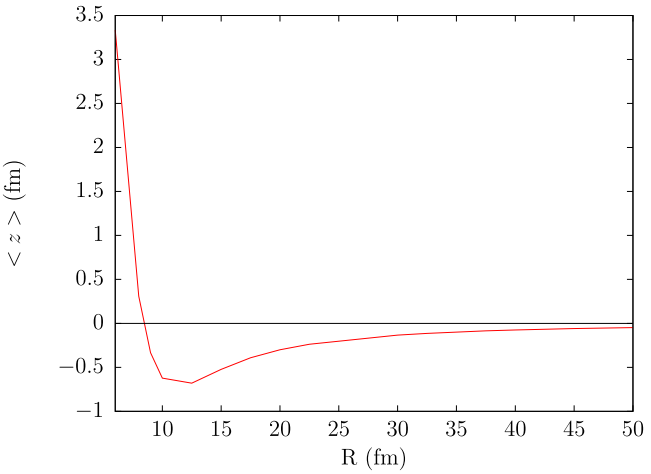

Fig. 22. Polarization $\langle z \rangle$ (Fm) of OHe as a function of the distance R (fm) of an external sodium nucleus, calculated in Ref. [299] in the framework of perturbation theory. Note that here R denotes the distance between OHe and the nucleus and not radius of the nucleus, as it was in Eqs. (108), (109), (111), and (112).

change of polarization may not be sufficient for the creation of the potential, given by Fig. 21. If the picture of Fig. 21 is not proven, one may need more sophisticated models retaining the ideas of the OHe scenario which involve more elements of new physics, as proposed in Ref. [300].

On the other hand, O-helium – being an α-particle with screened electric charge – can catalyze nuclear transformations, which can influence primordial light element abundance and cause primordial heavy element formation. It is especially important for the quantitative estimation of the role of OHe in Big Bang Nucleosynthesis and in stellar evolution. These effects need a special detailed and complicated study of OHe nuclear physics, and this work is under way.

The qualitative picture of OHe cosmological evolution is presented below, following Refs. [22,121,122,124,278–280, 292], and is based on the idea of the dominant role of elastic collisions in OHe interaction with baryonic matter.

6.3. Large scale structure formation by OHe dark matter

Due to elastic nuclear interactions of its helium constituent with nuclei in the cosmic plasma, the O-helium gas is in thermal equilibrium with plasma and radiation in the Radiation Dominance (RD) stage, while the energy and momentum transfer from plasma is effective. The radiation pressure acting on the plasma is then transferred to density fluctuations of the O-helium gas, and transforms them in acoustic waves at scales up to the size of the horizon.

At temperature $T < T_{od} \approx 1 S_3^{2/3}$ eV, the energy and momentum transfer from baryons to O-helium is not effective [22,122] because

$$n_B \langle \sigma v \rangle (m_p/m_o) t < 1$$

where m_o is the mass of the *OHe* atom, and $S_3 = m_o/(1\,\text{TeV})$. Here

$$\sigma \approx \sigma_o \sim \pi r_o^2 \approx 10^{-25}\,\text{cm}^2 \tag{115}$$

and $v = \sqrt{2T/m_p}$ is the baryon thermal velocity. Then, O-helium gas decouples from plasma. It starts to dominate in the universe after $t \sim 10^{12}$ s at $T \leq T_{RM} \approx 1$ eV, and O-helium "atoms" play the main dynamical role in the development of gravitational instability, triggering large scale structure formation. The composite nature of O-helium determines the specifics of the corresponding dark matter scenario.

At $T > T_{RM}$, the total mass of the *OHe* gas with density $\rho_d = (T_{RM}/T)\rho_{tot}$ is equal to

$$M = \frac{4\pi}{3}\rho_d t^3 = \frac{4\pi}{3}\frac{T_{RM}}{T} m_{Pl} (\frac{m_{Pl}}{T})^2$$

within the cosmological horizon $l_h = t$. In the period of decoupling $T = T_{od}$, this mass depends strongly on the O-helium mass S_3, and is given by [22]

$$M_{od} = \frac{T_{RM}}{T_{od}} m_{Pl} (\frac{m_{Pl}}{T_{od}})^2 \approx 2 \times 10^{44} S_3^{-2}\,\text{g} = 10^{11} S_3^{-2} M_\odot \tag{116}$$

where $M_\odot$ is the solar mass. O-helium is formed only at T_o and its total mass within the cosmological horizon in the period of its creation is $M_o = M_{od}(T_{od}/T_o)^3 = 10^{37}$ g.

In the RD stage before decoupling, the Jeans length λ_J of the *OHe* gas was restricted from below by the propagation of sound waves in plasma with a relativistic equation of state $p = \epsilon/3$, being on the order of the cosmological horizon and equal to $\lambda_J = l_h/\sqrt{3} = t/\sqrt{3}$. After decoupling at $T = T_{od}$, it falls down to $\lambda_J \sim v_o t$, where $v_o = \sqrt{2T_{od}/m_o}$. Though, after decoupling, the Jeans mass in the *OHe* gas correspondingly falls down

$$M_J \sim v_o^3 M_{od} \sim 3 \times 10^{-14} M_{od}$$

one should expect a strong suppression of fluctuations on scales $M < M_o$, as well as adiabatic damping of sound waves in the RD plasma for scales $M_o < M < M_{od}$. It can provide some suppression of small scale structure in the considered model for all reasonable masses of O-helium. The significance of this suppression and its effect on structure formation needs a special study in detailed numerical simulations. In any case, it cannot be as strong as the free streaming suppression in ordinary Warm Dark Matter (WDM) scenarios, but one can expect that, qualitatively, we deal with the Warmer Than Cold Dark Matter model.

At temperature $T < T_{od} \approx 1 S_3^{2/3}$ keV, the energy and momentum transfer from baryons to O-helium is not effective [122,278,292], and O-helium gas decouples from plasma. It starts to dominate in the universe after $t \sim 10^{12}$ s at $T \leq T_{RM} \approx 1$ eV, and O-helium "atoms" play the main dynamical role in the development of gravitational instability, triggering large scale structure formation. The composite nature of O-helium determines the specifics of the corresponding warmer than cold dark matter scenario.

Being decoupled from baryonic matter, the *OHe* gas does not follow the formation of baryonic astrophysical objects (stars, planets, molecular clouds, etc.) and forms dark matter halos of galaxies. It can be easily seen that O-helium gas is collisionless for its number density, saturating galactic dark matter. Taking the average density of baryonic matter, one can also find that the galaxy as a whole is transparent for O-helium in spite of its nuclear interaction. Only individual baryonic objects like stars and planets are opaque for it.

6.4. Anomalous component of cosmic rays

O-helium atoms can be destroyed in astrophysical processes, giving rise to the acceleration of free O^{--} in the galaxy.

O-helium can be ionized due to nuclear interaction with cosmic rays [122,298]. Estimations [122,301] show that for the number density of cosmic rays $n_{CR} = 10^{-9}\,\text{cm}^{-3}$ during the age of a galaxy, a fraction of about 10^{-6} of the total amount of OHe is disrupted irreversibly, since the inverse effect of recombination of free O^{--} is negligible. Near the solar system, it leads to the concentration of free O^{--} $n_O = 3 \times 10^{-10} S_3^{-1}\,\text{cm}^{-3}$. After OHe destruction, free O^{--} have momentum of order $p_O \cong \sqrt{2 \cdot m_o \cdot I_o} \cong 2\,\text{GeV} S_3^{1/2}$ and velocity $v/c \cong 2 \times 10^{-3} S_3^{-1/2}$, and due to effect of Solar modulation these particles initially can hardly reach Earth [293,301]. Their acceleration by Fermi mechanism or by collective acceleration forms the power spectrum of the O^{--} component at the level of $O/p \sim n_O/n_g = 3 \times 10^{-10} S_3^{-1}$, where $n_g \sim 1\,\text{cm}^{-3}$ is the density of baryonic matter gas.

At the stage of red supergiant, stars have the size $\sim 10^{15}$ cm, and during the period of this stage$\sim 3 \times 10^{15}$ s, up to $\sim 10^{-9} S_3^{-1}$ of O-helium atoms per nucleon can be captured [293,301]. In the Supernova explosion, these OHe atoms are disrupted in collisions with particles in the front of the shock wave and the acceleration of free O^{--} by the regular mechanism gives the corresponding fraction in cosmic rays. However, this picture needs detailed analysis, based on the development of OHe nuclear physics and numerical studies of OHe evolution in the stellar matter.

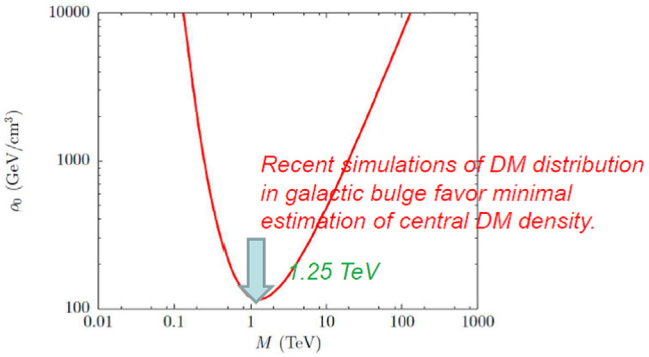

Fig. 23. De-excitation by pair production after *O*He collisions in the center of Galaxy can explain the excess in positronium annihilation line, observed by INTEGRAL at the central density shown by the curve pending on *O*He mass.

If these mechanisms of O^{--} acceleration are effective, the anomalous low Z/A component of -2 charged O^{--} can be present in cosmic rays at the level $O/p \sim n_O/n_g \sim 10^{-9}\, S_3^{-1}$, and be within the reach for PAMELA and AMS02 cosmic ray experiments.

In the framework of the Walking Technicolor model, the excess of both stable ζ^{--} and $(UU)^{++}$ is possible [293]; the latter being two to three orders of magnitude smaller than the former. This leads to the two-component composite dark matter scenario, with the dominant OHe accompanied by a subdominant WIMP-like component of $(\zeta^{--}(UU)^{++})$ bound systems. Technibaryons can be metastable, and decays of $(UU)^{++}$ can provide an explanation for anomalies observed in the high energy cosmic positron spectrum by PAMELA, FERMI-LAT, and AMS02.

6.5. Positron annihilation and gamma lines in galactic bulge

Inelastic interaction of O-helium with matter in the interstellar space and its de-excitation can give rise to radiation in the range from a few keV to a few MeV. In the galactic bulge with radius $r_b \sim 1$ kpc, the number density of O-helium can reach the value $n_o \approx 3 \times 10^{-3}/S_3\,\mathrm{cm}^{-3}$, and the collision rate of O-helium in this central region was estimated in [298]: $dN/dt = n_o^2 \sigma v_h 4\pi r_b^3/3 \approx 3 \times 10^{42}\, S_3^{-2}\,\mathrm{s}^{-1}$. At the velocity of $v_h \sim 3 \times 10^7$ cm/ s, energy transfer in such collisions is $\Delta E \sim 1\,\mathrm{MeV} S_3$. These collisions can lead to the excitation of O-helium. If the 2S level is excited, pair production dominates over two-photon channel in the de-excitation by $E0$ transition, and positron production with the rate $3 \times 10^{42}\, S_3^{-2}\,\mathrm{s}^{-1}$ is not accompanied by strong gamma signal. According to Ref. [302], this rate of positron production for $S_3 \sim 1$ is sufficient to explain the excess in positron annihilation line from bulge, measured by INTEGRAL (see Ref. [303] for review and references). If *OHe* levels with nonzero orbital momentum are excited, gamma lines should be observed from transitions $(n > m)$ $E_{nm} = 1.598$ MeV$(1/m^2 - 1/n^2)$ (or from the similar transitions corresponding to the case $I_o = 1.287$ MeV) at the level $3 \times 10^{-4}\, S_3^{-2}(\,\mathrm{cm}^2\,\mathrm{s\,MeV ster})^{-1}$. Cosmic high energy positron flux from decays of double charged constituents of composite dark matter as a possible explanation of the positron excess detected by PAMELA and AMS02 are displayed in Fig. 24. Gamma ray flux accompanying cosmic high energy positron flux from decays of double charged constituents of composite dark matter in confrontation with the measurements of FERMI/LAT are displayed in Fig. 25.

To explain the excess of positron annihilation line in the galactic bulge mass of double charged constituent of O-helium should be in a narrow window around

$$m_o = 1.25\,\mathrm{TeV}. \tag{117}$$

To explain the excess of high energy cosmic ray positrons by decays of constituents of composite dark matter with charge +2 and to avoid overproduction of gamma background, accompanying such decays, the mass of such constituent should be in the range

$$m_o < 1\,\mathrm{TeV}. \tag{118}$$

These predictions can be confronted with the experimental data on the accelerator search for stable double charged particles.

6.6. O-helium solution for dark matter puzzles

It should be noted that the nuclear cross section of the O-helium interaction with matter escapes the severe constraints [289–291] on strongly-interacting dark matter particles (SIMPs) [283–291] imposed by the XQC experiment [304,305]. More general class of dark matter with hadronic and hadron-like interaction was discussed in [306].

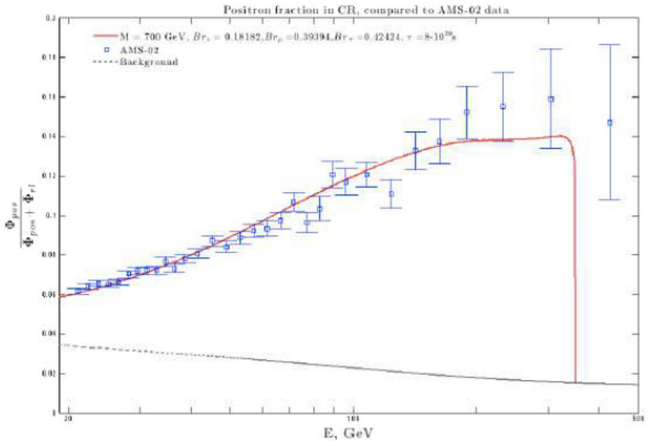

Fig. 24. Excess of high energy cosmic ray positrons measured in AMS02 experiment as a signature for decaying double charged constituents of dark atoms.

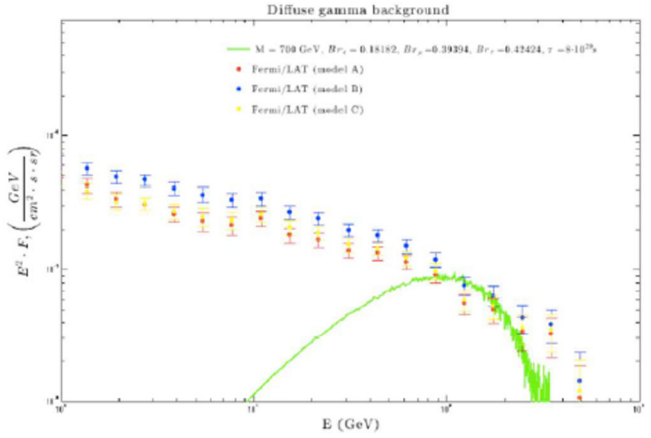

Fig. 25. Gamma ray flux that should accompany high energy cosmic ray positrons from decaying double charged constituents of dark atoms detected in PAMELA and AMS02 experiment in confrontation with the gamma ray background measured by FERMI/LAT.

6.6.1. O-helium in the terrestrial matter

The evident consequence of the O-helium dark matter is its inevitable presence in the terrestrial matter, which appears opaque to O-helium and stores all its in-falling flux.

After they fall down to the terrestrial surface, the in-falling *OHe* particles are effectively slowed down due to elastic collisions with matter. They then drift, sinking down towards the center of the Earth with velocity

$$V = \frac{g}{n\sigma v} \approx 80\, S_3 A_{med}^{1/2}\ \mathrm{cm/\,s} \tag{119}$$

Here $A_{med} \sim 30$ is the average atomic weight in terrestrial surface matter, $n = 2.4 \times 10^{24}/A$ is the number of terrestrial atomic nuclei, σv is the rate of nuclear collisions, and $g = 980\ \mathrm{cm/\,s^2}$.

Near the Earth's surface, the O-helium abundance is determined by the equilibrium between the in-falling and down-drifting fluxes.

At a depth L below the Earth's surface, the drift timescale is $t_{dr} \sim L/V$, where $V \sim 400\, S_3\ \mathrm{cm/\,s}$ is the drift velocity and $m_o = S_3$ TeV is the mass of O-helium. This means that the change of the incoming flux, caused by the motion of the Earth along its orbit, should lead at the depth $L \sim 10^5$ cm to the corresponding change in the equilibrium underground concentration of *OHe* on the timescale $t_{dr} \approx 2.5 \times 10^2\, S_3^{-1}$ s.

The equilibrium concentration – which is established in the matter of underground detectors at this timescale – is given by

$$n_{oE} = n_{oE}^{(1)} + n_{oE}^{(2)} \cdot sin(\omega(t - t_0)) \tag{120}$$

with $\omega = 2\pi/T$, $T = 1yr$ and t_0 the phase. So, there is an averaged concentration given by

$$n_{oE}^{(1)} = \frac{n_o}{320\, S_3 A_{med}^{1/2}} V_h \tag{121}$$

and the annual modulation of concentration characterized by the amplitude

$$n_{oE}^{(2)} = \frac{n_o}{640\, S_3 A_{med}^{1/2}} V_E \tag{122}$$

Here V_h is the speed of Solar System (220 km/s), V_E is the speed of the Earth (29.5 km/s), and $n_0 = 3 \times 10^{-4}\, S_3^{-1}\, \mathrm{cm}^{-3}$ is the local density of O-helium dark matter.

6.6.2. OHe in the underground detectors

The explanation [124,278,282] of the results of the DAMA/NaI [103] and DAMA/LIBRA [104] (see Ref. [105] for the latest review of these results) experiments is based on the idea that OHe – slowed down in the matter of detector – can form a few keV bound state with a nucleus, in which OHe is situated beyond the nucleus. Therefore, the positive result of these experiments is explained by annual modulation in reaction of radiative capture of OHe

$$A + (^4He^{++}O^{--}) \to [A(^4He^{++}O^{--})] + \gamma \tag{123}$$

by nuclei in DAMA detector.

To simplify the solution of the Schrödinger equation, the potential was approximated in Refs. [278,292] by a rectangular potential, presented in Fig. 21. The solution of the Schrödinger equation determines the condition under which a low-energy OHe–nucleus bound state appears in the shallow well of region III and the range of nuclear parameters was found at which OHe–sodium binding energy is in the interval 2–4 keV.

The rate of radiative capture of OHe by nuclei can be calculated [278,282] with the use of the analogy with the radiative capture of a neutron by a proton, accounting for: (i) absence of M1 transition that follows from the conservation of orbital momentum; and (ii) suppression of E1 transition in the case of OHe. Since OHe is isoscalar, the isovector E1 transition can take place in the OHe–nucleus system only due to the effect of isospin nonconservation, which can be measured by the factor $f = (m_n - m_p)/m_N \approx 1.4 \times 10^{-3}$, corresponding to the difference of mass of neutron, m_n, and proton, m_p, relative to the mass of nucleon, m_N. In the result, the rate of OHe radiative capture by a nucleus with atomic number A and charge Z to the energy level E in a medium with temperature T is given by

$$\sigma v = \frac{f\pi\alpha}{m_p^2} \frac{3}{\sqrt{2}} \left(\frac{Z}{A}\right)^2 \frac{T}{\sqrt{A m_p E}} \tag{124}$$

Formation of an OHe–nucleus bound system leads to energy release of its binding energy, detected as ionization signal. In the context of our approach, the existence of annual modulations of this signal in the range 2–6 keV and the absence of such an effect at energies above 6 keV means that binding energy E_{Na} of the Na–OHe system in the DAMA experiment should not exceed 6 keV, being in the range 2–4 keV. The amplitude of annual modulation of the ionization signal can reproduce the result of DAMA/NaI and DAMA/LIBRA experiments for $E_{Na} = 3$ keV. Accounting for the energy resolution in DAMA experiments [104] can explain the observed energy distribution of the signal from a monochromatic photon (with $E_{Na} = 3$ keV) emitted in OHe radiative capture.

At the corresponding nuclear parameters, there is no binding of OHe with iodine and thallium [278].

It should be noted that the results of the DAMA experiment also exhibit the absence of annual modulations of the energy of tens MeV. Energy release in this range should take place if the OHe–nucleus system comes to the deep level inside the nucleus. This transition implies tunneling through dipole Coulomb barrier, and is suppressed below the experimental limits.

For the chosen range of nuclear parameters, reproducing the results of DAMA/NaI and DAMA/LIBRA, the results of Ref. [278] indicate that there are no levels in the OHe–nucleus systems for heavy nuclei. In particular, there are no such levels in Xe, which seems to prevent direct comparison with DAMA results in the XENON100 experiment [109]. The existence of such levels in Ge and the comparison with the results of CDMS [106–108] and CoGeNT [110] experiments need special study. According to Ref. [278], OHe should bind with O and Ca, which is of interest for interpretation of the signal observed in the CRESST-II experiment [307].

In thermal equilibrium, OHe capture rate is proportional to the temperature. Therefore, it looks like it is suppressed in cryogenic detectors by a factor on the order of 10^{-4}. However, for the size of cryogenic devices (less than a few tens of meters), OHe gas in them has the thermal velocity of the surrounding matter, and this velocity dominates in the relative velocity of the OHe–nucleus system. This gives the suppression relative to room temperature only $\sim m_A/m_o$. Then, the rate of OHe radiative capture in cryogenic detectors is given by Eq. (124), in which room temperature T is multiplied by factor m_A/m_o.

6.7. The open problems of OHe model

The existence of heavy stable particles is one of the popular solutions for the dark matter problem. Usually they are considered to be electrically neutral. However, dark matter can potentially be formed by stable heavy charged particles bound in neutral atom-like states by Coulomb attraction. Analysis of the cosmological data and atomic composition of the universe gives constraints on the particle charge, showing that only -2 (in general, $-2n$) charged constituents – being trapped by primordial helium nuclei (in general by n He nuclei) in neutral O-helium states – can avoid the problem of overproduction of the anomalous isotopes of chemical elements, which are severely constrained by observations. A cosmological model of O-helium dark matter can even explain puzzles of direct dark matter searches.

The proposed explanation is based on the mechanism of low-energy binding of OHe with nuclei. Within the uncertainty of nuclear physics parameters, there exists a range at which OHe binding energy with sodium is in the interval 2–4 keV. Annual modulation in radiative capture of OHe to this bound state leads to the corresponding energy release observed as an ionization signal in DAMA/NaI and DAMA/LIBRA experiments.

Accounting for the for high sensitivity of the numerical results to the values of nuclear parameters and for the approximations made in the calculations, the presented results can be considered only as an illustration of the possibility of explaining puzzles of the dark matter search in the framework of the composite dark matter scenario. An interesting feature of this explanation is a conclusion that the ionization signal may be absent in detectors containing light (e.g., ^3He) or heavy (e.g., Xe) elements. Therefore, tests of results of the DAMA/NaI and DAMA/LIBRA experiments by other experimental groups can become a very nontrivial task. The signal of OHe binding should be absent in xenon detectors [109,275] and suppressed in cryogenic detectors. The specific temperature dependence of the signal should be taken into account for the same chemical content and even the same strategy of searches for annual modulation signal in the ANAIS [308] and COSINE-100 [309] experiments.

The present explanation contains distinct features, by which it can be distinguished from other recent approaches to this problem (see [310] for review and references).

An inevitable consequence of the proposed explanation is the appearance of anomalous superheavy isotopes in the matter of underground detectors, having mass roughly m_o larger than ordinary isotopes of the corresponding elements.

It is interesting to note that in the framework of the presented approach, positive results of the experimental search for WIMPs by effect of their nuclear recoil would be a signature for a multicomponent nature of dark matter. Such OHe+WIMPs multicomponent dark matter scenarios naturally follow from the AC model [121] and can be realized in models of Walking technicolor [293].

Stable -2 charge states (O^{--}) can be elementary, like AC-leptons or technileptons, or look like elementary as technibaryons. The latter, composed of techniquarks, reveal their structure at much higher energy scale and should be produced at the LHC as elementary species. The signature for AC leptons and techniparticles is unique and distinctive, which allows their separation from other hypothetical exotic particles.

Since simultaneous production of three $U\bar{U}$ pairs and their conversion in two doubly charged quark clusters UUU is suppressed, the only possibility to test the models of composite dark matter from fourth generation in the collider experiments is a search for the production of stable hadrons containing single U or $\bar{U}$-like Uud and $\bar{U}u/\bar{U}d$.

The presented approach sheds new light on the physical nature of dark matter. Specific properties of dark atoms and their constituents are challenging for the experimental search. The development of the quantitative description of OHe interaction with matter confronted with the experimental data will provide the complete test of the composite dark matter model. It challenges the search for stable doubly charged particles at accelerators and cosmic rays as direct experimental probe for charged constituents of the dark atoms of dark matter.

Collisions of OHe in the center of Galaxy lead to excess in positron annihilation line. The excess measured by INTEGRAL can be explained at the central density and OHe mass displayed in Fig. 23.

7. Conclusion. Towards unification of BSM physics and cosmology

The Ouroboros self-eating-snake illustrates the main problem of modern fundamental physics: *The theory of the universe is based on the predictions of particle theory, which in turn need cosmology for their test*. It is displayed in Fig. 26. The paradox of the current situation is that in spite of serious arguments in favor of BSM physics and its reflection in BSM cosmology the experimental data of high energy physics and precision cosmology only tighten the constraints on effects of this physics.

Except for the detection of neutrino oscillations there is no convincing experimental evidence for BSM physics.

Precision cosmology, supporting the BSM physics basis of the standard inflationary ΛCDM model, does not indicate any serious deviations from this now standard cosmological paradigm.

It may be possible that future accelerator experiments will only put more stringent constraints on BSM physics, which can be only restricted to a super high energy basis of the standard ΛCDM cosmology, specifying with higher accuracy its parameters in future CMB and LSS experiments.

However, reminding the situation of the end of XIX century, when the end of fundamental physics was declared, it looks much more probable that there is some conspiracy of BSM physics and cosmology, hiding their signatures under the cover of Standard models' effects [311]. It may need special efforts to reveal their existence and features. Probably

Fig. 26. The extremes of our knowledge in the largest and smallest physical scales converge as the Ouroboros self-eating snake.

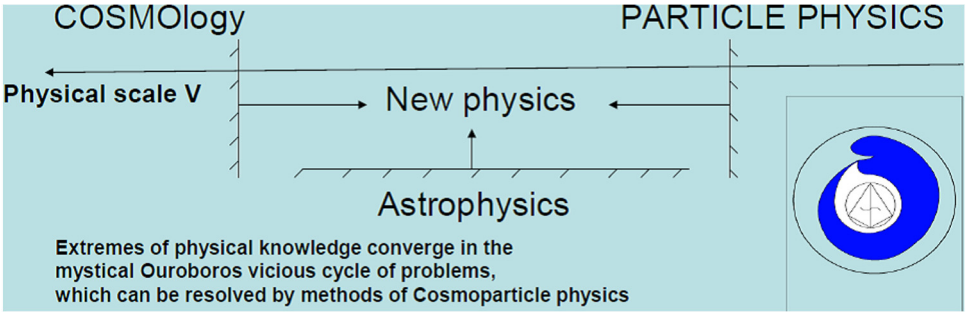

Fig. 27. Complementarity of cosmological, astrophysical and experimental physical tests of new physics, characterized by energy scale V.

first hints to deviation from the standard cosmological scenario come from the so called "Hubble tension" - difference in determination of the value of the modern Hubble constant from early and late cosmological data [312,313].

The expected progress in studies of precision cosmology, astroparticle physics and high energy physics and astrophysics will definitely help to uncover this secrecy. Multimessenger cosmology of new physics will provide both additional information on the physics of very early Universe as well as on the underlying physics. The analysis of the expected big data on the physical, astrophysical and cosmological signatures of new physics will accomplish these studies. It will involve technology of artificial intellect and machine learning.

We have presented some examples of possible cosmological and physical signatures of new physics and look forward to revealing of features of BSM symmetries, supporting multicomponent dark matter candidates and nonstandard cosmological scenarios.

Cosmological, astrophysical and experimental physical probes for new physics are complementary. This complementarity of studies of physics corresponding to a new physical scale V is displayed in Fig. 27.

The observed contours of the BSM physics and cosmology inspire a deep belief that after the Standard model the development of cosmoparticle physics, studying fundamental relationship of cosmology and particle physics in the set of indirect cosmological, astrophysical and microphysical effects [12,13], will lead to true history of our world based on the true physical nature of its unknown components that correspond to 95% of the modern Universe content.

Acknowledgments

I express the gratitude to all the co-authors of my original works on which the review is based. I am grateful to Prof. Shantanu Desai, Prof. Ken Ganga and Prof. George F. Smoot for reading the manuscript and important comments. I am grateful to Ekaterina Shlepkina for important help in preparation of the manuscript. The work has been performed with a support of the Ministry of Science and Higher Education of the Russian Federation, Project "Fundamental problems of cosmic rays and dark matter", No. 0723-2020-0040.

References

[1] A.D. Linde, Particle Physics and Inflationary Cosmology, Harwood, Chur, Switzerland, 1990.
[2] E.W. Kolb, M.S. Turner, The Early Universe, Addison-Wesley, Boston, MA, USA, 1990.
[3] D.S. Gorbunov, V.A. Rubakov, Introduction To the Theory of the Early Universe Hot Big Bang Theory. Cosmological Perturbations and Inflationary Theory, World Scientific, Singapore, Singapore, 2011.

[4] D.S. Gorbunov, V.A. Rubakov, Introduction To the Theory of the Early Universe Hot Big Bang Theory, World Scientific, Singapore, Singapore, 2011.
[5] G. Bertone, Particle Dark Matter: Observations, Models and Searches, Cambridge University Press, Cambridge, UK, 2010.
[6] C.S. Frenk, S.D.M. White, Ann. Phys. 524 (2012) 507.
[7] G.B. Gelmini, Internat. J. Modern Phys. A 23 (2008) 4273.
[8] E. Aprile, S. Profumo, New J. Phys. 11 (2009) 105002.
[9] J.L. Feng, Ann. Rev. Astron. Astrophys. 48 (2010) 495–545.
[10] A.D. Sakharov, Vestnik AN SSSR 4 (1989) 39.
[11] M.Y. Khlopov, Vestnik Russ. Acad. Sci. 71 (2001) 1133.
[12] M.Y. Khlopov, Cosmoparticle Physics, World Scientific, Singapore, Singapore, 1999.
[13] M.Y. Khlopov, Fundamentals of Cosmoparticle Physics, CISP-Springer, Cambridge, UK, 2012.
[14] Planck Collaboration, P.A.R. Ade, et al., Astron. Astrophys. 594 (2016) A13.
[15] M. Khlopov, Symmetry 8 (2016) 81.
[16] F. Sannino, K. Tuominen, Phys. Rev. D 71 (2005) 051901.
[17] D.K. Hong, S.D.H. Hsu, F. Sannino, Phys. Lett. B 597 (2004) 89.
[18] D.D. Dietrich, F. Sannino, K. Tuominen, Phys. Rev. D 72 (2005) 055001.
[19] D.D. Dietrich, F. Sannino, K. Tuominen, Phys. Rev. D 73 (2006) 037701.
[20] S.B. Gudnason, C. Kouvaris, F. Sannino, Phys. Rev. D 73 (2006) 115003.
[21] S.B. Gudnason, C. Kouvaris, F. Sannino, Phys. Rev. D 74 (2006) 095008.
[22] M.Yu. Khlopov, C. Kouvaris, Phys. Rev. D 77 (2008) 065002.
[23] M.Yu. Khlopov, C. Kouvaris, Phys. Rev. D 78 (2008) 065040.
[24] D.B. Kaplan, H. Georgi, Phys. Lett. B 136 (1984) 183.
[25] D.B. Kaplan, H. Georgi, S. Dimopoulos, Phys. Lett. B 136 (1984) 187.
[26] N. Arkani-Hamed, A.G. Cohen, E. Katz, A.E. Nelson, T. Gregoire, J.G. Wacker, J. High Energy Phys. 08 (2002) 021.
[27] N. Arkani-Hamed, A.G. Cohen, E. Katz, A.E. Nelson, J. High Energy Phys. 07 (2002) 034.
[28] K. Agashe, R. Contino, A. Pomarol, Nuclear Phys. B 719 (2005) 165.
[29] R. Contino, L. Da Rold, A. Pomarol, Phys. Rev. D 75 (2007) 055014.
[30] Y. Kats, M. McCullough, G. Perez, Y. Soreq, J. Thaler, J. High Energy Phys. 06 (2017) 126.
[31] S. Jaeger, S. Kvedaraite, G. Perez, I. Savoray, J. High Energy Phys 2019 (2019) 41.
[32] R.D. Peccei, H.R. Quinn, Phys. Rev. Lett. 38 (1977) 1440.
[33] F. Wilczek, Phys. Rev. Lett. 40 (1978) 279.
[34] S. Weinberg, Phys. Rev. Lett. 40 (1978) 223.
[35] J.E. Kim, Phys. Rep. 150 (1987) 1.
[36] H.Y. Cheng, Phys. Rep. 158 (1988) 1.
[37] M. Dine, W. Fischler, M. Srednicky, Phys. Lett. B 104 (1981) 199.
[38] A.R. Zhitnitcki, Yad. Fiz. 31 (1980) 197.
[39] J.E. Kim, Phys. Rev. Lett. 43 (1979) 103.
[40] M.A. Shifman, A.I. Vainshtein, V.I. Zakharov, Nuclear Phys. B 166 (1980) 493.
[41] Z.G. Berezhiani, J.K. Chkareuli, Pisma ZhETF 35 (1982) 494.
[42] Z.G. Berezhiani, J.K. Chkareuli, Pisma ZhETF 37 (1983) 285.
[43] Z.G. Berezhiani, Phys. Lett. B 129 (1983) 99.
[44] J.K. Chkareuli, Pisma ZhETF 32 (1980) 684.
[45] T. Appelquist, Y. Bai, M. Piai, Phys. Rev. D 75 (2007) 073005.
[46] T. Appelquist, Y. Bai, M. Piai, Phys. Rev. D 74 (2006) 076001.
[47] T. Appelquist, Y. Bai, M. Piai, Phys. Lett. B 637 (2006) 245.
[48] A.A. Anselm, N.G. Uraltzev, ZhETF 84 (1983) 1961.
[49] A.A. Anselm, Z.G. Berezhiani, Phys. Lett. B 162 (1985) 349.
[50] T.D. Lee, C.N. Yang, Phys. Rev. 104 (1956) 254.
[51] I.Y. Kobzarev, L.B. Okun, I.Y. Pomeranchuk, Sov. J. Nucl. Phys. 3 (1966) 837.
[52] Y.B. Zeldovich, M.Y. Khlopov, Sov. Phys. Usp. 24 (1981) 755.
[53] R. Foot, R.R. Volkas, Phys. Rev. D 52 (1995) 6595.
[54] S.I. Blinnikov, M.Y. Khlopov, Sov. J. Nucl. Phys. 36 (1982) 472.
[55] S.I. Blinnikov, M.Y. Khlopov, Sov. Astron. J. 27 (1983) 371.
[56] E.D. Carlson, S.L. Glashow, Phys. Lett. B 193 (1987) 168.
[57] R. Foot, R.R. Volkas, Astropart. Phys. 7 (1997) 283.
[58] Z. Berezhiani, D. Comelli, F. Villante, Phys. Lett. B 503 (2001) 362.
[59] Z. Berezhiani, Internat. J. Modern Phys. A 19 (2004) 3775.
[60] E.W. Kolb, D. Seckel, M.S. Turner, Nature 314 (1985) 415.
[61] M.Y. Khlopov, et al., Sov. Astron. 35 (1991) 21.
[62] L.B. Okun, Phys.-Usp. 50 (2007) 380.
[63] P. Ciarcelluti, Internat. J. Modern Phys. D 19 (2010) 2151.
[64] Ya.B. Zeldovich, M.Yu. Khlopov, Phys. Lett. B 79 (1978) 239.
[65] M.Yu. Khlopov, Priroda 12 (1979) 90.
[66] J.R. Preskill, Phys. Rev. Lett. 43 (1979) 1365.
[67] S. Ketov, M.Yu. Khlopov, Symmetry 11 (2019) 511.
[68] T. Kaluza, Sitzungsber. Preuss. Akad. Wiss. Berlin. (Math. Phys.), Zum Unitätsproblem Phys. (1921) 966.
[69] O. Klein, Nature 118 (1926) 516.
[70] J.H. Schwarz, Phys. Rep. 315 (1999) 107.
[71] M.B. Green, J.H. Schwarz, Phys. Lett. B 149 (1984) 117.
[72] D.J. Gross, J.A. Harvey, E. Martinec, R. Rohm, Phys. Rev. Lett. 54 (1985) 502.
[73] P. Candelas, G.T. Horowitz, A. Strominger, E. Witten, Nuclear Phys. B 258 (1985) 46.
[74] M.B. Green, J.H. Schwarz, Phys. Lett. B 109 (1982) 444.
[75] M. Maltoni, V.A. Novikov, L.B. Okun, A.N. Rozanov, M.I. Vysotsky, Phys. Lett. B 476 (2000) 107.
[76] M.Y. Khlopov, R.M. Shibaev, Adv. High Energy Phys. 2014 (2014) 406458, http://dx.doi.org/10.1155/2014/406458.
[77] K.M. Belotsky, M.Y. Khlopov, K.I. Shibaev, Gravit. Cosm. Suppl. 6 (2000) 140.

[78] K.M. Belotsky, D. Fargion, M.Y. Khlopov, R.V. Konoplich, K.I. Shibaev, Gravit. Cosm. 11 (2005) 16.
[79] K.M. Belotsky, D. Fargion, M.Y. Khlopov, R.V. Konoplich, Phys. Atom. Nucl. 71 (2008) 147.
[80] Ya.I. Kogan, M.Yu. Khlopov, Sov. J. Nucl. Phys. 44 (1986) 873.
[81] Ya.I. Kogan, M.Yu. Khlopov, Sov. J. Nucl. Phys. 46 (1987) 193.
[82] S. Weinberg, Gravitation and Cosmology, John Wiley and Sons, Inc., New York, NY, USA, 1972.
[83] Y.B. Zeldovich, I.D. Novikov, Structure and Evolution of the Universe, Nauka, Moscow, Russia, 1985.
[84] N.S. Mankoc Borstnik, J. Math. Phys. 34 (1993) 3731, space.
[85] N.S. Mankoc Borstnik, Phys. Rev. D 91 (2015) 065004.
[86] A. Merle, Internat. J. Modern Phys. D 22 (2013) 1330020.
[87] M.Y. Khlopov, A.D. Linde, Phys. Lett. B 138 (1984) 265.
[88] F. Balestra, et al., Sov. J. Nucl. Phys. 39 (1984) 626.
[89] Y.L. Levitan, I.M. Sobol, M.Y. Khlopov, V.M. Chechetkin, Sov. J. Nucl. Phys. 47 (1988) 109.
[90] M.Y. Khlopov, Yu.L. Levitan, E.V. Sedel'Nikov, I.M. Sobol', Phys. Atom. Nucl. 57 (1994) 1393.
[91] E.V. Sedel'nikov, S.S. Filippov, M.Y. Khlopov, Phys. Atom. Nucl. 58 (1995) 235.
[92] K. Jedamzik, Phys. Rev. D 70 (2004) 063524.
[93] M. Kawasaki, K. Kohri, T. Moroi, Phys. Lett. B 625 (2005) 7.
[94] A. Sommerfeld, Atombau Und Spektrallinien, F. Vieweg and Sohn, Brunswick, Germany, 1921.
[95] G. Gamow, Z. Phys. 51 (1928) 204.
[96] A.D. Sakharov, Sov. Phys. Usp. 34 (1991) 375.
[97] K.M. Belotsky, M.Y. Khlopov, K.I. Shibaev, Gravit. Cosmol. 6 (2000) 140.
[98] A.B. Arbuzov, T.V. Kopylova, J. High Energy Phys. 2012 (2012) 9.
[99] Y.B. Zeldovich, A.A. Klypin, M.Y. Khlopov, V.M. Chechetkin, Sov. J. Nucl. Phys. 31 (1980) 664.
[100] G. Jungman, M. Kamionkowski, K. Griest, Phys. Rep. 267 (1996) 195.
[101] D. Fargion, M.Y. Khlopov, R.V. Konoplich, R. Mignani, Phys. Rev. D 52 (1995) 1828.
[102] R. Bernabei, et al., Phys. Lett. B 480 (2000) 23.
[103] R. Bernabei, et al., Riv. Nuovo Cimento 26 (2003) 1.
[104] R. Bernabei, et al., Eur. Phys. J. C 56 (2008) 333.
[105] R. Bernabei, et al., Internat. J. Modern Phys. A 28 (2013) 1330022.
[106] D. Abrams, D.S. Akerib, P.D. Barnes Jr., Phys. Rev. D 66 (2002) 122003.
[107] D.S. Akerib, M.S. Armel-Funkhouser, M.J. Attisha, B.A. Young, Phys. Rev. D 72 (2005) 052009.
[108] Z. Ahmed, D.S. Akerib, S. Arrenberg, Phys. Rev. Lett. 102 (2009) 011301.
[109] E. Aprile, K. Arisaka, F. Arneodo, Phys. Rev. Lett. 105 (2010) 131302.
[110] C.E. Aalseth, P.S. Barbeau, N.S. Bowden, Phys. Rev. Lett. 106 (2011) 131302.
[111] Y.A. Golubkov, et al., JETP Lett. 69 (1999) 434.
[112] D. Fargion, R.V. Konoplich, M. Grossi, M.Y. Khlopov, Astropart. Phys. 12 (2000) 307.
[113] K.M. Belotsky, M.Y. Khlopov, Gravit. Cosmol. Suppl. 8 (2002) 112.
[114] K.M. Belotsky, D. Fargion, M.Y. Khlopov, R.V. Konoplich, Phys. Atom. Nucl. 71 (2008) 147.
[115] K.M. Belotsky, M.Y. Khlopov, K.I. Shibaev, Part. Nucl. Lett. 108 (2001) 5.
[116] K.M. Belotsky, M.Y. Khlopov, K.I. Shibaev, Phys. Atom. Nucl. 65 (2002) 382.
[117] K.M. Belotsky, T. Damour, M.Y. Khlopov, Phys. Lett. B 105 (2010) 131302.
[118] D. Fargion, M.Y. Khlopov, Gravit. Cosmol. 19 (2013) 219.
[119] K.M. Belotsky, M.Y. Khlopov, Gravit. Cosmol. 7 (2001) 189.
[120] K.M. Belotsky, et al., Gravit. Cosmol. Suppl. 11 (2005) 3.
[121] D. Fargion, M.Y. Khlopov, C.A. Stephan, Classical Quantum Gravity 23 (2006) 7305.
[122] M.Y. Khlopov, JETP Lett. 83 (2006) 1.
[123] K.M. Belotsky, M.Y. Khlopov, K.I. Shibaev, Gravit. Cosmol. 12 (2006) 1.
[124] M.Y. Khlopov, Modern Phys. Lett. A 26 (2011) 2823.
[125] A. Ibarra, D. Tran, C. Weniger, Internat. J. Modern Phys. A 28 (2013) 1330040.
[126] O. Adriani, et al., Nature 458 (2009) 607.
[127] M. Ackermann, M. Ajello, A. Allafort, Phys. Rev. Lett. 108 (2012) 011103.
[128] M. Aguilar, G. Alberti, B. Alpat, Phys. Rev. Lett. 110 (2013) 141102.
[129] A. Kounine, Internat. J. Modern Phys. E 21 (2012) 1230005.
[130] K. Petraki, R.R. Volkas, Internat. J. Modern Phys. A 28 (2013) 1330028.
[131] S.L. Glashow, 2005, preprint hep-ph/0504287.
[132] M.Y. Khlopov, V.M. Chechetkin, Sov. J. Part. Nucl. 18 (1987) 267.
[133] A.S. Sakharov, M.Y. Khlopov, Phys. Atom. Nucl. 57 (1994) 651.
[134] A.G. Doroshkevich, M.Y. Khlopov, Sov. J. Nucl. Phys. 39 (1984) 551.
[135] A.G. Doroshkevich, M.Y. Khlopov, Mon. Not. R. Astron. Soc. 211 (1988) 279.
[136] A.G. Doroshkevich, A.A. Klypin, M.Y. Khlopov, Sov. Astron. 32 (1984) 127.
[137] A.G. Doroshkevich, A.A. Klypin, M.Y. Khlopov, Mon. Not. R. Astron. Soc. 239 (1989) 923.
[138] Z.G. Berezhiani, M.Y. Khlopov, Sov. J. Nucl. Phys. 52 (1990) 60, symmetry.
[139] Z.G. Berezhiani, M.Y. Khlopov, Z. Phys. C 49 (1991) 73.
[140] M.S. Turner, G. Steigman, L.M. Krauss, Phys. Rev. Lett. 52 (1984) 2090.
[141] G. Gelmini, D.N. Schramm, J.W.F. Valle, Phys. Lett. B 146 (1984) 311.
[142] E.V. Sedelnikov, M.Y. Khlopov, Phys. Atom. Nucl. 59 (1996) 1000.
[143] S. Dimopoulos, R. Esmailzadeh, G.D. Starkman, L.J. Hall, Astrophys. J. 330 (1988) 545.
[144] A.G. Doroshkevich, M.Y. Khlopov, Sov. Astron. Lett. 11 (1985) 236.
[145] A.G. Polnarev, M.Y. Khlopov, Sov. Phys. Usp. 28 (1985) 213.
[146] M.Y. Khlopov, A.G. Polnarev, Phys. Lett. B 97 (1980) 383.
[147] A.G. Polnarev, M.Y. Khlopov, Sov. Astron. 25 (1981) 406.
[148] A. Mazumdar, G. White, Rep. Progr. Phys. 82 (2019) 076901.
[149] R.V. Konoplich, et al., Phys. Atom. Nucl. 62 (1999) 1593.
[150] M.Y. Khlopov, S.G. Rubin, Cosmological Pattern of Microphysics in Inflationary Universe, Kluwer, Dordrecht, The Netherlands, 2004.
[151] M.Y. Khlopov, Magnetic Stars, Nauka, Leningrad, Russia, 1988, p. 201.
[152] Y.B. Zeldovich, I.Y. Kobzarev, L.B. Okun, Sov. Phys.—JETP 40 (1975) 1.

[153] Y.B. Zeldovich, Mon. Not. R. Astron. Soc. 192 (1980) 663.
[154] A. Vilenkin, Phys. Rev. Lett. 46 (1981) 1169.
[155] A.S. Sakharov, M.Y. Khlopov, Phys. Atom. Nucl. 57 (1994) 485.
[156] A.S. Sakharov, M.Y. Khlopov, P. D.D. Sokoloff, hys. Atom. Nucl. 59 (1996) 1005; Phys. Atom. Nucl. 59 (1996) 1005–1010.
[157] A.S. Sakharov, M.Y. Khlopov, D.D. Sokoloff, Nuclear Phys. B Proc. Suppl. 72 (1999) 105.
[158] J. Jaeckel, A. Ringwald, Ann. Rev. Nucl. Part. Sci. 60 (2010) 405.
[159] A. Vilenkin, E.P.S. Shellard, Cosmic Strings and Other Topological Defects, Cambridge University Press, Cambridge, UK, 1994.
[160] J.R. Oppenheimer, H. Sneider, Phys. Rev. 56 (1939) 455.
[161] Y.B. Zeldovich, I.D. Novikov, Relativistic Astrophysics, Volume 1: Stars and Relativity, University of Chicago Press, Chicago, IL, USA, 1971.
[162] Y.B. Zeldovich, I.D. Novikov, Sov. Astron. 10 (1967) 602.
[163] S.W. Hawking, Mon. Not. R. Astron. Soc. 152 (1971) 75.
[164] B.J. Carr, S.W. Hawking, Mon. Not. R. Astron. Soc. 168 (1974) 399.
[165] J.S. Bullock, J.R. Primack, Phys. Rev. D 55 (1997) 7423.
[166] B.J. Carr, Astroph. J. 201 (1975) 1.
[167] A.G. Polnarev, M.Y. Khlopov, Sov. Astron. 26 (1982) 391.
[168] M.Y. Khlopov, A.G. Polnarev, in: G. Gibbons, S. Hawking, E. Siclos (Eds.), The Very Early Universe, Cambridge University Press, Cambridge, UK, 1983, 407 early Universe. –432.
[169] M.Y. Khlopov, B.A. Malomed, Y.B. Zel'dovich, Mon. Not. R. Astron. Soc. 215 (1985) 575.
[170] Y.B. Zeldovich, M.A. Podurets, Sov. Astron. 9 (1965) 742.
[171] V.G. Gurzadian, G.K. Savvidi, Astrophys. J. 160 (1986) 203.
[172] O.K. Kalashnikov, M.Y. Khlopov, Phys. Lett. B 127 (1983) 407; Theory. Phys. Lett. 127B (1983) 407–422.
[173] A.F. Kadnikov, V.I. Maslyankin, M.Y. Khlopov, Astrophysics 31 (1990) 523.
[174] L.A. Kofman, A.D. Linde, Nuclear Phys. B 282 (1987) 555.
[175] A.S. Sakharov, M.Y. Khlopov, Phys. Atom. Nucl. 56 (1993) 412.
[176] Z. Berezhiani, M.Y. Khlopov, Sov. J. Nucl. Phys. 51 (1990) 739.
[177] Z. Berezhiani, M.Y. Khlopov, Sov. J. Nucl. Phys. 51 (1990) 935.
[178] Z. Berezhiani, M.Y. Khlopov, R.R. Khomeriki, Sov. J. Nucl. Phys. 52 (1990) 344.
[179] R. Watkins, M. Widrow, Nuclear Phys. B 374 (1992) 446.
[180] S.W. Hawking, I.G. Moss, J.M. Stewart, Phys. Rev. D 26 (1982) 2681, Bubble collisions in the very early universe; Phys. Rev. D 26 (1982) 2681–2693, http://dx.doi.org/10.1103/PhysRevD.26.2681.
[181] I.G. Moss, Phys. Rev. D 50 (1994) 676.
[182] R.V. Konoplich, S.G. Rubin, A.S. Sakharov, M.Y. Khlopov, Astron. Lett. 24 (1998) 413.
[183] M.Y. Khlopov, R.V. Konoplich, S.G. Rubin, A.S. Sakharov, Gravit. Cosmol. 6 (2000) 153.
[184] D. La, P.J. Steinhardt, Phys. Rev. Lett. 62 (1989) 376.
[185] R. Holman, E.W. Kolb, Y. Wang, Phys. Rev. Lett. 65 (1990) 17.
[186] R. Holman, E.W. Kolb, S.L. Vadas, Y. Wang, Phys. Rev. D 43 (1991) 3833.
[187] F.C. Adams, K. Freese, Phys. Rev. D 43 (1991) 353.
[188] E.J. Copeland, A.R. Liddle, D.H. Lyth, E.D. Stewart, D. Wands, Phys. Rev. D 49 (1994) 6410.
[189] F. Occhionero, L. Amendola, Phys. Rev. D 50 (1994) 4846.
[190] L. Amendola, C. Baccigalupi, R. Konoplich, Phys. Rev. D 54 (1996) 7199.
[191] M.S. Turner, E.J. Weinberg, L.M. Widrow, Phys. Rev. D 46 (1992) 2384.
[192] S.W. Hawking, Comm. Math. Phys. 43 (1975) 199.
[193] S.W. Hawking, Nature 248 (1974) 30.
[194] J.D. Barrow, E.J. Copeland, A.R. Liddle, Phys. Rev. D 46 (1992) 645.
[195] B.J. Carr, J.H. Gilbert, J.E. Lidsey, Phys. Rev. D 50 (1994) 4853.
[196] S.O. Alexeyev, M.V. Pomazanov, Phys. Rev. D 55 (1997) 2110.
[197] I.G. Dymnikova, Internat. J. Modern Phys. D 5 (1996) 529.
[198] Y.B. Zeldovich, A.A. Starobinsky, JETP Lett. 24 (1976) 571.
[199] S. Miyama, K. Sato, Progr. Theoret. Phys. 59 (1978) 1012.
[200] P.D. Naselsky, Sov. Astron. Lett. 4 (1978) 209.
[201] D. Lindley, Mon. Not. R. Astron. Soc. 193 (1980) 593.
[202] Y.B. Zeldovich, A.A. Starobinskii, M. Yu. Khlopov, V.M. Chechetkin, Sov. Astron. Lett. 3 (1977) 110.
[203] T. Rothman, R. Matzner, Astrophys. Space. Sci. 75 (1981) 229.
[204] J.H. MacGibbon, B.J. Carr, Astrophys. J. 371 (1991) 447.
[205] I.D. Novikov, A.G. Polnarev, A.A. Starobinskii, Ya.B. Zeldovich, Astron. Astrophys. 80 (1979) 104.
[206] V.M. Chechetkin, M.Y. Khlopov, M.G. Sapozhnikov, Riv. Nuovo Cimento 5 (1982) 1.
[207] J.H. MacGibbon, B.J. Carr, Phys. Rep. 307 (1998) 141.
[208] A.R. Liddle, A.M. Green, Phys. Rep. 307 (1998) 125.
[209] M. Lemoine, Phys. Lett. B 481 (2000) 333.
[210] A.M. Green, Phys. Rev. D 60 (1998) 063516.
[211] M.Y. Khlopov, A. Barrau, J. Grain, Classical Quantum Gravity 23 (2006) 1875.
[212] A. Guth, Phys. Rev. D 23 (1981) 347.
[213] A.D. Linde, Rep. Progr. Phys. 47 (1984) 925.
[214] E.B. Gliner, ZhETF 49 (1965) 542.
[215] A.D. Sakharov, Sov. Phys.—JETP 22 (1966) 241.
[216] E.B. Gliner, Dokl. Akad. Nauk 192 (1970) 771.
[217] E.B. Gliner, I.G. Dymnikova, Pisma Astron. Zh. 1 (1975) 7.
[218] A.I. Bugrii, A.A. Trushevsky, Astrophysica 13 (1977) 361.
[219] A.A. Starobinsky, Phys. Lett. B 91 (1980) 99.
[220] V.Ts. Gurovich, A.A. Starobinsky, Sov. Phys.—JETP 50 (1979) 844.
[221] Ya.B. Zeldovich, Sov. Phys. Usp. 24 (1981) 216, Affil.
[222] D. Kazanas, Astrophys. J. 241 (1981) L59.
[223] A.D. Linde, Phys. Lett. B 108 (1982) 389.
[224] A. Albrecht, P.J. Steinhardt, Phys. Rev. Lett. 48 (1982) 1220.
[225] A.D. Linde, Phys. Lett. B 129 (1983) 177.

[226] J.J.M. Carrasco, R. Kallosh, A. Linde, Phys. Rev. D 93 (2016) 061301.
[227] A. Addazi, M. Khlopov, Modern Phys. Lett. A 32 (2017) 1740002.
[228] A. Addazi, S. Ketov, M. Khlopov, A. Marciano, Internat. J. Modern Phys. D 27 (2018) 1841011.
[229] Y. Akrami, et al., Planck 2018 results. X. Constraints on inflation, 2018, preprint-arXiv:1807.06211.
[230] A.D. Sakharov, JETP Lett. 5 (1967) 24.
[231] V.A. Kuzmin, Pis'ma Zh. Eksp. Teor. Fiz. 12 (1970) 335.
[232] I. Affleck, M. Dine, Nuclear Phys. B 249 (1985) 361.
[233] A.D. Linde, Phys. Lett. B 158 (1985) 375.
[234] V.A. Kuzmin, V.A. Rubakov, M.E. Shaposhnikov, Phys. Lett. B 155 (1985) 36.
[235] M.E. Shaposhnikov, in: I.M. Dremin, A.M. Semikhatov (Eds.), Proc. 2 Sakharov Conf. on Physics, World Scientific, Singapore, 1997, p. 320.
[236] S.G. Rubin, M.Y. Khlopov, A.S. Sakharov, Gravit. Cosmol. Suppl. 6 (2000) 51.
[237] M.Y. Khlopov, S.G. Rubin, A.S. Sakharov, Gravit. Cosmol. Suppl. 8 (2002) 57.
[238] S.G. Rubin, A.S. Sakharov, M.Y. Khlopov, JETP 92 (2001) 921.
[239] V. Dokuchaev, Y. Eroshenko, S. Rubin, Gravit. Cosmol. 11 (2005) 99.
[240] M.Y. Khlopov, Res. Astron. Astrophys. 10 (2010) 495.
[241] M.Y. Khlopov, S.G. Rubin, A.S. Sakharov, Astropart. Phys. 23 (2005) 265.
[242] B.P. Abbott, et al., Phys. Rev. Lett. 116 (2016) 061102.
[243] B.P. Abbott, et al., Phys. Rev. Lett. 116 (2016) 241103.
[244] B.P. Abbott, et al., Phys. Rev. Lett. 118 (2017) 221101.
[245] B.P. Abbott, et al., Phys. Rev. Lett. 119 (2017) 141101.
[246] B.P. Abbott, et al., Astrophys. J. Lett. 851 (2017) L35.
[247] K.M. Belotsky, et al., Eur. Phys. J. C 79 (2019) 246, M.Y. Khromykh, L.A. Kirillov, A.A. Nikulin, V.V. Rubin, S.G.
[248] B.J. Carr, Lecture Notes in Phys. 631 (2003) 301.
[249] D. Blais, C. Kiefer, D. Polarski, Phys. Lett. B 535 (2002) 11.
[250] N. Afshordi, P. McDonald, D.N. Spergel, Astrophys. J. 594 (2003) L71.
[251] B. Carr, F. Kuehnel, M. Sandstad, Phys. Rev. D 94 (2016) 083504.
[252] Y. Ali-Haimoud, M. Kamionkowski, Phys. Rev. D 95 (2017) 043534.
[253] The LIGO Scientific Collaboration, The Virgo Collaboration, B.P. Abbott, et al., 2018, Preprint 1811.12907.
[254] The LIGO Scientific Collaboration, the Virgo Collaboration, R. Abbott, et al., Phys. Rev. Lett. 125 (2020) 101102.
[255] The LIGO Scientific Collaboration, the Virgo Collaboration, R. Abbott, et al., Astrophys. J. Lett. 900 (2020) L13.
[256] T. Bringmann, P.F. Depta, V. Domcke, K. Schmidt-Hoberg, Phys. Rev. D 99 (2019) 063532.
[257] V.M. Chechetkin, M.Y. Khlopov, M.G. Sapozhnikov, Y.B. Zeldovich, Phys. Lett. B 118 (1982) 329.
[258] M.Y. Khlopov, J. Phys. Conf. Ser. 66 (2007) 012032.
[259] F.W. Stecker, J.-L. Puget, Astrophys. J. 178 (1972) 57.
[260] G.A. Steigman, Annu. Rev. Astron. Astrophys. 14 (1976) 339.
[261] A.G. Cohen, A. De Rujula, S.L. Glashow, Astrophys. J. 495 (1998) 539.
[262] W.H. Kinney, E.W. Kolb, M.S. Turner, Phys. Rev. Lett. 79 (1997) 2620.
[263] A.D. Dolgov, Nuclear Phys. Proc. Suppl. 113 (2002) 40.
[264] M.Y. Khlopov, S.G. Rubin, A.S. Sakharov, Phys. Rev. D 62 (2000) 083505.
[265] A. Dolgov, J. Silk, Phys. Rev. D 47 (1993) 4244.
[266] A.D. Dolgov, M. Kawasaki, N. Kevlishvili, Nuclear Phys. B 807 (2009) 229.
[267] M.Y. Khlopov, et al., Astropart. Phys. 12 (2000) 367.
[268] M.Y. Khlopov, Gravit. Cosmol. 4 (1998) 69.
[269] Y.A. Golubkov, M.Y. Khlopov, Phys. Atom. Nucl. 64 (2001) 1821.
[270] K.M. Belotsky, et al., Phys. Atom. Nucl. 63 (2000) 233.
[271] D. Fargion, M.Y. Khlopov, Astropart. Phys. 19 (2003) 441.
[272] V. Poulin, P. Salati, I. Cholis, M. Kamionkowski, J. Silk, Phys. Rev. D 99 (2019) 023016.
[273] S.I. Blinnikov, A.D. Dolgov, K.A. Postnov, Phys. Rev. D 92 (2015) 023516.
[274] R. Bernabei, et al., Bled Workshops Phys. 19 (2018) 27.
[275] D. Akerib, et al., Phys. Rev. D 98 (2018) 062005.
[276] M. Khlopov, Modern Phys. Lett. A 26 (2011) 2823.
[277] M. Khlopov, Internat. J. Modern Phys. A 29 (2014) 1443002.
[278] M.Y. Khlopov, A.G. Mayorov, E.Y. Soldatov, Prespacetime J 309 (2011) 012013.
[279] M.Y. Khlopov, AIP Conf. Proc. 1241 (2010) 388.
[280] M.Y. Khlopov, 2008, Preprint 0801.0167.
[281] M.Y. Khlopov, 2008, Preprint 0801.0169.
[282] M.Y. Khlopov, A.G. Mayorov, E.Y. Soldatov, Bled Workshops Phys. 11 (2010) 186.
[283] C.B. Dover, T.K. Gaisser, G. Steigman, Phys. Rev. Lett. 42 (1979) 1117.
[284] S. Wolfram, Phys. Lett. B 82 (1979) 65.
[285] G.D. Starkman, A. Gould, R. Esmailzadeh, S. Dimopoulos, Phys. Rev. D 41 (1990) 3594.
[286] D. Javorsek, D. Elmore, E. Fischbach, D. Granger, T. Miller, D. Oliver, V. Teplitz, Phys. Rev. Lett. 87 (2001) 231804.
[287] S. Mitra, Phys. Rev. D 70 (2004) 103517.
[288] G.D. Mack, J.F. Beacom, G. Bertone, Phys. Rev. D 76 (2007) 043523.
[289] B.D. Wandelt, R. Dave, G.R. Farrar, P.C. McGuire, D.N. Spergel, P.J. Steinhardt, 2000, preprint astro-ph/0006344.
[290] P.C. McGuire, P.J. Steinhardt, 2001, Preprint astro-ph/0105567.
[291] G. Zaharijas, G.R. Farrar, Phys. Rev. D 72 (2005) 083502.
[292] M.Y. Khlopov, A.G. Mayorov, E.Y. Soldatov, Bled Workshops Phys. 11 (2010) 73.
[293] M.Y. Khlopov, C. Kouvaris, Phys. Rev. D 78 (2008) 065040.
[294] R.N. Cahn, S.L. Glashow, Science 213 (1981) 607.
[295] M. Pospelov, Phys. Rev. Lett. 98 (2007) 231301.
[296] K. Kohri, F. Takayama, Phys. Rev. D 76 (2007) 063507.
[297] M.Y. Khlopov, A.G. Mayorov, E.Y. Soldatov, Internat. J. Modern Phys. D 19 (2010) 1385.
[298] M.Y. Khlopov, 2008, Preprint 0806.3581.
[299] J.-R. Cudell, M.Y. Khlopov, Q. Wallemacq, Bled Workshops Phys. 13 (2012) 10.
[300] Q. Wallemacq, Phys. Rev. D 88 (2013) 063516.

[301] K.M. Belotsky, A.G. Mayorov, M.Y. Khlopov, Scientific Session NRNU MEPhI-2010, vol. 4, World Scientific Publishing Company, Singapore, Singapore, 2010, p. 127.
[302] D.P. Finkbeiner, N. Weiner, Phys. Rev. D 76 (2007) 083519.
[303] B.J. Teegarden, et al., Astrophys. J. 621 (2005) 296.
[304] D. McCammon, et al., Nucl. Instrum. Methods 370 (1996) 266.
[305] D. McCammon, et al., Astrophys. J. 576 (2002) 188.
[306] V. Beylin, M. Khlopov, V. Kuksa, N. Volchanskiy, Symmetry 11 (2019) 587.
[307] G. Angloher, et al., Eur. Phys. J. C 72 (2012) 1971.
[308] J. Amare, et al., Eur. Phys. J. C 79 (2019) 412.
[309] The COSINE-100 Collaboration, Nature 564 (2018) 83.
[310] M. Khlopov, Internat. J. Modern Phys. A 28 (2013) 1330042.
[311] M.Yu. Khlopov, Internat. J. Modern Phys. D 587 (2019) 1941012.
[312] E. Mörtsell, S. Dhawan, J. Cosmol. Astropart. Phys. 2018 (2018) 025.
[313] S. Vagnozzi, Phys. Rev. D 102 (2020) 023518.